DOCTOR OF PHILOSOPHY

Synthetic studies on ferrocenylamines and ferrocenylphosphines

Quayle, Scott Calvin

Award date:
1998

Awarding institution:
University of Wales, Bangor

Synthetic Studies on Ferrocenylamines and Ferrocenylphosphines

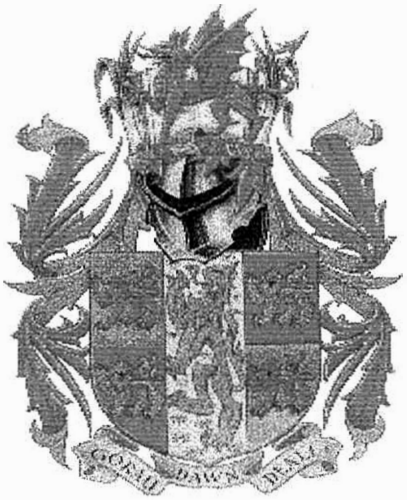

A thesis submitted to the University of Wales, Bangor
in candidature for the degree of Doctor of Philosophy

by

Scott Calvin Quayle

November, 1998

Abstract

A synthetic route for the preparation of 1,1'-heterosubstituted aminoferrocenes has been devised. The key precursor, 1-bromo-1'-aminoferrocene, is generated in a one-pot reaction from the readily available 1,1'-dibromoferrocene, and has been additionally characterised as its *N*-borane adduct. 1-Amino-1'-ferrocenecarboxylic acid and its methyl ester are reported as the first examples of 1,1'-heterosubstituted aminoferrocenes, and 1-(diphenylphosphino)-1'-aminoferrocene is representative of a new class of *P,N*-donor ferrocene ligands in which both heteroelements are bonded directly to the ferrocene backbone. Protection of air-sensitive ferrocenylphosphines as their *P*-borane adducts has allowed for the synthesis of novel 1,1'- and 1,2-substituted ferrocenylphosphine-boranes which, while air-stable and crystalline, can be readily deprotected to yield the corresponding 1,1'- or 1,2-diphosphines.

Nickel and palladium (II) chloride complexes of the previously reported ligand 1,1'-bis(diisopropylphosphino)ferrocene and the palladium (II) chloride complex of 1,1'-bis(diisopropylphosphino)-2-[(*N,N*-dimethylamino)ethyl]ferrocene have been prepared and their single crystal X-ray structures determined: as with their diphenylphosphino-analogues, the palladium complexes are square-planar and *cis* while the nickel complex is tetrahedral. The crystal structures are presented, together with preliminary electrochemical characterisation.

cis-Dichloro[1,1'-bis(diisopropylphosphino)ferrocene]palladium (II) has been tested as a catalyst precursor for carbon-carbon bond forming reactions and is found to be considerably more efficient than its phenylphosphino-analogue in catalysis of the Heck reaction. A range of related (diisopropylphosphino)- and (diphenylphosphino)ferrocenes is also compared and, in general, the complexes with (diisopropylphosphino)ferrocene ligands are shown to produce greater reaction rates. The scope of the new complexes in other cross-coupling reactions, namely the coupling of organomagnesium and organoboron reagents, is also assessed.

Acknowledgements

I should like to thank my supervisors Dr Ian Butler and Dr Alastair Boyes for their wholehearted involvement with the project. I am also grateful to the technical staff, in particular Mr Eric Lewis, Mr Glyn Connolly, Mr Denis Williams and Mr Gwynfor Davies, and to Mrs Barbara Kinsella, Mrs Helen Hughes, Miss Caroline Naylor, Mrs Margaret Calvert and Mrs Linda Edwards of the Department of Chemistry, and Mrs Annwen Francis of Coleg Menai. My gratitude is extended to those involved with X-ray crystallography at the University of Wales, Cardiff, mass spectrometry at the University of Wales, Swansea and electrochemistry at the University of Siena, for their services and helpful discussions.

I wish to acknowledge the support and assistance of my esteemed colleagues, Miss Rachel Davies, Mr Richard Dickinson, Miss Claire Gravil, Herr Ulrich Griesbach, Herr Tobias Herzig, Mr Glenn Kelly, Srta María Méndez Pérez, Herr Philipp Müller, Mr Robert Noden, Mr Richard Parry, Mr Martin Rugen-Hankey, Mr John Szewczyk, Mr Dafydd Thomas, Srta Eléna Valles Valles and Mr Mark Wild.

I am extremely grateful to my parents, my family and all my friends for the unfailing encouragement and benevolence they have demonstrated over the last three years.

The project was funded by a University of Wales, Bangor/ Department of Chemistry studentship, for which I remain indebted.

Abbreviations and Acronyms

An	anthracenyl
b	broad
BINAP	2,2'-bis(diphenylphosphino)-1,1'-binaphthyl
bp	boiling point
BPPFA	1,1'-bis(diphenylphosphino)-2-[(*N*,*N*-dimethylamino)ethyl]-ferrocene
cat.	catalyst
CIP	Cahn-Ingold-Prelog
Cp	η^5-cyclopentadienyl
Cy	cyclohexyl
COD	1,5-cyclooctadiene
dec.	decomposes
DIOP	2,3-*O*-isopropylidene-2,3-dihydroxy-1,4-bis(diphenyl-phosphino)butane
DIPPB	1,4-bis(diisopropylphosphino)butane
DIPPE	1,2-bis(diisopropylphosphino)ethane
DIPPF	1,1'-bis(diisopropylphosphino)ferrocene
DIPPP	1,3-bis(diisopropylphosphino)propane
DME	1,2-dimethoxyethane; glyme
DMF	*N*,*N*-dimethylformamide
DPPB	1,4-bis(diphenylphosphino)butane
DPPE	1,2-bis(diphenylphosphino)ethane
DPPF	1,1'-bis(diphenylphosphino)ferrocene
DPPM	bis(diphenylphosphino)methane
DPPP	1,3-bis(diphenylphosphino)propane
d	doublet
DI	direct insertion
e.e.	enantiomeric excess
EI	electron impact

FAB	fast-atom bombardment
Fc	ferrocenyl
GLC	gas-liquid chromatography
IMS	industrial methylated spirits
IPPFA	1,1'-bis(diisopropylphosphino)-2-[(*N*,*N*-dimethylamino)-ethyl]ferrocene
IR	infra-red
L	ligand
LDA	lithium *N*,*N*-diisopropylamide
m	multiplet (NMR); medium (IR)
m-	*meta*-
mp	melting point
MS	mass spectrometry
NBD	2,5-norbornadiene; bicyclo[2.2.1]hepta-2,5-diene
NMR	nuclear magnetic resonance
o-	*ortho*-
OTf	trifluoromethylsulfonyl; triflate
p-	*para*-
PPFA	1-(diphenylphosphino)-2-[(*N*,*N*-dimethylamino)ethyl]-ferrocene
pt	*pseudo*-triplet
q	quartet
R	as defined, otherwise an alkyl or aryl group
rt	room temperature
s	singlet (NMR); strong (IR)
SCE	saturated calomel electrode
sept	septet
sxt	sextet
t	triplet
THF	tetrahydrofuran
TLC	thin-layer chromatography
TMEDA	*N*,*N*,*N*',*N*'-tetramethylethane-1,2-diamine
TRIPHOS	bis(2-diphenylphosphinoethyl)phenylphosphine

w	weak

Nomenclature

Where reference is made herein to substituted ferrocenes, the substituents R and R' are named in order of their CIP priority[1] rather than alphabetically as is often the convention, *e.g.* 1-bromo-1'-aminoferrocene, R > R'. The CIP priority rules also apply in those cases where there is more than one substituent on the same cyclopentadienyl ring, *e.g.* 1,1'-dibromo-2-[(*N*,*N*-dimethylamino)ethyl]ferrocene. The stereochemistry of such compounds is defined according to the convention of Schlögl[2] and explained in Chapter 1.2.3.

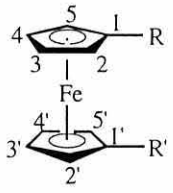

For the interpretation of NMR data the carbon and hydrogen atoms at the 2-, 2'-, 5- and 5'-positions are identified collectively as *alpha* while those in the 3-, 3'-, 4- and 4'- are *beta*. Where reference is made to ferrocenes with phenyl or tolyl substituents, the convention of *ortho*-, *meta*- and *para*- is followed for those substituents in order to distinguish between the ferrocenyl and phenyl resonances.

Contents

1. Introduction 1

1.1 Objectives 2

1.2 Ligand Synthesis 3

1.2.1 1,1'-Disubstituted Ferrocenes 4

1.2.2 1,1'-Heterodisubstituted Ferrocenes 6

1.2.3 1,2-Heterodisubstituted Ferrocenes 7

1.3 Representative Ligands 11

1.3.1 Ferrocenylamines 11

1.3.2 Ferrocenylphosphines 13

1.4 Applications in Cross-Coupling Catalysis 17

1.4.1 The Heck Reaction 18

1.4.2 Organomagnesium Cross-Coupling 27

1.4.3 Other Cross-Couplings 36

1.5 Summary 37

2. Aims 38

2.1 General Aims 39

2.2 Target Ligands 40

2.3 Catalysis 42

2.4 Summary 42

3. Results and Discussion 43

3.1 Outline 44

3.2 Synthesis 44

3.2.1 1,1'-Dibromoferrocene 44

3.2.2 1-Bromo-1'-aminoferrocene 45

3.2.3 Protection of 1-Bromo-1'-aminoferrocene 48

3.2.4 1-Amino-1'-ferrocenecarboxylic Acid 50

3.2.5 1-(Diphenylphosphino)-1'-aminoferrocene 51
3.2.6 1-Ferrocenyl(*N,N*-dimethyl)ethylamine 52
3.2.7 1,1'-Dibromo-2-[(*N,N*-dimethylamino)ethyl]-ferrocene 53
3.2.8 1,1'-Bis(diisopropylphosphino)ferrocene 56
3.2.9 1,1'-Bis(diphenylphosphino)ferrocene 59
3.2.10 1,1'-Bis[diisopropylphosphino(borane)]ferrocene .. 59
3.2.11 (*R,S*)-1,1'-Bis(diisopropylphosphino)-2-[(*N,N*-dimethylamino)ethyl]ferrocene 62
3.2.12 (*S,S*)-1-(*p*-Tolylsulfinyl)-2-[diisopropylphosphino(borane)]ferrocene 63
3.2.13 Attempted Synthesis of (*S*)-1-[Diphenyl-phosphino(borane)]-2-[diisopropylphosphino-(borane)]ferrocene 64
3.2.14 1,2-Bis[diisopropylphosphino(borane)]ferrocene .. 66
3.3 Co-ordination Chemistry 68
3.3.1 Dichloro[1,1'-bis(diisopropylphosphino)-ferrocene]nickel (II) 68
3.3.2 *cis*-Dichloro[1,1-bis(diisopropylphosphino)-ferrocene]palladium (II) 71
3.3.3 *cis*-Dichloro[(*R,S*)-1,1'-bis(diisopropylphosphino)-2-[(*N,N*-dimethylamino)ethylferrocene]-palladium (II) Dichloromethane Solvate 75
3.4 Catalysis 79
3.4.1 The Heck Reaction 79
3.4.2 Organomagnesium Cross-Coupling 88
3.4.5 Other Cross-Couplings 92

4. Conclusions and Further Work 96
4.1 Outline 97
4.2 Synthesis 97
4.2.1 Ferrocenylamines 97
4.2.2 Ferrocenylphosphines 101

4.3 Catalysis 103
4.3.1 The Heck Reaction 103
4.3.2 Organomagnesium Cross-Coupling 104
4.3.3 Other Cross-Couplings 104
4.3 Summary 105

5. Experimental 106
5.1 General 107
5.1.1 Techniques 107
5.1.2 Materials 108
5.1.3 Chemicals 108
5.2 Synthesis 109
5.2.1 Preparation of 1,1'-Dibromoferrocene 109
5.2.2 Preparation of 1-Bromo-1'-(*N*-phthalimido)-ferrocene 110
5.2.3 Preparation of 1-Bromo-1'-aminoferrocene 111
5.2.4 Preparation of 1-Bromo-1'-[amino(borane)]-ferrocene 113
5.2.5 Preparation of (*N*,*N*-Dicarboethoxyl)amino-ferrocene 114
5.2.6 Preparation of 1-Amino-1'-ferrocene-carboxylic Acid 115
5.2.7 Preparation of Methyl 1-Amino-1'-ferrocene-carboxylate 116
5.2.8 Preparation of 1-Diphenylphosphino-1'-aminoferrocene 118
5.2.9 Preparation of (±)-1,1'-Dibromo-2-[(*N*,*N*-dimethylamino)methyl]ferrocene 119
5.2.10 Preparation of (*R*)-1-Ferrocenyl(*N*,*N*-dimethyl)-ethylamine 120
5.2.11 Preparation of (*R*,*S*)-1,1'-Dibromo-2-[(*N*,*N*-dimethylamino)ethyl]ferrocene 121
5.2.12 Lithiation of (*R*,*S*)-1,1'-Dibromo-2-[(*N*,*N*-

dimethylamino)ethyl]ferrocene 122
5.2.13 Preparation of (*R*,*S*)-1,1'-Bis(diisopropyl-phosphino)-2-[(*N*,*N*-dimethylamino)ethyl]-ferrocene 123
5.2.14 Preparation of 1,1'-Bis(diisopropyl-phosphino)ferrocene 125
5.2.15 Preparation of 1,1'-Bis(diphenyl-phosphino)ferrocene 126
5.2.16 Preparation of Triphenylphosphine-borane 127
5.2.17 Preparation of 1,1'-Bis[diphenylphosphino-(borane)]ferrocene 128
5.2.18 Preparation of 1,1'-Bis[diisopropylphosphino-(borane)]ferrocene 129
5.2.19 Preparation of (*S*)-Ferrocenyl *p*-Tolyl Sulfoxide . . 130
5.2.20 Preparation of (*S*,*S*)-1-(*p*-Tolylsulfinyl)-2-[diisopropylphosphino(borane)]ferrocene 131
5.2.21 Preparation of (*S*)-1-(Diphenylphosphoryl)-2-[diisopropylphosphino(borane)]ferrocene 133
5.2.22 Preparation of 1,2-Bis[diisopropylphosphino-(borane)]ferrocene 135
5.3 Co-ordination Chemistry 137
5.3.1 Preparation of [$NiCl_2$(DIPPF)] 137
5.3.2 Preparation of [$NiCl_2$(DPPF)] 138
5.3.3 Preparation of *cis*-[$PdCl_2$(DIPPF)] 139
5.3.4 Preparation of *cis*-[$PdCl_2$(DPPF)] 140
5.3.5 Preparation of *cis*-[$PdCl_2$(IPPFA)].CH_2Cl_2 141
5.4 Catalysis 142
5.4.1 The Heck Reaction - General Method for *cis*-[$PdCl_2$(DIPPF)] Catalysis 142
5.4.2 The Heck Reaction - General Method for Reaction of Aryl Iodides and Methyl Acrylate 144
5.4.3 Organomagnesium Cross-Coupling - General Method 145

5.4.4 Suzuki Cross-Coupling - General Method 146

6. References. 147

Appendix - X-ray crystal structure data. 156

List of Figures

1.1 Target ferrocene derivatives 2
1.2 Reactions of 1,1'-dilithioferrocene 5
1.3 Phosphine ligands from 1,1'-dibromoferrocene 6
1.4 Amino-phosphine ligands from [1]-ferrocenophanes 7
1.5 Synthesis of 1-ferrocenyl(*N,N*-dimethyl)ethylamine 8
1.6 Synthesis of ferrocenyloxazoline ligands 9
1.7 Chiral sulfoxides in the synthesis of chiral ferrocene ligands 10
1.8 Synthesis of chiral ferrocenylamine ligands 12
1.9 Phosphine protection to prevent oxidation 15
1.10 Catalytic cross-coupling 17
1.11 The Heck reaction 18
1.12 Catalyst decomposition in the presence of phosphine ligands 19
1.13 Generation of palladacycles 20
1.14 Intermolecular asymmetric Heck reaction 22
1.15 Intramolecular asymmetric Heck reaction 22
1.16 Heck coupling of *n*-butyl vinyl ether and 1-naphthyl triflate 23
1.17 Possible insertion mechanisms in the catalytic Heck reaction 25
1.18 Catalytic Grignard cross-coupling 27
1.19 Kinetic resolution of secondary alkyl Grignard reagents 28
1.20 The effect of metal choice on cross-coupling catalysis 30
1.21 Hydrogenation using rhodium-phosphine complexes 30
1.22 Grignard cross-coupling catalytic cycle 32
1.23 Observed terminating species in the Grignard cross-coupling 33
1.24 Evidence for palladium (IV) oxidative addition products 34
1.25 Palladium (IV) intermediate in the Grignard cross-coupling 34
1.26 Suzuki cross-coupling catalysis using [$NiCl_2$(DPPF)]. 36
3.1 Synthesis of 1,1'-dibromoferrocene 44
3.2 Synthesis of 1-bromo-1'-aminoferrocene 47
3.3 Lithium-bromine exchange leading to formation of (*N,N*-dicarboethoxyl)-

aminoferrocene 49
3.4 Phosphine and amine protection 49
3.5 Synthesis of 2-ferrocenyl-2-(*N,N*-dimethylamino)acetonitrile 52
3.6 Synthesis of 1-ferrocenyl(*N,N*-dimethyl)ethylamine 53
3.7 Dibromination of ferrocenyl(*N,N*-dimethyl)methylamine 53
3.8 Synthesis of 1,1'-bis(diisopropylphosphino)ferrocene 56
3.9 ^{1}H NMR spectrum of 1,1'-bis(diisopropylphosphino)ferrocene 58
3.10 Cyclic voltammogram of 1,1'-bis(diisopropylphosphino)ferrocene 59
3.11 Immeasurable integration in the borane region of a ^{1}H NMR spectrum . . . 62
3.12 Synthesis of (*S,S*)-1-(*p*-tolylsulfinyl)-2-[diisopropylphosphino-(borane)]ferrocene 64
3.13 Attempted synthesis of (*R*)-1-[diisopropylphosphino-(borane)]-2-diphenylphosphino(borane)]ferrocene 65
3.14 Cyclic voltammogram of [$NiCl_2$(DIPPF)]. 69
3.15 Single crystal X-ray structure of [$NiCl_2$(DIPPF)]. 70
3.16 Cyclic voltammogram of *cis*-[$PdCl_2$(DIPPF)]. 72
3.17 Single crystal X-ray structure of *cis*-[$PdCl_2$(DIPPF)]. 74
3.18 Cyclic voltammogram of *cis*-[$PdCl_2$(IPPFA)]. 76
3.19 Single crystal X-ray structure of *cis*-[$PdCl_2$(IPPFA)]. 77
3.20 Heck coupling of iodobenzene with methyl acrylate 79
3.21 Possible explanations for copper (I) iodide rate increase 80
3.22 Allylic coupling in major and minor products from methyl methacrylate coupling 82
3.23 Formation of a η^3-allyl intermediate in the reaction of methyl methacrylate 82
3.24 Formation of phenyl acetaldehyde by-product 83
3.25 Attempted asymmetric Heck reaction 87
3.26 Catalytic cross-coupling of bromobenzene and *sec*-butylmagnesium chloride 88
3.27 Cross-coupling reaction profiles for different catalysts 89
3.28 Isomerisation of metal-alkenyl intermediate 90
3.29 Cross-coupling of 4-chlorotoluene and phenylboronic acid 94
4.1 Possible synthesis of 1-amino-2-ferrocenecarboxylic acid 99

4.2 Alternative possible synthesis of 1-amino-2-ferrocenecarboxylic acid 99

List of Tables

1.1 Isopropylphosphines in the catalysis of the Heck reaction 21
1.2 $Pd(OAc)_2$-phosphine catalysed Heck reaction of *n*-butyl vinyl ether and 1-naphthyl triflate 25
1.3 Cross-coupling reaction of *sec*-butylmagnesium chloride with bromobenzene 29
1.4 The effect of bond angles on catalysis 29
3.1 Attempted selective lithiation of 1,1'-dibromo-2-[(*N,N*-dimethyl amino)ethyl]ferrocene 56
3.2 Comparison of $^{31}P-\{^1H\}$ NMR shifts for phosphines and phosphine-boranes 61
3.3 Crystal data and structure refinement for $[NiCl_2(DIPPF)]$. 69
3.4 Crystal data and structure refinement for *cis*-$[PdCl_2(DIPPF)]$. 74
3.5 Crystal data and structure refinement for *cis*-$[PdCl_2(IPPFA)]$. 78
3.6 Heck coupling of aryl iodides with methyl acrylate in the presence of ferrocenylphosphines 86
3.7 Comparison of $^{31}P-\{^1H\}$ NMR shifts for phosphines and phosphine oxides 92
3.8 Cross-coupling of aryl halides with arylboronic acids in the presence of metal-phosphine catalysts 94

Chapter 1

Introduction

1.1 Objectives

The objectives of this project comprise the synthesis of a number of ferrocenylamines and ferrocenylphosphines of the types illustrated in Figure 1.1, and the subsequent testing of some ferrocenylphosphines as ligands in homogeneous catalysis.

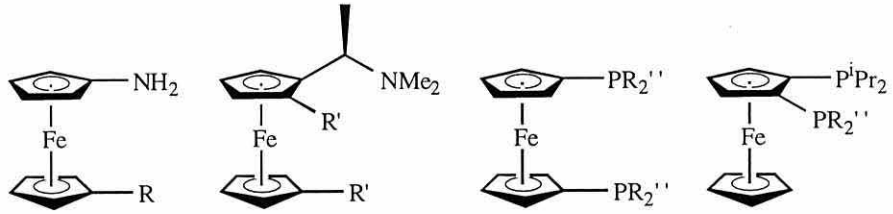

1 R = Br
2 R = CO_2H
3 R = PPh_2
4 R' = Br
5 R' = P^iPr_2
6 R'' = Ph
7 R'' = ^{i}Pr
8 R'' = Ph
9 R'' = ^{i}Pr

Figure 1.1 Target ferrocene derivatives

Ferrocenylamines **1-4** and ferrocenylphosphines **8** and **9** are novel, but the known ferrocenylphosphines **5-7** are also to be prepared in order to compare their efficiency as ligands in cross-coupling catalyses. The following discussion will explain the precedence and reasoning behind the current investigation and outline the relevant synthetic methodologies together with some aspects of the catalyses concerned.

1.2 Ligand Synthesis

The principal roles of an organic or organometallic ligand in homogeneous transition metal catalysis are to homogenise the transition metal and to stabilise the active catalyst. However, the steric and electronic effects of a ligand can strongly influence the efficiency of a catalyst and because these subtle effects are neither general nor entirely predictable, many catalysts are chosen largely by analogy. The designed synthesis of new ligands is currently seeing continued development in response to the ever-increasing demand for more efficient catalysis.

Since the 1970s, ferrocenylamines and ferrocenylphosphines have proved both successful and popular as ligands for homogeneous catalysis. Reported applications of ferrocene ligands include cross-coupling, carbonylation, substitution, polymerisation, hydroformylation, hydrogenation, hydroboration, hydrosilylation and isomerisation catalyses.[3] The fixed yet flexible geometry of ferrocene lends itself to the synthesis of structurally well-defined ligands which retain sufficient freedom to accommodate any spatial modifications required during a catalytic cycle. The reactivity of the compound towards electrophiles facilitates the synthesis of ligands by methods such as Friedel-Crafts substitution or more commonly metallation and in particular lithiation. Meanwhile, the chemical and physical stability of ferrocene contribute to the longevity of the ligands, and the redox-active iron centre introduces the added dimension of electrochemically-controlled catalysis.

Ferrocene ligands, being for the most part bidentate in their co-ordination to a metal, generally fall into one of the following categories:-

- symmetrically 1,1'-disubstituted
- 1,1'-heterodisubstituted
- 1,2-heterodisubstituted

All three classes of ligand can be synthesised by variations on the general method of metallation, and the available protocols for each class will now be discussed together with notable examples of ligands. Other modes of substitution are far less common and are beyond the scope of the current discussion.

1.2.1 1,1'-Disubstituted Ferrocenes

Symmetrically 1,1'-disubstituted ferrocene ligands bearing, for example, diphenylphosphino-,[4] dicyclohexylphosphino-,[5] dibutylphosphino-[6] and dipropylphosphino-[7] donor groups can be generated by the one-pot reaction of 1,1'-dilithioferrocene **10** with commercially available chlorodiorganophosphine reagents. Figure 1.2 (overleaf) illustrates some of the reactions of 1,1'-dilithioferrocene **10**, many of which will be discussed in further detail elsewhere in this chapter.

In addition to phosphines, other donor groups such as sulfides[8] can be introduced directly, while derivatives such as 1,1'-dibromoferrocene **11**[9] and 1,1'-bis(tri-*n*-butylstannyl)ferrocene **12**[10] are used in the synthesis of 1,1'-heterodisubstituted ferrocenes (Chapter 1.2.2). Reaction of **10** with dichloroorganophosphines gives rise to [1]-ferrocenophanes which can be ring-opened to produce symmetrically and asymmetrically substituted ligands (also Chapter 1.2.2).[11-13] Some historically important derivatives such as mercurioferrocenes and ferrocenylboronic acids have been omitted because the use of these compounds as synthons is largely now obsolete as a result of the introduction of more convenient methodologies.

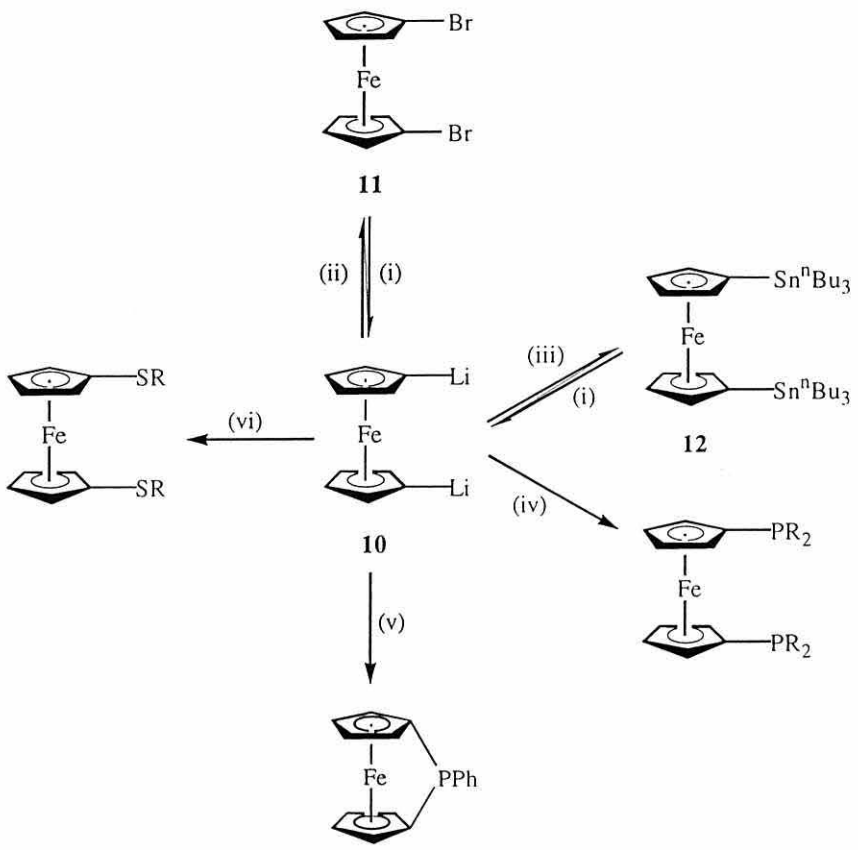

Figure 1.2 Reactions of 1,1'-dilithioferrocene **10**: (i) ^{n}BuLi; (ii) $BrCF_2CF_2Br$; (iii) $ClSn^nBu_3$; (iv) $ClPR_2$; (v) Cl_2PR; (vi) R_2S_2 (R = alkyl, aryl, etc)

The reaction of ferrocene with *n*-butyllithium is accelerated by the addition of *N,N,N',N'*-tetramethylethane-1,2-diamine (TMEDA) **13** which forms an insoluble 1:1 complex with 1,1'-dilithioferrocene, thereby shifting the equilibrium in favour of double deprotonation. Complete dilithiation is achieved in *n*-hexane at room temperature over 18h. A crystal of the complex formed by 1,1'-dilithioferrocene with TMEDA has been studied by X-ray crystallography and has been shown to contain a number of different adducts with both TMEDA and the co-ordinating solvent.[14]

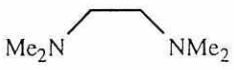

13

1.2.2 1,1'-Heterodisubstituted Ferrocenes

Lithiation of the unsubstituted cyclopentadienyl ring of a substituted ferrocene is disfavoured as a result of the second ring becoming deactivated by the substituent on the first. Monolithiation of ferrocene, while achievable with *tert*-butyllithium, generally returns maximum yields of 70%.[15] A recent report has suggested that monolithiation is in fact optimised by the use of a "superbase" combination of *tert*-butyllithium and potassium *tert*-butoxide.[16]

However, it was also shown recently that stoichiometric lithiation of 1,1'-dibromoferrocene **11** in tetrahydrofuran at -78°C gives almost quantitatively 1-bromo-1'-lithioferrocene **10**, with little or no by-product formation.[9] This method, therefore, provides an efficient route to 1,1'-heterodisubstituted ferrocenes and has been employed in the synthesis of ferrocene analogues of bis(2-diphenylphosphinoethyl)phenylphosphine (TRIPHOS) **14** (Fig. 1.3).[17]

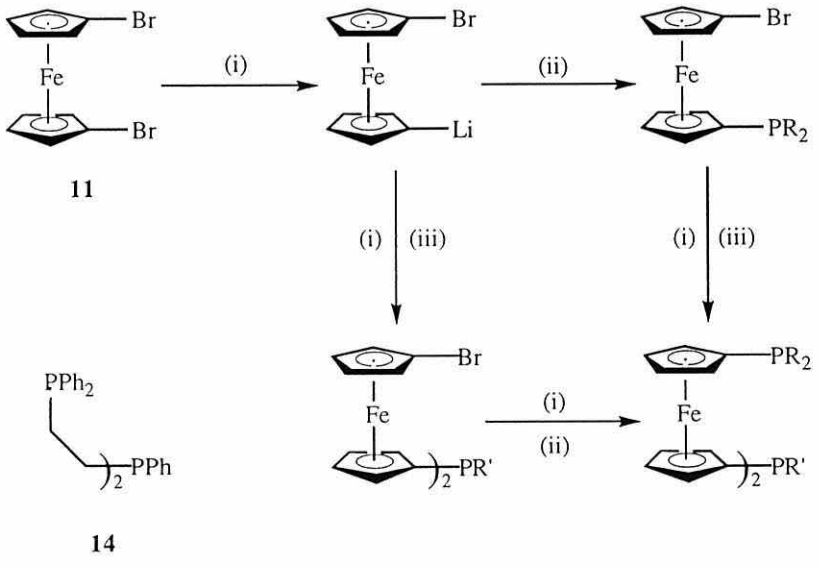

Figure 1.3 Phosphine ligands from 1,1'-dibromoferrocene **1**: (i) ^{n}BuLi; (ii) $ClPR_2$ (R = Ph, ^{i}Pr); (iii) Cl_2PR (R = Ph, ^{i}Pr)

The lithiation of 1,1'-dibromoferrocene **11** mirrors the chemistry of Wright[10] and Kagan,[18] who reported the use of (tri-*n*-butylstannyl)ferrocene as a source of pure lithioferrocene. The tin derivative **12** and its monosubstituted analogue can be separated by distillation and transmetallated independently in high yield with *n*-butyllithium, but the method suffers from the high toxicity of the tin species, especially on large-scale preparation. Quantitative lithiation of bromoferrocene to give pure lithioferrocene was reported as early as 1969.[19]

An alternative method for the preparation of 1,1'-heterodisubstituted ferrocenes is the ring-opening of [1]-ferrocenophanes,[11] particularly applicable in the synthesis of heterosubstituted phosphine ligands.[20,21] Indeed, the ring-opening of phosphorus-bridged [1]-ferrocenophanes has recently provided access to a number of phosphine[22] and mixed amino-phosphine ligands (Fig. 1.4).[23-25] In related work, the ring-opening polymerisation of strained silicon-bridged [1]-ferrocenophanes has seen increasing interest in the field of materials science and has been reviewed by Manners.[26]

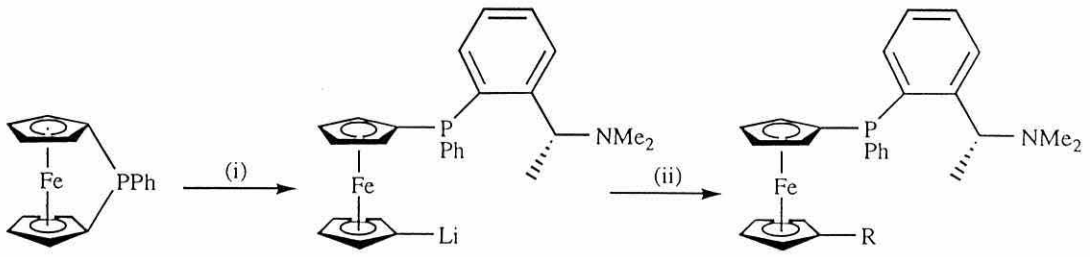

Figure 1.4 Amino-phosphine ligands from [1]-ferrocenophanes: (i) *o*-$LiC_6H_4CH(CH_3)NMe_2$, (ii) R-X (*e.g.* $ClPPh_2$)

1.2.3 1,2-Heterodisubstituted Ferrocenes

Any derivative of ferrocene bearing two or more different substituents on one of its cyclopentadienyl rings possesses planar chirality, which does not undergo racemisation. This chirality has been defined by Schlögl[2] such that a 1,2- or 1,3-heterodisubstituted

ferrocene has (*R*) planar chirality if its substituents decrease in CIP priority[1] in a clockwise direction when viewed from the substituted cyclopentadienyl ring towards the unsubstituted ring and (*S*) if *vice versa*. If a compound possesses both central and planar chirality then the central chirality is described first. Thus, the ligand (*R,S*)-1-diphenylphosphino-2-[(*N,N*-dimethylamino)ethyl]ferrocene (PPFA) **15** possesses (*R*) central chirality in its amine substituent and (*S*) planar chirality in the ferrocene backbone.

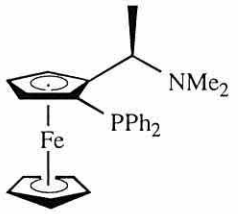

(*R,S*)-**15**

With regard to asymmetric catalysis, it is desirable to have control over the planar chirality, so the requirement for a method for the preparation of 1,2-heterodisubstituted ferrocenes is coupled with the need for a stereocontrolled synthesis. The different methods for achieving this stereocontrolled synthesis have been reviewed recently by Togni[27] and Kagan.[28] By far the most widely used is the employment of a chiral directing group such as the amine substituent of 1-ferrocenyl(*N,N*-dimethyl)ethylamine **16** (Fig. 1.5)[29] which was first resolved and exploited by Ugi *et al.*[30-33]

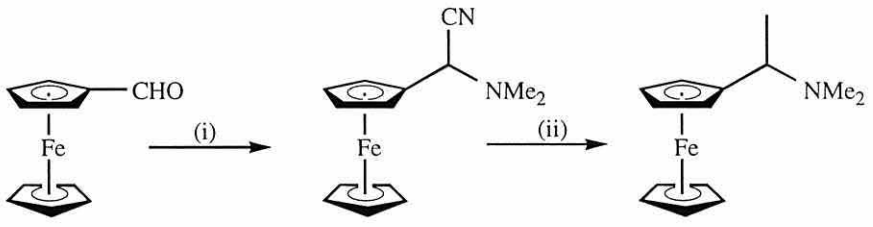

16

Figure 1.5 Synthesis of 1-ferrocenyl(*N,N*-dimethyl)ethylamine **16**: (i) $NaHSO_3$, KCN, $HNMe_2$; (ii) MeMgI

Several alternative methods for the synthesis of 1-ferrocenyl(*N,N*-dimethyl)ethylamine **16** have also been reported[34,35] and most make use of the unusually high stability of the

1-ferrocenylethyl carbocation, which allows for stereoretentive substitution *alpha* to the cyclopentadienyl ring of ferrocene; thus an acyl group at this position is readily displaced by dimethylamine.[30,31] The racemic amine is traditionally resolved by kinetically-controlled crystallisation of its diastereomeric tartrate salts,[32] and the resolved amine has come to be used as the standard chiral ferrocene reagent. The *ortho*-directing effect of the amine substituent confers 92% diastereoselectivity upon metallation with butyllithium[30] and studies using the nuclear Overhauser effect have shown there to be a spatial correlation between the *N,N*-dimethylamino-group and the site of stereoselective lithiation.[36]

Recently there has been an increasing interest in ferrocenyloxazolines.[37-39] The reported synthesis (Fig. 1.6)[39] incorporates an amino alcohol which, being the reduction product of an amino acid, is already a single enantiomer. Thus, the advantage of this methodology is the removal of the necessity to resolve the product ferrocene derivative. As a result of synthetic studies involving constrained oxazolines, it has been shown that it is the nitrogen and not the oxygen of the heterocycle which is responsible for the *ortho*-directing effect.[40]

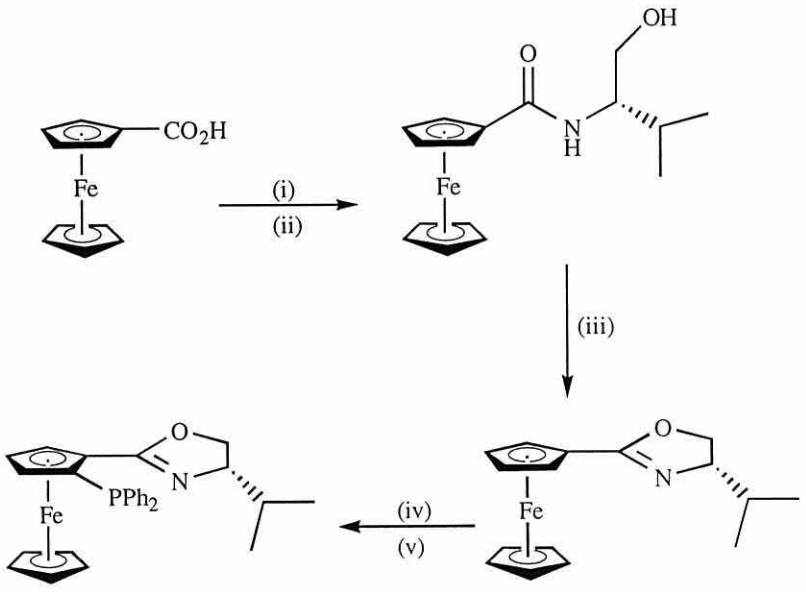

Figure 1.6 Synthesis of ferrocenyloxazoline ligands: (i) $(COCl)_2$, pyridine, (ii) L-valinol, pyridine, (iii) PPh_3, CCl_4, (iv) ^nBuLi, (vi) $ClPPh_2$

Ferrocenyloxazolines, however, are not without their disadvantages: commercially available amino alcohols are expensive and the oxazoline synthesis is not as straightforward as that of 1-ferrocenyl(*N,N*-dimethyl)ethylamine **16**. Also, since oxazolines are merely protected carboxylic acids, the scope of these ligands in terms of tolerating a range of reaction conditions is perceivably limited.

More recently, Kagan *et al.*[41] reported the use of removable chiral sulfoxides in the synthesis of enantiopure 1,2-heterodisubstituted ferrocenes, extending previous work which used sulfoxides as directing groups.[42] This method was used to generate the first example of a chiral 1,2-diphosphinoferrocene, *viz.* 1-(dicyclohexylphosphino)-2-(diphenylphosphino)ferrocene **17**, in which the chirality arises solely from the planar chirality of the ferrocene (Fig. 1.7).

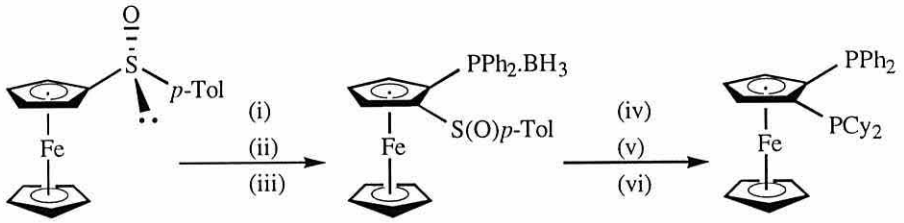

17

Figure 1.7 Chiral sulfoxides in the synthesis of chiral ferrocene ligands: (i) LDA, (ii) $ClPPh_2$, (iii), BH_3.THF, (iv), ^tBuLi, (v) $ClPCy_2$, (vi) $HNEt_2$

Other notable methods for the stereoselective synthesis of 1,2-heterodisubstituted ferrocenes have included the use of chiral auxiliaries such as *N,N,N',N'*-tetramethyl-cyclohexadiamine,[43] proline[44] and spartiene,[45] and the use of chiral protecting groups such as acetals.[46]

1.3 Representative Ligands

The diversity of available methods for the substitution of ferrocene outlined above has allowed for the production of a wide range of ligands bearing phosphorus, nitrogen, sulfur and oxygen donor groups. Historically, however, it is possible to highlight a small number of significant prototype ligands from which the more recent ligands have been developed, using advanced synthetic methodologies. There is invariably a considerable time interval between the reporting of a new ligand and the application of that ligand in an organic synthesis and as a result prototype ligands tend also to become archetypal.

1.3.1 Ferrocenylamines

The most notable of ferrocenylamines is the aforementioned 1-ferrocenyl(*N,N*-dimethyl)ethylamine **16** which has been used to create a large number of chiral ferrocene ligands. The ligand 1,1'-bis(diphenylphosphino)-2-[(*N,N*-dimethylamino)ethyl]ferrocene (BPPFA) **18** first synthesised by Kumada *et al.*,[47] has found great success in asymmetric cross-coupling reactions.[48] Although many chiral phosphines achieve high selectivity, BPPFA and its analogues have a number of advantages: they have planar chirality, they have exchangeable functional groups *alpha* to the ferrocene and, like most ferrocene derivatives, their distinctive orange colour facilitates purification by chromatographic methods. Furthermore, both the mono- and diphosphines **18** and **15** can be generated from the same chiral precursor **16** (Fig. 1.8, overleaf).

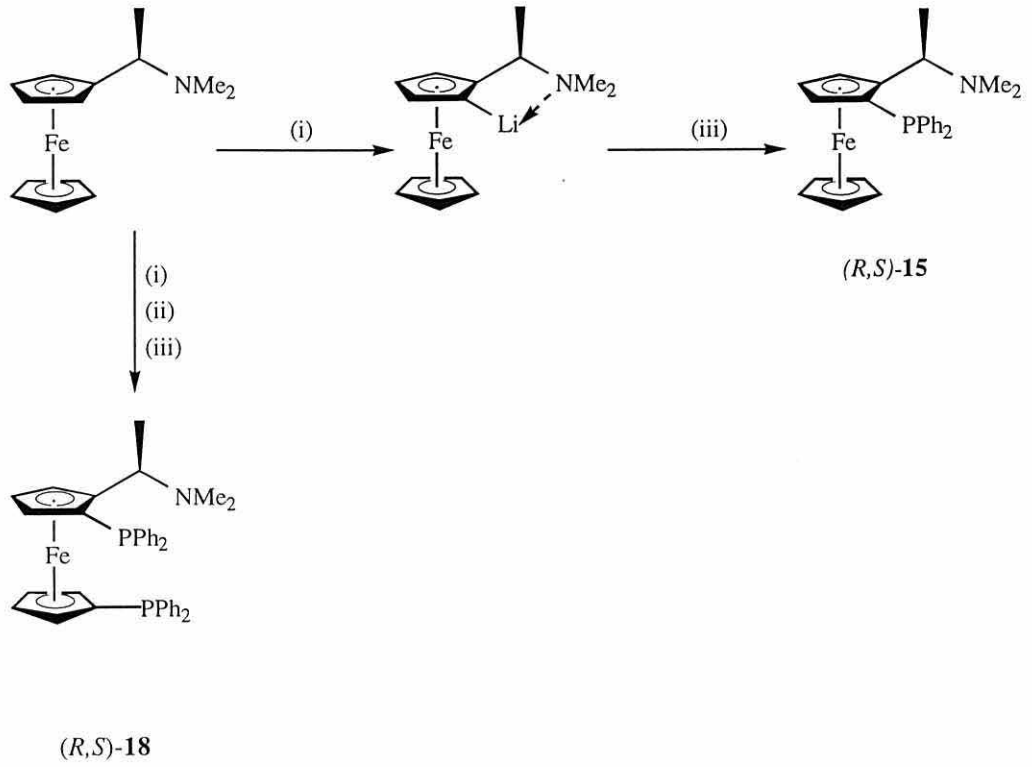

Figure 1.8 Synthesis of chiral ferrocenylamine ligands: (i) ^{n}BuLi, (ii) ^{n}BuLi/TMEDA, (iii) $ClPPh_2$

A wide variety of chiral, bidentate phosphorus-nitrogen and diphosphine ligands have been produced as a result of the ease of substitution of the dimethylamino-group of BPPFA **18**. The group can be displaced by an acyl group in the presence of acetic anhydride or methylated with methyl iodide, then substituted with complete retention of stereochemistry by virtually any other amine.[49] Thus, the major advantage of ferrocenylamine ligands over their purely phosphine counterparts is the secondary interaction resulting from the amine substituent or side chain. While the phosphine groups chelate to the transition metal, the side chain has been shown to enhance enantioface differentiation and so enhance the enantiomeric excess in the products of, for example, the cross-coupling catalysis (Chapter 1.4.2). The functional group on the side chain is directed spatially towards the reaction site of the catalyst and can, therefore, interact electrostatically and sterically with the functional groups in the substrate.

PPFA **15** forms a number of useful transition metal complexes, including the palladium (II) complex *cis*-$[PdCl_2(PPFA)]$.[50] The single crystal X-ray structure of this complex

(as its $CDCl_3$ solvate) shows that both the phosphorus and the nitrogen chelate to the metal, producing a red, slightly distorted square-planar complex with a large bite angle P-Pd-N of 96.1° and a small Cl-Pd-Cl angle of 86.4°. BPPFA **18**, on the other hand, chelates to palladium (II) only through its phosphines, also forming a distorted square-planar complex with a bite angle of 98.8° and a Cl-Pd-Cl angle of 87.8°, thus the amine substituent is pendent and capable of partaking in secondary interactions during catalysis.[51]

1.3.2 Ferrocenylphosphines

Of the many reported ferrocenylphosphine ligands, the most widely used is 1,1'-bis(diphenylphosphino)ferrocene (DPPF) **6**, which is prepared by the dilithiation methodology outlined above.[4]

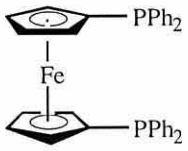

6

The ligand readily forms complexes with a wide range of transition metals, the most significant being the Group 10 metals, palladium and nickel. *cis*-[$PdCl_2$(DPPF)] has proven to be a highly efficient catalyst precursor for organomagnesium cross-couplings and indeed in a wide range of other catalyses. The reasons for its exceptional behaviour have been attributed in part to the large bite angle (99.1°) of DPPF compared to other bidentate phosphines and the consequently small Cl-Pd-Cl bond angle (87.8°), which facilitate the reductive elimination in the final step of the cross-coupling catalytic cycle (*vide infra*).[52]

cis-[$PdCl_2$(DPPF)] is a square-planar, red complex, with a co-ordination shift (*i.e.* the difference between the chemical shift of the complex and that of the free ligand) of Δ =

51.2ppm in the ^{31}P NMR spectrum.[52] The nickel analogue [$NiCl_2$(DPPF)] is tetrahedral, green and paramagnetic, and possesses a bite angle of 105°.[6] The reason for the difference between the palladium and nickel complexes has been attributed to the large steric bulk of the DPPF ligand, which forces the nickel to adopt its high-spin tetrahedral geometry instead of the low-spin, diamagnetic, planar geometry. *cis*-[$PtCl_2$(DPPF)] is structurally similar to its palladium counterpart, being square-planar, but exhibits a smaller co-ordination shift of Δ = 30.3ppm.[53] The co-ordination shift is dependent upon the metal, its co-ordination geometry and its auxiliary ligands, the former having the greatest effect in this case, but the latter two also being of importance in the elucidation of catalysis mechanisms.

By no means as popular as its diphenylphosphino-analogue, the ligand 1,1'-bis(diisopropylphosphino)ferrocene (DIPPF) **7** nonetheless represents an important electron-rich ligand.

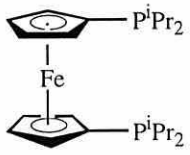

7

The synthesis of the ligand was first reported in 1985,[7] but recognition of the difference in electronic and configurational properties did not appear until very recently. Part of the reason for the lack of interest in the ligand can be attributed to the universal success of DPPF **6**. However, DIPPF **7** can be oily at room temperature and the effective synthesis requires chromatographic purification: such problems do not arise with DPPF. A number of complexes of the ligand have been reported, including those of the Group 9 metals iridium and rhodium. In a complexation study Chaloner *et al.*[54] showed that both the [Ir(COD)(DIPPF)]$^+$[PF_6]$^-$ and [Rh(NBD)(DIPPF)]$^+$[BF_4]$^-$ complexes have a distorted square-planar geometry, the distortion arising from a twist in the ferrocene backbone. The authors also showed that DIPPF **7** is highly labile and can be displaced from the rhodium complex by reaction with other bidentate diphosphines.

Ferrocenylphosphine ligands, being electron-rich, are generally air-sensitive to some extent, especially when in solution. They are usually stored under an inert atmosphere to prevent oxidation to the phosphine oxide, this oxidation being facilitated by the redox-active iron centre. Indeed, oxidation in solution under aerobic conditions can be rapid and practically irreversible on account of the ferrocene-ferrocenium redox equilibrium and very few truly air-stable ferrocenylphosphines are known; those which have been reported typically have an alkyl spacer between the phosphine and the ferrocene.[55] In order to be of use as ligands, phosphine oxides must first be reduced back to their respective phosphines. This commonly involves reaction with, for example, lithium aluminium hydride, which is an inconvenient method since $LiAlH_4$ is both air- and moisture-sensitive and is often used in excess to effect complete reaction. Other more convenient reagents which effect the same reduction are trichlorosilane[56] and alane.[57]

Phosphine-boranes,[58] the adducts of phosphines with borane, which are air-stable, readily crystallised, easily manipulated and can be purified by chromatography, have received much interest recently as a means of preventing phosphine oxidation.[59] The conventional synthesis of phosphine-boranes is by direct reaction of the phosphine with borane, usually as its dimethylsulfide[60] or tetrahydrofuran adduct.[61] Thus, the borane adduct of a ferrocenylphosphine was used recently in conjunction with sulfoxides (Fig. 1.7 and Fig. 1.9).[41]

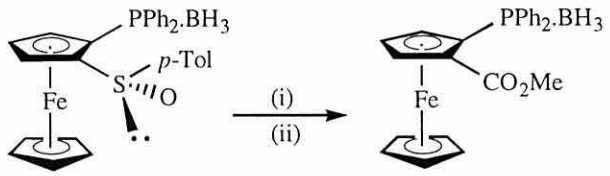

Figure 1.9 Phosphine protection to prevent oxidation: (i) 'BuLi, (ii) $ClCO_2Me$

Borane-protected ferrocenylphosphines such as **19** (overleaf) have also been synthesised in one-pot reactions from 1,1'-dilithioferrocene **10** using borane-protected chloroorganophosphine reagents.[62]

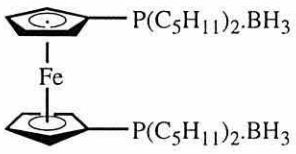

19

Other high-yielding syntheses of phosphine-boranes include the reaction of a phosphine with sodium borohydride and iodine,[63] or the treatment of a phosphine oxide with a mixture of lithium aluminium hydride, sodium borohydride and cerium (III) chloride.[64] The protected phosphine can be then deprotected using a secondary amine such as diethylamine[64] and 1,4-diazabicyclo[2.2.2]octane (Dabco®)[65] or an acid such as boron trifluoride-methanol complex[58] and in all cases the deprotection is much more convenient than a $LiAlH_4$ reduction.

1.4 Applications in Cross-Coupling Catalysis

The applications of ferrocene ligands in catalysis are manifold and have been the subject of much review.[3] One of the widest applications has been in the catalytic cross-coupling reaction of organic electrophiles (*e.g.* organic halides R-X) and organic nucleophiles (*e.g.* organometallic reagents R'-M) (Fig. 1.10).

$$\text{R-X} + \text{R'-M} \xrightarrow{[\text{cat.}]} \text{R-R'} + \text{MX}$$

Figure 1.10 Catalytic cross-coupling: M = metal, *e.g.* magnesium

As a means of carbon-carbon and carbon-heteroelement bond formation, cross-coupling has largely supplanted many of the traditional, purely organic methodologies. Early coupling reactions were achieved in the presence of simple metal salts [for example, cobalt (II) chloride in the formation of biaryls],[66] then in 1971 the cross-coupling of a Grignard reagent was reported to be catalysed by iron (III).[67]

A significant advance, however, followed in 1972 when Kumada *et al.*[68] and Corriu and Masse[69] independently demonstrated efficient catalysis using nickel complexes. Simple salts and complexes of palladium were shown by Heck *et al.*,[70] also in the early 1970s, to catalyse the coupling of aryl and vinyl halides with alkenes, and in 1975 Murahashi *et al.*[71] demonstrated the application of palladium in the cross-coupling of organolithium and organomagnesium reagents. The Group 10 metals thenceforth formed the basis of most cross-coupling catalysts.

The rapid development of the cross-coupling reaction over the ensuing two decades allowed for the efficient coupling of a wide variety of substrates. Nickel and palladium catalysts, generally bearing phosphine ligands and often bearing ferrocenylphosphine ligands, have been shown to be effective in the cross-coupling of organic electrophiles

with organoboron and -silicon compounds and organometallic compounds of zinc, mercury, copper, aluminium, zirconium and tin.[72]

1.4.1 The Heck Reaction

The term *cross-coupling* has been used to describe the coupling of virtually any type of organic R and R', including[73] that of aryl or vinyl halides or triflates with alkenes, a coupling which has come to be known as the Heck reaction (Fig. 1.11). As the only known one-step method for accomplishing such a coupling, the Heck reaction is now invaluable in organic synthesis.

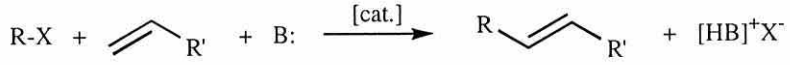

Figure 1.11 The Heck reaction: R = aryl, vinyl; B = base; X = OTf, I, Br, Cl

The reaction was developed by Heck[70] in parallel with similar work by other groups.[74,75] It has become the standard method for the formation of styrene derivatives and polyenes[76] and since it is regioselective, it is finding increasing use in the synthesis of natural products.[77] Many types of alkene are capable of Heck coupling, including the simple alkenes, electron-deficient alkenes such as acrylates and conjugated polyenes and electron-rich alkenes such as enol ethers and enamides, all of which have been reviewed recently by Soderberg.[72]

The Heck reaction is widely accepted to be catalysed by a nucleophilic d^{10} palladium (0) species. Palladium (II) acetate is a common precursor for palladium (0) complexes because its acetate ligands are labile and readily removed by a reducing agent.[78] The reduction requires the presence of several equivalents of a hindered base such as tri-*n*-butyl- or triethylamine and typically two or more equivalents of a triarylphosphine. In addition to its reductive properties, the phosphine also provides catalyst stabilisation,

however, in the coupling of aryl iodides the presence of phosphine ligands can lead to inhibition of the reaction by removal of the aryl iodide from the reaction mixture as a quaternary phosphonium iodide. Under such conditions palladium metal is often precipitated as the catalyst decomposes (Fig. 1.12).[79]

$$[Pd^0(PPh_3)_2] + 2\,Ar\text{-}I \longrightarrow Pd^0 + 2(Ph_3PAr)^+I^-$$

Figure 1.12 Catalyst decomposition in the presence of phosphine ligands

Typically, the reaction conditions for the Heck coupling involve refluxing a mixture of alkene, aryl halide, phosphine and base with a catalytic amount of palladium (II) acetate in acetonitrile. There have been many modifications to the reaction conditions in order to overcome the limitations of unstable catalysts and the inertness of some aryl halides, notably the chlorides, towards reaction. The coupling can be achieved under milder conditions, proceeding at room temperature in the presence of tetra-*n*-butylammonium chloride using a water-soluble base such as a carbonate in dimethylformamide solution.[80] It is believed that halide ions act so as to stabilise the palladium (0) complexes during these catalytic reactions, and so affect the activity of the catalyst.[73] The tetra-*n*-butylammonium chloride, therefore, provides a high concentration of soluble halide in the phase-transfer reaction mixture. Tri(*o*-tolyl)phosphine **20** is more hindered than the traditional triphenylphosphine and so is more reluctant to form phosphonium iodides and can reduce unwanted isomerisation.[79]

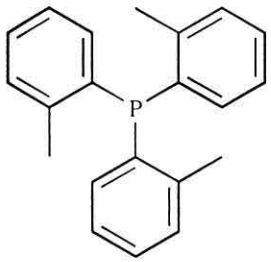

20

Tri(*o*-tolyl)phosphine **20** also forms the basis of an alternative type of catalyst, the palladacycle (Fig. 1.13).

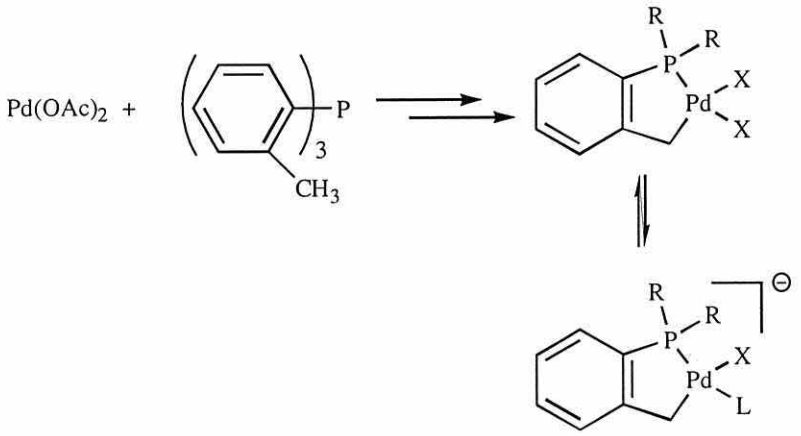

Figure 1.13 Generation of palladacycles: R = *o*-tolyl, X = Cl, Br, L = DMSO, DMF, CH_3CN

Recent work by Herrmann *et al.*[81] has shown that palladacycles present several advantages over their chelate counterparts by virtue of their well-defined structure and stability. Firstly, they are much more thermally stable than palladium-phosphine chelate complexes and as a result have a longer lifetime both in the solid state and in solution; furthermore, this increased stability does not adversely affect their catalytic activity. Secondly, since the ratio of phosphine to palladium is 1:1, there is no excess phosphine available to compromise the reaction by phosphonium formation. Thirdly, palladacycles give rise to higher turnover rates and avoid the formation of by-products caused by phosphorus-carbon (aryl) bond cleavage, a common problem with the conventional catalyst mixture. Finally, and perhaps most significantly, the greater efficiency of palladacycles means that they can be used to activate aryl chlorides, so overcoming one of the greatest limitations of the Heck reaction.

Bidentate phosphines have provided another alternative to the traditional triphenylphosphine ligand. It was shown recently that a series of bis(diisopropyl)-phosphine ligands used in conjunction with palladium (II) acetate enable the coupling of aryl chlorides.[82] The bidentate feature is believed to promote the catalysis by a chelate effect, with the possibility of one phosphine group dissociating during the catalytic cycle to open up a co-ordination site: in this respect 1,4-bis(diisopropylphosphino)butane

(DIPPB) **21** was found to be optimal for the arylation of styrene with chlorobenzene, as shown in Table 1.1.

LIGAND	UNREACTED Ph-Cl, %	YIELD OF STILBENE, %	
		cis	*trans*
DIPPB, 21	**15.6**	**4.4**	**80**
DIPPP	97	0	3
DIPPE	100	0	0
DPPE	83.4	1.6	15
$^{i}Pr_2P^{n}Bu$	85.0	3.0	12
$^{i}Pr_3P$	74.4	1.6	24

Table 1.1 Isopropylphosphines in the catalysis of the Heck reaction

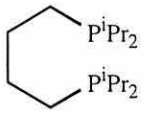

21

The axially chiral bidentate ligand (*R*)-2,2'-bis(diphenylphosphino)-1,1'-binaphthyl [(*R*)-BINAP] **22**, has been used recently to effect an intermolecular asymmetric Heck coupling, that of a dihydrofuran with aryl and alkenyl triflates (Fig. 1.14, overleaf).[83] The asymmetric induction was shown to be the result of a kinetic resolution during the catalytic cycle.[84]

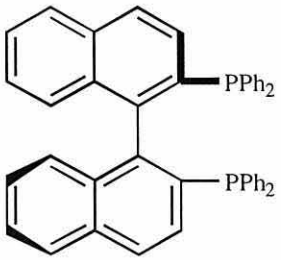

22

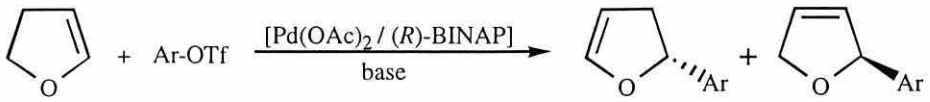

Figure 1.14 Intermolecular asymmetric Heck reaction: Ar = Ph, 4-ClC_6H_4, 3-ClC_6H_4, 2-ClC_6H_4, 4-AcC_6H_4, 4-NCC_6H_4, 4-$MeOC_6H_4$, 2-naphthyl

The same ligand has also been used to effect intramolecular asymmetric Heck coupling with the cyclisation of alkenyl iodides in the synthesis of *cis*-decalins, important chiral synthons for biologically active compounds (Fig. 1.15).[85]

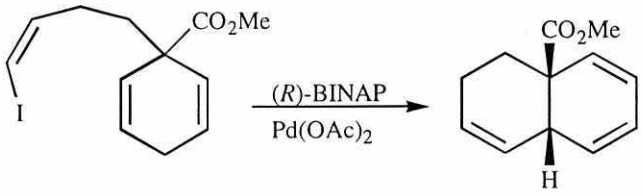

Figure 1.15 Intramolecular asymmetric Heck reaction

The advantage of the ferrocenylphosphine DPPF **6** over other bidentate phosphine ligands in the Heck reaction has been demonstrated by Cabri *et al.*[86] *n*-Butyl vinyl ether was regioselectively arylated by palladium complexes of DPPF in higher yield than was achieved using a range of other phosphines and diphosphines (Table 1.2; Fig. 1.16, both overleaf). The observed preferential formation of the α-substituted product suggested that the phosphine does not dissociate from the palladium active catalyst; instead a cationic intermediate is thought to be formed which polarises the alkene and reduces the likelihood of β-substitution (*vide infra*).

PHOSPHINE	L/Pd	TRIFLATE/ Pd	YIELD %
DPPF, 6	**2**	**50**	**73**
DPPF	2	100	72
DPPF	2	200	70
DPPF	1	50	13
DPPB	2	50	24
DPPP	2	50	10
DPPE	2	50	trace
PPh_3	3	50	15

Table 1.2 $Pd(OAc)_2$-phosphine catalysed Heck reaction of *n*-butyl vinyl ether and 1-naphthyl triflate

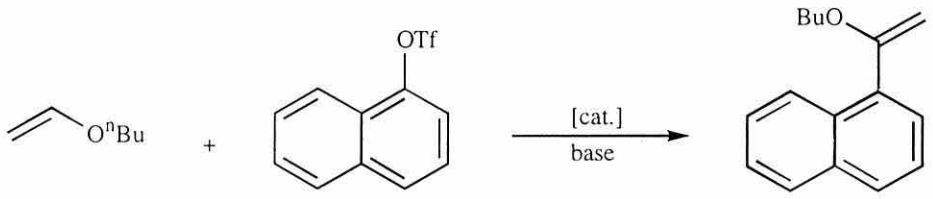

Figure 1.16 Heck coupling of *n*-butyl vinyl ether and 1-naphthyl triflate

The mechanism of the Heck reaction has not been unequivocally determined, but many texts and studies on the subject describe a sequence of observed events believed to constitute the catalytic cycle.[87] Since the traditional palladium (II) acetate, triphenylphosphine and triethylamine mixture has been the most widely studied, the following discussion also assumes these reaction conditions, although in principle palladium-ferrocenylphosphine complexes should produce a similar catalytic cycle.

As indicated above, it is believed that a palladium (0) active catalyst is formed by reduction of the palladium (II) precursor in the presence of a base. Ignoring solvent co-ordination, this catalyst has the formula $[Pd^0(PPh_3)_2]$. The formation of this species has been studied in some depth and has been shown to involve water, phosphine and triethylamine, according to the following equation (overleaf):-[88]

$$[Pd^{II}(OAc)_2] + H_2O + nPPh_3 + 2NEt_3 \rightarrow [Pd^0(PPh_3)_{n-1}] + O{=}PPh_3 + 2Et_3N.HOAc$$

The result of adding an aryl halide to the active catalyst is oxidative addition of the substrate, generating $[Pd^{II}(Ar)X(PPh_3)_2]$. The alkene co-ordinates to this species and subsequently undergoes a migratory insertion into the aryl-palladium bond. The regiochemistry of this intramolecular insertion is determined on steric grounds so as to place the aryl and alkene moieties R and R' *trans* to one another with respect to the alkene double bond. There are several possible mechanistic pathways by which the insertion can occur (Fig. 1.17, overleaf).

The first (**A**) involves the direct co-ordination of the alkene to give a five co-ordinate, 18-electron palladium (II) species. A second possibility (**B**) is that dissociation of the halide opens up a co-ordination site for the alkene, giving a halide salt of the alkenyl-palladium complex, while a third possibility (**C**) is that dissociation of a phosphine ligand allows for the alkene co-ordination.

Route (**A**), while unlikely for palladium (II) on geometrical grounds, offers the further possibility of a hydride abstraction to yield an octahedral palladium (IV) intermediate. Although only a few organo-palladium (IV) species have been isolated[89] due to their documented instability, such an intermediate would certainly be highly reactive and its instability would favour its ephemeral role in the cycle. Route (**B**) is thought to explain the high regioselectivity involved in the insertion, since the polarisation of the alkene which controls the reactivity of the α-carbon site towards co-ordination would be enhanced by the ionisation of the complex. Route (**C**) is perhaps the most conventional pathway, and it undoubtedly explains the success of the highly labile triphenylphosphine ligand in the reaction.

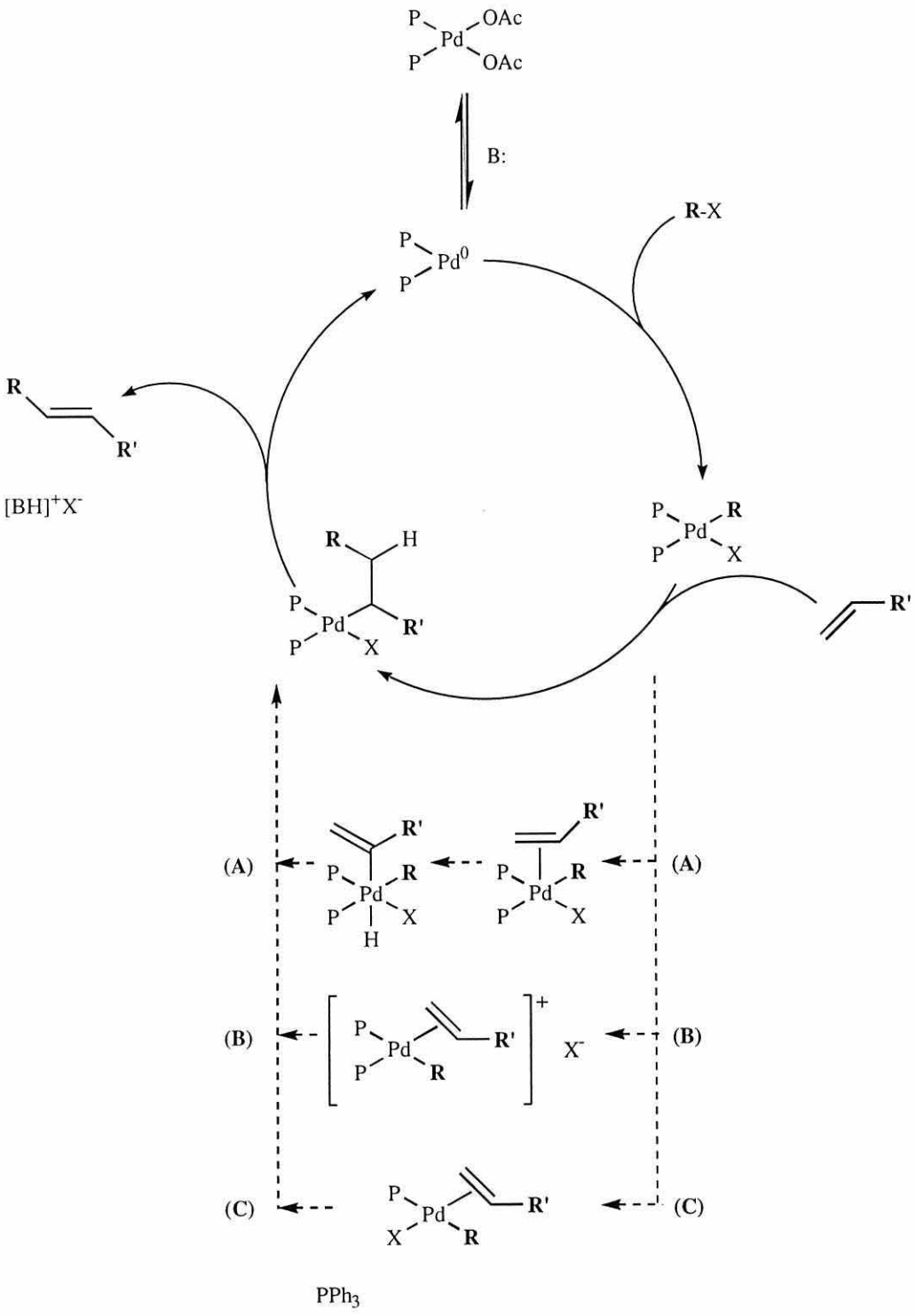

Figure 1.17 Possible insertion mechanisms in the catalytic Heck reaction: P = PPh_3, B = base

The precise reaction mechanism of the insertion is not satisfactorily described by any one of these possible explanations, but is likely to combine some of the rudiments of all three. Moreover, for numerous specific examples in the literature, the catalytic cycle is claimed with great confidence to follow one or other mechanism and can, therefore, be concluded to be highly dependent upon the case under consideration.

In the next step in the cycle, however, the aryl-alkene coupled product is liberated by β-hydride elimination. The palladium (II) is left with hydride and halide ligands which are removed by the base to complete the cycle and return the palladium (0) active catalyst. The limiting factors of the whole process are the relative reactivities of the reactant and product alkenes and the strength of the carbon-halide bond in the starting material, bromides being optimal. The product alkene must be sufficiently deactivated with respect to reaction with the catalyst so that it does not compete with the co-ordination of the reactant alkene. The flexibility of route (**A**) offers the possibility of high selectivity, since it enjoys the retention of a number of labile groups. The square-planar geometry about the palladium in routes (**B**) and (**C**) again determines the stereochemistry and in this case the configuration about the metal is retained: both the addition and the elimination of the coupled fragments are *cis*.

As one of the most widely used palladium-catalysed reactions, the Heck coupling has received much attention, and many applications of the reaction have been reported. The compatibility with functional groups is unusually high, so that in addition to a host of standard halide-alkene couplings having been demonstrated, many more complex systems have also been studied. Although more advanced catalytic systems such as palladacycles are capable of efficiently coupling aryl chlorides, there is still a need for further research in this area: at current prices chlorobenzene is less than half the price of bromobenzene.[90] With regard to ferrocenylphosphine ligands, it is clear from the above considerations that electron-rich alkylphosphine ligands such as DIPPB **21** are more efficient than their arylphosphine counterparts and there is, therefore, good precedence for the application of the isopropylphosphinoferrocenes **5** and **7** in Heck-type reactions.

1.4.2 Organomagnesium Cross-Coupling

The catalytic cross-coupling (Fig. 1.18) of organomagnesium (Grignard) reagents R'MgX with organic halides or triflates or with allylic alcohols R-X remains the most extensively studied of cross-coupling reactions.

$$R\text{-}X + R'MgX \xrightarrow{[cat.]} R\text{-}R' + MgX_2$$

Figure 1.18 Catalytic Grignard cross-coupling

The catalytic Grignard cross-coupling reaction has been applied to alkyl, alkenyl, alkynyl, alkenyl-heteroelement, aryl, aryl-heteroelement, heteroaryl, acyl and polyfunctional halide couplings, with various degrees of success and using a wide range of nickel- and palladium-phosphine catalysts, as reviewed recently by Farina.[72]

As described above, bidentate phosphine complexes of nickel and palladium have been used in the cross-coupling reaction since the early 1970s. Kumada *et al.*[68] pioneered the use of bidentate phosphines *in lieu* of unidentate phosphines because they favour a *cis* configuration of the substrate fragments about the central metal catalyst and therefore confer greater selectivity.

Asymmetric Grignard cross-coupling has been studied extensively since its introduction, also in the early 1970s, employing a number of chiral bidentate ligands. Early successes were achieved using 2,3-*O*-isopropylidene-2,3-dihydroxy-1,4-bis(diphenylphosphino)-butane (DIOP) **22**,[91,92] but this ligand was later superseded by a series of chiral ligands based on the aforementioned (*R,S*)-PPFA **15**.[93]

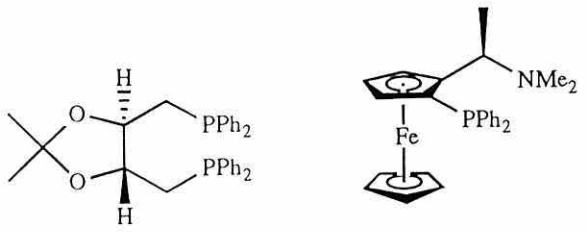

(*R*,*R*)-**22** (*R*,*S*)-**15**

Such ligands have been pivotal in establishing asymmetric methodologies and achieving high enantioselectivity in, for example, the coupling of secondary alkyl Grignards with aryl halides.[93] The asymmetric cross-coupling reaction provides a method for the transformation of a racemic Grignard reagent into an optically active product *via* a kinetic resolution of the Grignard reagent: secondary alkyl Grignard reagents undergo racemisation at a rate similar to that of the cross-coupling (Fig. 1.19), so the product is optically active even if the cross-coupling is quantitative.

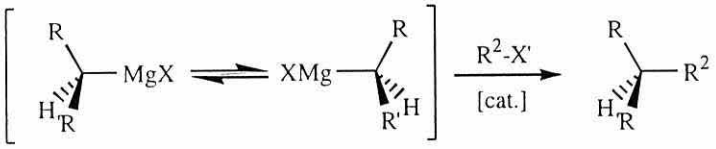

Figure 1.19 Kinetic resolution of secondary alkyl Grignard reagents

The cross-coupling of Grignard reagents using ferrocene ligands began in the late 1970s, with organic bromides[94] and allylic alcohols[95] and the literature covering the many applications of DPPF **6** and BPPFA **18** since then has been reviewed thoroughly.[3] The clear advantage of DPPF over other phosphine ligands in the cross-coupling reaction is illustrated by the work of Hayashi *et al.* (Table 1.3, overleaf).[52] Prior to the introduction of *cis*-[$PdCl_2$(DPPF)] the reaction of secondary alkyl Grignard reagents resulted in considerable isomerisation of the alkyl fragment, yielding isomeric mixtures of cross-coupled products.[96] The effect of DPPF **6** was to allow for such a cross-coupling to proceed without isomerisation by reducing the susceptibility to β-elimination.

CATALYST PRECURSOR	REACTION CONDITIONS		GLC YIELD %		
	TEMP.	TIME, h	*sec*-Bu-Ph	^{n}Bu-Ph	Ph-Br
[$PdCl_2$(DPPF)]	**rt**	**1**	**95**	**0**	**0**
[$Pd(PPh_3)_4$]	rt	24	4	6	31
[$PdCl_2(PPh_3)_2$]	rt	24	5	6	9
[$PdCl_2$(DPPE)]	rt	48	0	0	96
[$PdCl_2$(DPPP)]	reflux	8	4	1	30
[$PdCl_2$(DPPB)]	rt	24	43	19	23
[$NiCl_2(PPh_3)_2$]	rt	8	51	25	1
[$NiCl_2$(DPPP)]	rt	23	3	5	4
[$NiCl_2$(DPPP)]	rt	23	29	3	5

Table 1.3 Cross-coupling reaction of *sec*-butylmagnesium chloride with bromobenzene (in diethyl ether using 1 mol% catalyst precursor)

Table 1.3 shows that *cis*-[$PdCl_2$(DPPF)] returns the highest yield of the required *sec*-butylbenzene, the lowest degree of isomerisation and the highest reaction rate of all the catalyst precursors compared. This superiority was attributed to the large bite angle encouraging reductive elimination of the cross-coupled product (Chapter 1.3.2), and (more tentatively) to the strain resulting from the large bite angle promoting prior ligand dissociation. The contrast between different bidentate ligands can be seen in Table 1.4, which shows a comparison of these parameters and their correlation with the yield in the above reaction.

[$PdCl_2$L] L =	BOND ANGLE, degrees		YIELD OF *sec*-Bu-Ph %
	P-Pd-P	Cl-Pd-Cl	
DPPF, 6	**99.1**	**87.8**	**95**
DPPP	90.6[97]	90.8[97]	43
DPPE	85.8[97]	94.2[97]	0-4

Table 1.4 The effect of bond angles on catalysis

It has been shown that the nature of the Group 10 metal used in conjunction with DPPF **6** in related reactions can make a considerable difference to the regiochemistry of the cross-coupling reaction. Indeed, the difference between the square-planar palladium (II) and tetrahedral nickel (II) catalysts can radically affect the outcome of a reaction, as exemplified by the product distribution in the reaction of two isomeric allylic silyl ethers with aryl Grignard reagents under the effect of each metal catalyst (Fig. 1.20).[98]

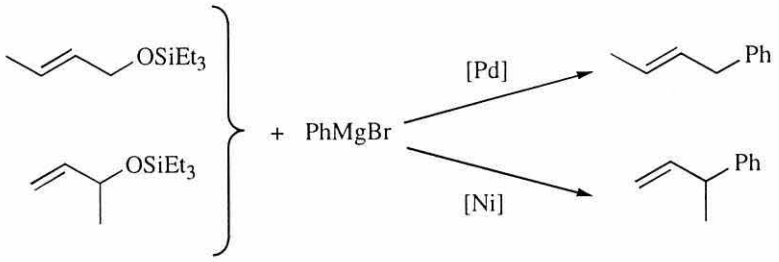

Figure 1.20 The effect of metal choice on cross-coupling catalysis: [Pd] = *cis*-[$PdCl_2$(DPPF)], [Ni] = [$NiCl_2$(DPPF)]

The ligand DIPPF **7** has not been hitherto been employed in cross-coupling catalysis. However, precedence for such an application can be found in the use of the ligand in hydrogenation catalysis in conjunction with rhodium and iridium. The rhodium (I) complex [Rh(COD)(DIPPF)]$^+$OTf$^-$ was used recently by Burk *et al.* [99] in the hydrogenation of aldehydes, ketones, alkenes, imines and *N*-acylhydrazones, with great success; for example, in the hydrogenation of acetophenone to phenylethanol DIPPF produced a twenty-fold increase in yield compared to the analogous DPPF **6** complex under the same conditions (Fig. 1.21).

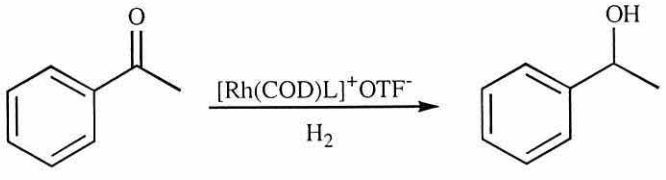

L = **6**, 5%
7, 100%

Figure 1.21 Hydrogenation using rhodium-phosphine complexes

The rationalisation of this result was that electron-rich phosphines are required for efficient hydrogenation catalysis. Metal hydrides of rhodium (I) complexes of DIPPF **7** and some *tert*-butylphosphino-analogues, which represent catalyst precursors for hydrogenation, have previously been prepared and characterised by Cullen *et al.*[100] The extension to cross-coupling catalysis is, therefore, justified on the grounds that both homogeneous hydrogenation and cross-coupling require an initial oxidative addition of the substrate in order to activate that species. The basicity of the ligand is of critical importance, since it must be strong enough to stabilise the active catalyst and yet not be so strong as to compromise the oxidative addition of the substrate.

Catalytic cycles describing the mechanism of the palladium catalysed cross-coupling reaction have been postulated as the result of much spectroscopic and isolated intermediate probing. Nevertheless, due to the instability (and conversely apparent inertness) of many of the proposed intermediates, there still remains some ambiguity. The most widely accepted mechanism (Fig. 1.22, overleaf) assumes again that the active catalyst is a palladium (0) species. Under the Grignard reaction conditions, however, this is formed by the substitution of the halide ligands of a palladium (II) complex such as $[PdCl_2(P\frown P)]$ (where P⁀P is a bidentate phosphine ligand). Figure 1.22 assumes that the Grignard reagent is an alkylmagnesium and the substrate is an aryl halide.

The palladium (II) precursor is reduced either by some co-ordinating solvent or by the Grignard reagent, both of which are present in relative excess. The solvent-substituted complex contains palladium (0) which may partake directly in the cycle, but the complex substituted by Grignard fragments must firstly lose its alkyl substituents by a reductive elimination in order to attain the requisite palladium oxidation state.

The palladium (0) active catalyst then undergoes oxidative addition of the aryl halide which is transmetallated by the nucleophilic Grignard reagent. Reductive elimination gives the desired product and returns the palladium (0) active catalyst. The elimination of the coupled product has been shown by extended Hückel calculations on *cis*-$[Pd(PH_3)_2(CH_3)CH{=}CH_2]$ to be a migration of the Pd-R bond rather than a concerted elimination.[101]

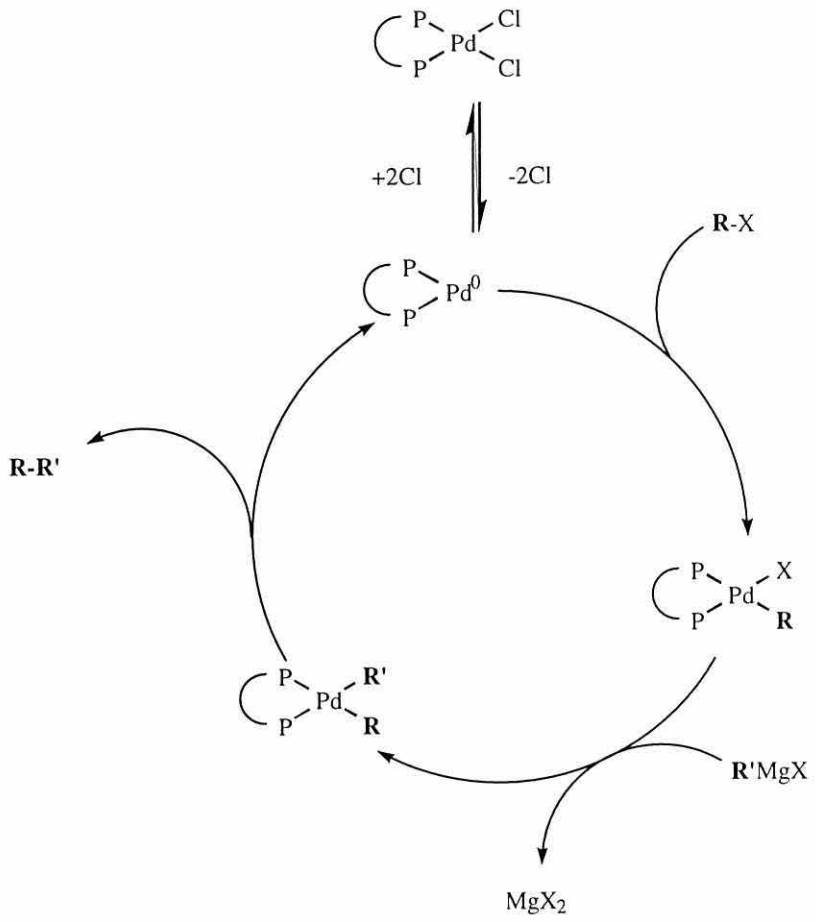

Figure 1.22 Grignard cross-coupling catalytic cycle

This overall mechanism is supported by the isolation of the coupled Grignard fragments R'-R' in certain reactions, but the absence of such a product merely infers a solvent-substituted system and does not preclude a similar catalytic cycle. Many of the active palladium (II) intermediates have been isolated and it has been shown that for bidentate phosphine ligands the rate of reductive elimination increases with increasing bite angle.[102] From a logical point of view, the restriction to palladium (0) and (II) is desirable: from a logistical point of view, the square-planar arrangement about the palladium would force the two coupling fragments (at least in the presence of a bidentate ligand) into the required *cis* geometry.

The palladium (0)/ palladium (II) mechanism is arguably flawed, however, in that the required reductive elimination is theoretically not spontaneous. The palladium-carbon

bond enthalpy is in the order of 200-250 $kJmol^{-1}$ and this increases with increasing *s*-character in the metal-carbon bond such that it is highly unlikely for two saturated alkyl fragments to couple and produce the required elimination.[78] Indeed the outcome of such an event is equally likely to be β-elimination, giving an unstable hydride complex and ultimately isomerisation without coupling of the alkyl components. The same argument can be applied if the Grignard reagent adds before the aryl halide, which is possible if the catalyst and substrate are not pre-mixed, but with the added complication that more than one equivalent of the Grignard reagent (which is present in excess) may undergo oxidative addition and thus impede further reaction (Fig. 1.23).

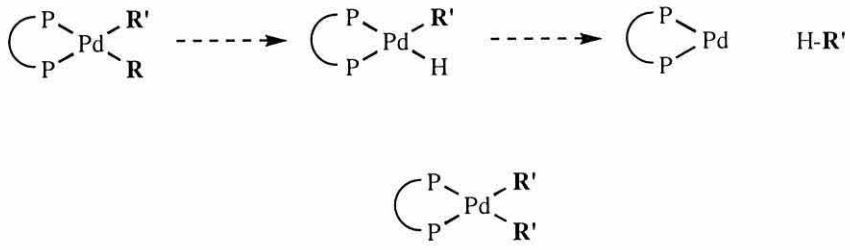

Figure 1.23 Observed terminating species in the Grignard cross-coupling: ABOVE β-elimination
BELOW stable dialkyl complex

The required activation of metal-carbon bonds is usually only possible in the presence of a co-catalyst such as a halide which increases the polarity of the system and competes with the β-hydride elimination by blocking co-ordination sites. Such blocking by oxidative addition also increases the rate of elimination by further increasing the oxidation state of the metal.

An alternative mechanism involves the oxidative addition of the alkyl halide to a palladium (II) active catalyst to produce a palladium (IV) species.[103] The oxidative addition of an alkyl halide to an alkyl-palladium (II) complex has been shown to be solvent-dependent and to exhibit second-order kinetics, consistent with a formal S_N2 mechanism: furthermore, isotopic labelling experiments have also indicated that the intermediate in the reaction is an unstable palladium (IV) species (Fig. 1.24, overleaf).[104]

$$cis\text{-}[PdMe_2(PPh_2Me)_2] + CH_3I \xrightarrow{\text{slow}} [Pd^{IV}] \xrightarrow{\text{fast}} trans\text{-}[PdIMe(PPh_2Me)_2] + Me\text{-}Me$$

$$cis\text{-}[PdMe_2(PPh_2Me)_2] + CD_3I \xrightarrow{\text{slow}} [Pd^{IV}] \xrightarrow{\text{fast}} trans\text{-}[PdIMe(PPh_2Me)_2] + Me\text{-}CD_3$$

Figure 1.24 Evidence for palladium (IV) oxidative addition products

The organo-palladium (IV) intermediate formed by this oxidative addition is then thought to lose the coupled product by reductive elimination (Fig. 1.25). As with the Heck catalytic cycle outlined above, a palladium (IV) intermediate can seem unlikely in view of the instability of organo-palladium (IV) species, but paradoxically an unstable intermediate is more likely to be present in the real catalytic cycle; far from accelerating the rate of a reaction, anything too stable is liable to curtail the process.

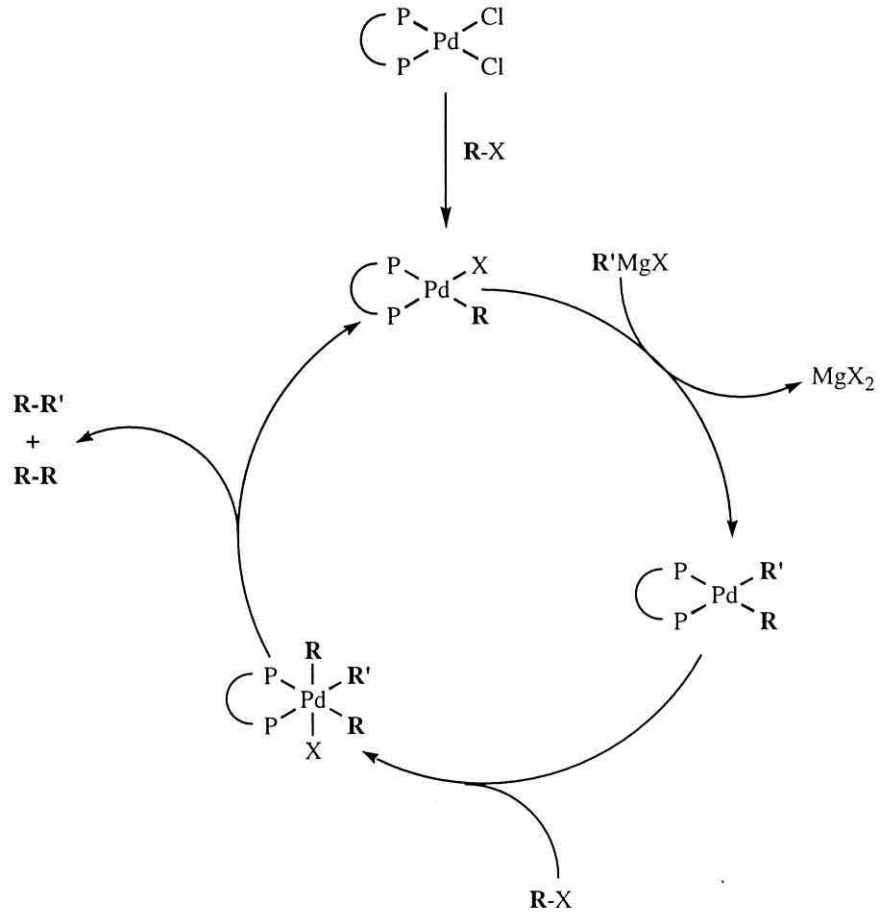

Figure 1.25 Palladium (IV) intermediate in the Grignard cross-coupling

The only criterion by which this mechanism would be governed would be the stereochemistry about the now octahedral palladium, since the coupling components now have the possibility of being *trans* to one another. This potential problem can be averted, however, since the dissociation and isomerisation necessary to attain a *cis* geometry is facilitated by the lower available oxidation state (II) and by the capacity of palladium to adopt a transient square-planar geometry. As would be expected, the evidence for this mechanism includes the formation of some homo-coupled product R-R; it is noteworthy that the homo-coupled fragments in this mechanism originate in the aryl halide and not the Grignard reagent, although this could be more the result of the volatility of the alternative homo-coupled product R'-R'.

Organomagnesium reagents, like their organolithium counterparts, are very reactive species. As a result they are capable of coupling with a wide range of electrophiles and are limited in their application only by their high basicity and nucleophilicity which can preclude the presence of a number of functional groups. On a practical level, the greatest drawback of Grignard coupling is that the Grignard reagent usually has to be prepared freshly from the corresponding alkyl or aryl halide and used *in situ*. This preparation is rarely quantitative and necessitates the employment of inconvenient and often inaccurate titrations in order to determine the concentration of active reagent in the reaction mixture.

Nevertheless, being one of the earliest coupling reactions, the amount of research which has been devoted to the Grignard cross-coupling is substantial. The lack of versatility of organomagnesiums is more than compensated by the reservoir of literature precedents and, in general, this type of research is based on recognition and analogy. Furthermore, the more recently reported coupling reactions such as those of organosilicons, -tins, -borons and -zincs owe much of their mechanistic understanding to analogies drawn from the proposed mechanisms for the Grignard cross-coupling.

Ferrocenylphosphine ligands have been used extensively in the cross-coupling reaction, particularly in the coupling of organomagnesium reagents. The delicate balance between electronic and steric parameters required in order to promote catalysis but restrict

isomerisation means that there is always scope for improvement.

1.4.3 Other Cross-Couplings

DPPF **6** has recently been employed in the nickel catalysed Suzuki-type cross-coupling.[105,106] Coupling of arylboronic acids with aryl chlorides was achieved, a reaction which has previously proved problematic due to the low reactivity of aryl chlorides (Fig. 1.26).[107] The addition of a base such as a phosphate is required due to the reluctance of the oxidative addition product [Pd^{II}(Ar)X(P⌒P)] to undergo direct transmetallation with the boronic acid.[106]

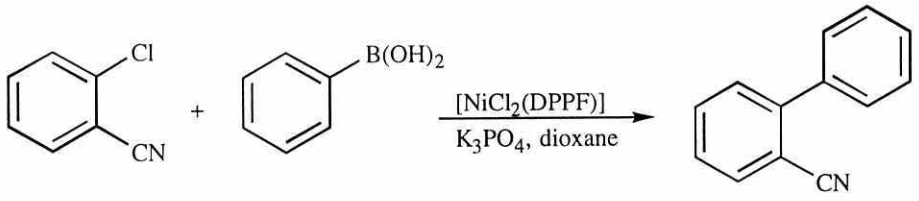

Figure 1.26 Suzuki cross-coupling catalysis using [$NiCl_2$(DPPF)]

The homo-coupling of aryl chlorides has also been reported to proceed in the presence of nickel-phosphine complexes with zinc metal as reductive co-catalyst and it has been suggested that the use of bidentate phosphine ligands might reduce by-product formation.[108]

Although these two examples represent only a fraction of the literature available on cross-couplings other than the Heck and Grignard reactions, they both illustrate a common theme which is that current interest in the cross-coupling reaction is focussed on the activation of aryl chlorides. Given that isopropylphosphines have been used successfully in the activation of aryl chlorides in the Heck reaction,[82] it is clearly of interest to examine the contrast between the isopropylphosphinoferrocene **7** and the phenylphosphinoferrocene **6** in similar reactions.

1.5 Summary

Ferrocene-based ligands are highly versatile and have been applied across a wide range of homogeneous catalyses. The cross-coupling reactions, in particular, have benefited tremendously from the introduction of ferrocenylphosphine complexes. *cis*-[$PdCl_2$(DPPF)] remains one of the most efficient catalyst precursors for the cross-coupling of organomagnesium reagents. New and improved techniques for the preparation of various types of ferrocene ligand are continually being reported. Current interest in asymmetric synthesis and selective lithiation of ferrocene is ongoing, providing an ever-increasing range of alternative methodologies for ligand synthesis. The application of novel ferrocene ligands in homogeneous catalysis, therefore, continues to approach optimal efficiency and industrial viability.

Chapter 2

Aims

2.1 General Aims

As described in Chapter 1.1, the overall aim of the current investigation was to produce a number of novel ferrocenylphosphines and ferrocenylamines. Work in ligand synthesis is ongoing within our research group, in particular the synthesis of ligands based on ferrocenylphosphines,[95] -amines,[23] -pyridines[109] and mixed ligands thereof.[110] The methodologies already employed within the group were, therefore, to be implemented in the preparation of the new ligands.

Additionally, a wide range of ligands produced within the group have not hitherto been tested with regard to their application in homogeneous catalysis, although as outlined in Chapter 1, there is good literature precedence for such a study. In order to test the ligands, however, it was first necessary to prepare suitable transition metal complexes.

The general aims of the project can be divided into three sections:-

- ligand synthesis
- co-ordination chemistry
- catalysis

The choice of transition metal and catalysis are closely related, so the following sections consist of an outline of the target ligands and methodology, and the proposed complexes and test catalyses.

2.2 Target Ligands

Previous work within the research group demonstrated the use of 1,1'-dibromoferrocene **11** in the synthesis of a series of 1,1'-heterosubstituted ferrocenylphosphines (Chapter 1.2.2).[17]

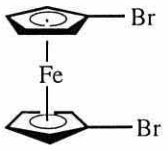

11

It was envisaged that a similar strategy could be adopted for the synthesis of 1,1'-heterosubstituted primary ferrocenylamines (aminoferrocenes), to produce a series of *N*-donor analogues. The target precursor was, therefore, 1-bromo-1'-aminoferrocene **1** which could in principle be used to generate the novel amino acid **2** and the mixed *P,N*-donor ligand **3**.

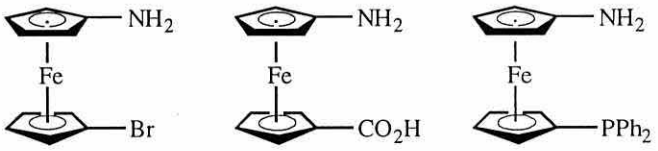

1 **2** **3**

A wide range of ferrocenylamine ligands based on 1-ferrocenyl(*N,N*-dimethyl)ethylamine **16** has been reported (Chapter 1.3.1), but it was hoped that the variety of donor groups on these ligands could be extended by adaptation of the above stepwise methodology for 1,1'-heterodisubstitution, starting from a dibrominated derivative of **16**, compound **4** (overleaf).

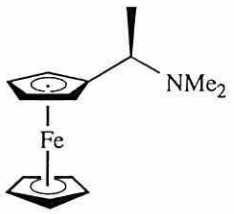

16

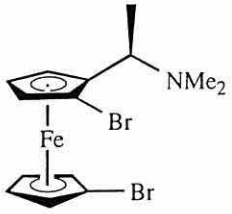

4

The chemistry of 1,1'-bis(diphenylphosphino)ferrocene (DPPF) **6** and 1,1'-bis(diphenylphosphino)-2-[(*N,N*-dimethylamino)ethyl]ferrocene (BPPFA) **18** is well documented and there are many reported applications of the ligands (Chapters 1.3.2-1.4),[3] however, the previously reported isopropylphosphine analogues, **7** and **5** respectively, have seen little application in catalysis. It was of interest, therefore, to prepare both ligands and to investigate the catalytic properties of their Group 10 metal complexes compared to those of the phenylphosphine ligands.

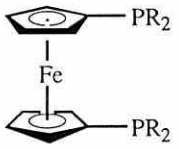

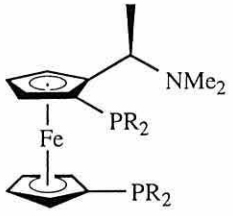

6 R = Ph
7 R = ^{i}Pr

18 R = Ph
5 R = ^{i}Pr

Planar chiral 1,2-substituted ferrocenylphosphines have only recently been reported (Chapter 1.2.3). It was envisaged that the 1,2-analogue of ligand **7**, compound **23**, would be of interest in catalytic studies due to its restricted co-ordination chemistry compared to the 1,1'-substituted ligand.

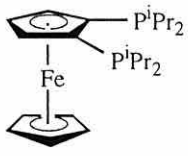

23

2.3 Catalysis

cis-[$PdCl_2$(DPPF)] is well known as a cross-coupling catalyst,[52] so a logical starting point for testing the ligands prepared, and specifically for comparing the phenyl and isopropyl ligands, was to look at the cross-coupling reaction using the palladium (II) chloride complex of the isopropylphosphine ligand **7**. Isopropylphosphines are known to promote catalysis in the Heck reaction[82] and as a bidentate isopropylphosphino-complex, the palladium complex of **7** was expected to be highly effective in this catalysis (Chapter 1.4.1). Cross-coupling can also be achieved with [$NiCl_2$(DPPF)][111] so it was hoped that the corresponding nickel complex of **7** might also provide effective cross-coupling catalysis (Chapter 1.4.2).

2.4 Summary

The target ligands identified in Chapter 1.1 were to be prepared using a number of recently reported synthetic methodologies. Group 10 metal complexes of a series of ferrocenylphosphines were to be tested in their application as catalyst precursors in cross-coupling reactions such as the Heck reaction and organometallic couplings.

Chapter 3

Results and Discussion

3.1 Outline

The results and discussion of the current investigation are described in the order introduced in Chapter 2. A report of the synthesis of ferrocenylamines and ferrocenylphosphines from their respective precursors is followed by a description of the co-ordination chemistry of the Group 10 complexes of DIPPF **7** and preliminary results from catalytic tests in cross-coupling reactions.

3.2 Synthesis

3.2.1 1,1'-Dibromoferrocene

As the precursor for many of the proposed reactions, the first objective was to obtain a sufficient quantity of 1,1'-dibromoferrocene **11**. Although the compound has recently become commercially available,[90] it is much more economically obtained from ferrocene using a modification of the literature procedure[9] which has been in use within our research group for some time and which generally furnishes a higher yield than that reported in the literature (typically > 90% *vs.* 60%[9]). Ferrocene was thus reacted with *n*-butyllithium in the presence of TMEDA **13**, then cooled and treated with 1,2-dibromotetrafluoroethane (Fig. 3.1).

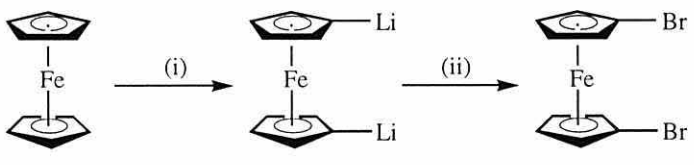

10 **11**

Figure 3.1 Synthesis of 1,1'-dibromoferrocene, **11**: (i) ^{n}BuLi, TMEDA, (ii) $BrF_2C\text{-}CF_2Br$

Work-up consisting of a series of brine and water washes yielded a solution of the product sufficiently pure to be crystallised directly from the dried organic extracts. The product gave satisfactory analytical data and was characterised by NMR and IR spectroscopy and by mass spectrometry. All results were found to be in accordance with the literature [mp 51-52°C (*n*-hexane), lit. 50-51° (ethanol)].[9] In general, the protons of ferrocene derivatives couple to one another in a $^3J_{2,3}$ and $^4J_{2,4}$ manner, but the coupling constants for each are so similar that the signals overlap and produce the pattern of a *pseudo*-triplet in the ^{1}H NMR spectrum. The spectrum of 1,1'-dibromoferrocene **11**, therefore, shows two *pseudo*-triplets at δ = 4.08 and 4.42ppm. The majority of ferrocene derivatives with electron-withdrawing substituents such as the halogens produce downfield α-proton resonances and upfield β-proton resonances, thus the two signals observed for 1,1'-dibromoferrocene correspond respectively to the β- and α-protons.[112] The ^{13}C-{^{1}H} spectrum mirrors this distribution, but for other ferrocene derivatives ^{13}C-{^{1}H} spectroscopy is of limited applicability due to the ferrocene resonances being coincident with those of the solvent $CDCl_3$. In the spectrum of compound **11** the signals range from δ = 69.9 to 78.3ppm and are not masked by the solvent resonance at δ = 77ppm.

3.2.2 1-Bromo-1'-aminoferrocene

The proposed starting material for the heterosubstitution of aminoferrocenes was 1-bromo-1'-aminoferrocene **1**. Synthesis of the compound was investigated using a number of available methods, of which only two gave reasonable yields and only one gave synthetically useful results.

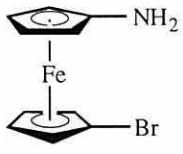

1

The first method involved a Gabriel-type synthesis using 1-bromo-1'-(*N*-phthalimido)-ferrocene **24**, which was prepared in a melt from 1,1'-dibromoferrocene and copper (I) phthalimide in a yield of 28%. *N*-Phthalimidoferrocene has previously been prepared from bromoferrocene using a similar method in the synthesis of aminoferrocene **25**.[113]

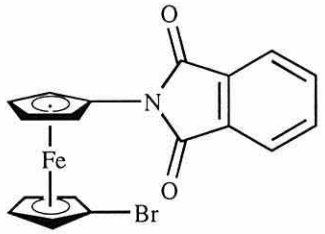

24

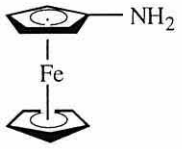

25

Compound **24** was characterised by NMR and IR spectroscopy and by mass spectrometry and gave a satisfactory elemental analysis. The ^{1}H NMR of the product showed a considerable range of chemical shifts for the ferrocene proton resonances, due to the electronegative substituents and in particular the amide functional groups; δ = 4.17ppm for the β-protons on the bromine-substituted cyclopentadienyl ring, while δ = 5.21ppm for those *alpha* to the phthalimido-substituent. Assignment was made by analogy with 1,1'-dibromoferrocene **11** and aminoferrocene **25**.[112] The carbonyl stretching frequency was observed to be 1780cm^{-1}, which is within the range expected.[113] While the product is both air- and light-stable, forming dark red crystals, there was considerable decomposition in the reaction mixture. The resultant low yield of 28% would subsequently be exacerbated by the need for further reaction with ethanolic hydrazine in order to generate the corresponding primary amine **1**.[112]

It was decided instead to examine the synthesis of 1-bromo-1'-aminoferrocene **1** by the monolithiation of 1,1'-dibromoferrocene **11**, followed by reaction with a protected hydroxylamine as a source of electrophilic "$^+NH_2$" (the Kochetkov reaction), according to a similar method reported for the synthesis of aminoferrocene from lithioferrocene.[114] The monolithiated intermediate was thus reacted with *O*-benzylhydroxylamine and produced a yield of 53% (Fig. 3.2, overleaf). The pale yellow crystalline solid **1** obtained may be stored indefinitely at low temperature under an inert atmosphere, however, the

need for a rapid work-up soon became clear, as the product decomposed rapidly in solution under aerobic conditions to a black oil.

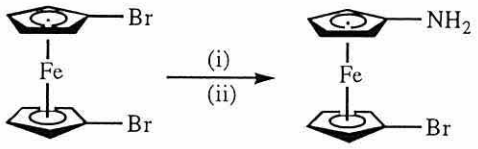

11 **1**

Figure 3.2 Synthesis of 1-bromo-1'-aminoferrocene **1**: (i) ^{n}BuLi, (ii) $BnONH_2$

The relatively high yield in comparison to the corresponding literature preparation of aminoferrocene **25**[114] is the result of the slow addition of a limited amount of the quenching reagent; 0.4 equivalents of *O*-benzylhydroxylamine was found to be optimal. It is assumed that reaction of the aminoferrocene with unreacted lithioferrocene detracted from the yield in the literature preparation.[114] Compound **1** was characterised by NMR spectroscopy and by mass spectrometry and gave satisfactory elemental analysis. Aminoferrocene **25** and its derivatives are unusual in that the protons *alpha* to the substituent produce the highest field resonance; notably, this resonance is further upfield than that of the unsubstituted cyclopentadienyl ring in the parent compound.[112] This can be accounted for by the electronic effect of the amine lone pair being in direct conjugation with the π-system of ferrocene. Furthermore, aminoferrocene possesses a redox potential of -0.37V with respect to ferrocene,[115] a property which explains its readiness to oxidise and, therefore, its air-sensitivity. By analogy with **11** and **25**, the α'-protons of 1-bromo-1'-aminoferrocene **1** produce the signal at δ = 3.94ppm and the amine protons resonate at δ = 2.71ppm.

A small quantity (*ca.* 14%) of the *N*-butyl-substituted amine by-product **26** and an even smaller quantity (6%) of the dibutyl-substituted amine product **27** were also isolated. The primary amine **1**, being more polar than the alkyl-substituted by-products, was separated by chromatography. The trace of 1,1'-diaminoferrocene **28** observed by TLC (having a much lower R_f value than the other products) decomposed during work-up.

All of the compounds were characterised as fully as possible under the limitations of air-sensitivity.

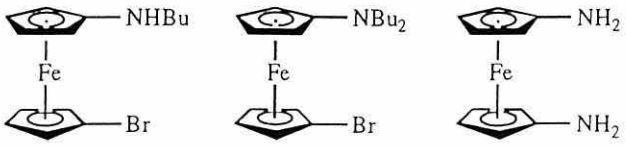

26 27 28

3.2.3 Protection of 1-Bromo-1'-aminoferrocene

In order to further stabilise the precursor 1-bromo-1'-aminoferrocene **1**, it became clear that some form of amine protection was necessary. Several techniques were, therefore, examined. It was found that lithiation of the amine with *n*-butyllithium would lead to removal of both of the $-NH_2$ protons before removal of the bromine substituent, despite lithium-halogen exchange being itself a rapid process. Attempts to protect the amine using ethyl chloroformate following reaction with two molar equivalents of *n*-butyllithium, however, gave rise only to the *N,N*-disubstituted product **29** and none of the protected compound bearing a bromine substituent.

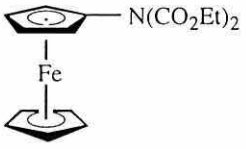

29

The absence of the desired product can be attributed to intra- and intermolecular lithium-halogen exchange resulting from the lithio-amine intermediate: immediately the amine is lithiated, the bromine is cleaved, leaving a lithioferrocene intermediate which is either quenched during the reaction or during work-up (Fig. 3.3, overleaf).

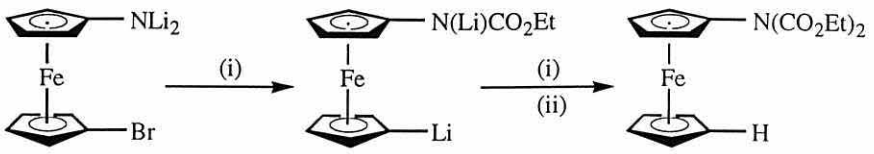

Figure 3.3 Lithium-bromine exchange leading to formation of (*N,N*-dicarboethoxyl)aminoferrocene **29**: (i) $ClCO_2Et$, (ii) H_2O

Nevertheless, the product **29** formed bright yellow, air- and light-stable crystals which were characterised by NMR and IR spectroscopy and by mass spectrometry and gave a satisfactory elemental analysis. The protons *alpha* to the nitrogen are shifted downfield to $\delta = 4.52$ppm in the protected compound (*cf.* $\delta = 3.89$ppm in the parent compound, aminoferrocene **25**) and there is a distinctive carbonyl stretching resonance in the IR spectrum at 1722cm^{-1}.

In line with concurrent work on phosphine protection (*vide infra*), an alternative protocol for amine protection was investigated, which made use of borane chemistry.[58] Phosphine- and amine-boranes can be formed under reductive conditions, according to the following general equation (Fig. 3.4).[116]

$$2XR_3 + 2NaBH_4 + I_2 \rightarrow 2XR_3.BH_3 + 2NaI + H_2$$

Figure 3.4 Phosphine and amine protection: X = P, N; R = H, alkyl or aryl

1-Bromo-1'-aminoferrocene **1** was thus protected as its *N*-borane adduct **30** and characterised by NMR and IR spectroscopy and by mass spectrometry. Importantly, the protected amine melts without decomposition at a temperature considerably higher than the decomposition temperature of its unprotected counterpart [132°C *vs.* 90°C (*n*-hexane)]. The presence of the borane is also supported by the observation of a boron-hydrogen stretch in the IR spectrum at 2330cm^{-1}.

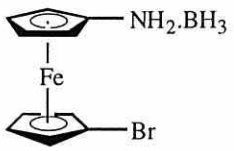

30

3.2.4 1-Amino-1'-ferrocenecarboxylic Acid

As a novel compound, it was hoped that 1-bromo-1'-aminoferrocene **1** could be converted to 1-amino-1'-ferrocenecarboxylic acid **2**, by stepwise lithiation and quenching using carbon dioxide as the electrophile. To allow for deprotonation of the amine preceding lithium-halogen exchange, lithiation was performed using three molar equivalents of *n*-butyllithium. The addition of dry carbon dioxide either as pellets or preferably as the gas resulted in the immediate precipitation of 1-amino-1'-ferrocene-carboxylic acid **2** which was filtered off and washed with ether.

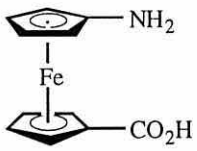

2

The crude product, while water-soluble, could be extracted neither from acidic nor from basic aqueous solutions, and attempts at organic solvent washing, evaporation and extraction into dry methanol met with only limited success. The instability of the crude product meant that it was only possible to characterise the amino acid using NMR and IR spectroscopy and mass spectrometry.

It was decided instead to form the methyl ester **31** of the acid by treatment of the crude solid initially obtained with methanolic hydrogen chloride.[117] Along with the methyl ester **31**, aminoferrocene **25** and the *N*-butylated methyl ester **32** were also isolated by

flash chromatography, in the ratio 62:9:24. The methyl ester was obtained as deep orange crystals which, while still air-sensitive, were found to be considerably more stable than either aminoferrocene **25** or the *N*-butylated methyl ester **32**. Compound **31** was characterised by high resolution FAB accurate mass spectrometry and NMR spectroscopy.

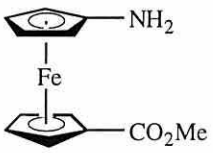

31

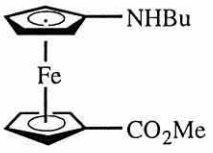

32

3.2.5 1-(Diphenylphosphino)-1'-aminoferrocene

From a catalysis point of view, a useful target compound was 1-(diphenylphosphino)-1'-aminoferrocene **3**.

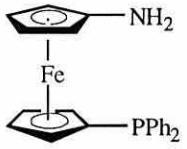

3

The synthesis of such a ligand could theoretically be approached either by lithiation of 1-bromo-1'-aminoferrocene **1** or by lithiation of 1-bromo-1'-(diphenylphosphino)-ferrocene **33**.[17]

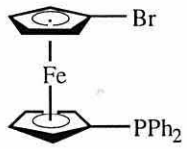

33

In light of the difficulties experienced with the amino acid **2**, the latter of these methodologies was deemed preferable. The reaction of 1-diphenylphosphino-1'-

lithioferrocene prepared *in situ* from a previously prepared sample of 1-bromo-1'-(diphenylphosphino)ferrocene **33** with *O*-benzylhydroxylamine resulted in the formation of the target ligand, but the product was observed to darken on standing in air and thus is not such a useful ligand, for want of ease of handling. Characterisation of the compound was incomplete as a consequence, however, the $^{31}P-\{^{1}H\}$ NMR spectrum consists of a singlet at δ = -17.6ppm which is shifted only slightly upfield when compared to DPPF **6** (δ = -17.9ppm, *vide infra*), suggesting that it is the amine functionality which is responsible for the instability of the product.

3.2.6 1-Ferrocenyl(*N,N*-dimethyl)ethylamine

The examination of the dibromination chemistry of 1-ferrocenyl(*N,N*-dimethyl)ethylamine **16** required a large scale synthesis of the starting material, which is economically achieved using the procedure of Hauser and Lindsay.[29] Ferrocenecarboxaldehyde **34** was thus treated with sodium bisulfite, sodium cyanide and dimethylamine to give 2-ferrocenyl-2-(*N,N*-dimethylamino)acetonitrile **35** (Fig. 3.5), a light brown crystalline compound, identified by its ^{1}H NMR spectrum. This compound was used without purification in the subsequent reaction, since it has a tendency to decompose to a black oil fairly rapidly.

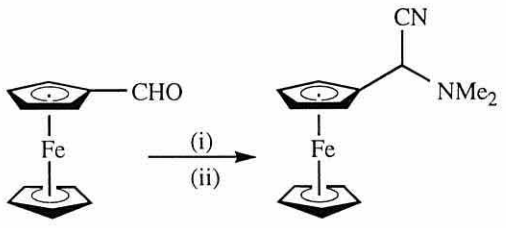

3 **35**

Figure 3.5 Synthesis of 2-ferrocenyl-2-(*N,N*-dimethylamino)acetonitrile **35**: (i) $NaHSO_3$, (ii) NaCN, $HNMe_2$

The nitrile group was then displaced by methylmagnesium iodide, prepared by the reaction of methyl iodide on magnesium in ether solution (Fig. 3.6, overleaf). The product amine **16** was isolated as a dark yellow air-stable oil and purified by flash

chromatography on basic alumina, then characterised by comparison of its physical data with the literature [bp 115-7°C/5mm (lit. 120-1°C/7mm)].[33]

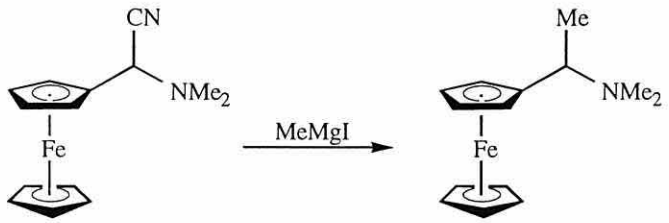

35 16

Figure 3.6 Synthesis of 1-ferrocenyl(*N,N*-dimethyl)ethylamine **16**

Resolution of the compound was also achieved according to the method of Ugi *et al.*,[33] using tartaric acid in saturated methanolic solution. The two enantiomers were obtained in high optical purity after being recrystallised twice, giving $[\alpha]^{25}_{D}$ = +13 and -13 (lit.+14.1 and -14.1, c = 1.5, ethanol).[33]

3.2.7 1,1'-Dibromo-2-[(*N,N*-dimethylamino)ethyl]ferrocene

As precedence for the dibromination of the chiral amine **16** it was necessary first to demonstrate the viability of such a reaction on the commercially available achiral analogue ferrocenyl(*N,N*-dimethyl)methylamine **36** (Fig. 3.7).

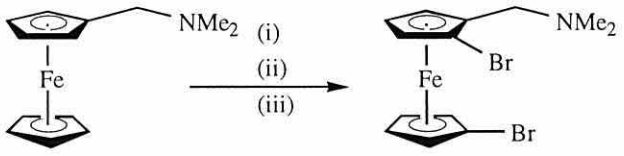

36 37

Figure 3.7 Dibromination of ferrocenyl(*N,N*-dimethyl)methylamine **36**: (i) ^{n}BuLi, (ii) ^{n}BuLi, TMEDA, (iii) $BrF_2C\text{-}CF_2Br$

The dibromination of ferrocenyl(*N,N*-dimethyl)methylamine was achieved by dilithiation in the presence of TMEDA **13** followed by reaction of the lithio-intermediate with 1,2-dibromotetrafluoroethane, in the same manner as the preparation of 1,1'-dibromoferrocene **11**.[54] The reaction proceeded in rather lower yield (36%) than had been expected but the product (±)-1,1'-dibromo-2-[(*N,N*-dimethylamino)methyl]ferrocene **37** was unexpectedly straightforward to purify. Whereas the separation of 1,1'-dibromoferrocene **11** in the preparation of bromoferrocene is virtually impossible by conventional column chromatography,[118] the impurities from the amine synthesis were fortuitously separable. The product dibromo-amine **37** was characterised by NMR and IR spectroscopy and by mass spectrometry.

The resolved chiral amine (*R*)-1-ferrocenyl(*N,N*-dimethyl)ethylamine (*R*)-**16** was then dilithiated in the presence of TMEDA **13** and treated with 1,2-dibromotetrafluoroethane, to afford (*R,S*)-1,1'-dibromo-2-[(*N,N*-dimethylamino)ethyl]ferrocene **38**, also a dark yellow oil, which was purified by chromatography on basic alumina. This product, while air-stable, was observed to darken upon prolonged exposure to daylight. The characterisation of the product was supported by proton-proton decoupling experiments which showed that the proton H-3, *ortho* to the amine substituent on the cyclopentadienyl ring, gave rise to a resonance at $\delta = 4.15$ppm, while the other protons on the same ring, H-4 and H-5, gave rise to resonances at $\delta = 4.20$ and 4.48ppm respectively.

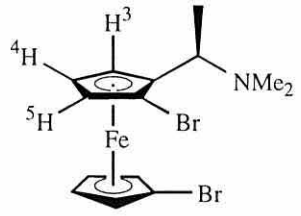

38

This upfield shift of H-3 is evidence for the *ortho*-directing effect of the amine substituent, which causes a downfield shift in one *ortho*-position (in this case the position occupied by the bromine at C-1) and an upfield shift in the other *ortho*-position, where lithiation is disfavoured.[36] The chirality of the compound led to each ferrocene

resonance being diastereotopic and therefore slightly inequivalent: the protons in the α'- and β'-positions produced irresolvable multiplets at 250MHz instead of the expected *pseudo*-triplets.

It was hoped that upon lithiation with one molar equivalent of *n*-butyllithium, the *ortho*-directing effect of the amine substituent might favour lithium-bromine exchange at -80°C on the cyclopentadienyl ring bearing the amine functionality. However, lithiation was indiscriminate under the conditions examined: there was only minimal selectivity in THF solution and no appreciable selectivity in either *n*-hexane or diethyl ether when the reactions were quenched with water and the NMR spectra of the products were compared. An additional experiment was performed in THF, whereby the amine was lithiated at different temperatures over the range -80 to +20°C. Comparison of the respective NMR spectra from the different reactions showed that the selectivity was limited to under -60°C, a limitation which restricts the number of useful electrophilic quenches since, for example, the reaction with chlorophosphines generally takes place at between -30 and -20°C. The results are summarised in Table 3.1 (overleaf), with assignments made by comparison of the integrals of the downfield H-5 signal (δ = 4.48ppm) and the characteristic cyclopentadienyl signal (δ = 4.12ppm). The H-5 signal disappears as the protons on the amine-substituted ring assume equivalence upon removal of the *ortho*-bromine (C1), while removal of the bromine from the "lower" ring (C1') leads to the appearance of a disproportionately tall cyclopentadienyl singlet.

SOLVENT	APPROX. TEMP., °C	H / Br SUBSTITUTION, %		
		C1	C1'	neither
n-hexane	20	52	48	0
	-80	37	34	29
diethyl ether	20	51	49	0
	-80	50	50	0
THF	20	51	49	0
	0	54	46	0
	-20	60	40	0
	-40	63	37	0
	-60	65	35	0
	-80	73	27	0

Table 3.1 Attempted selective lithiation of 1,1'-dibromo-2-[(*N*,*N*-dimethylamino)ethyl]ferrocene **38**

3.2.8 1,1'-Bis(diisopropylphosphino)ferrocene

The synthesis of 1,1'-bis(diisopropylphosphino)ferrocene, DIPPF **7**, was carried out according to the procedure of Cullen *et al.*[7] (Fig. 3.8), in 86% yield.

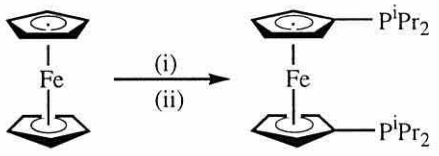

7

Figure 3.8 Synthesis of 1,1'-bis(diisopropylphosphino)ferrocene **7**: (i) ^{n}BuLi, TMEDA, (ii) ClP^{i}Pr$_2$

The advantage of this one-pot lithiate and quench methodology is the exclusion of mono-(diisopropylphosphino)ferrocene from the reaction mixture: the alternative Friedel-Crafts introduction of phosphine groups on to the ferrocene using the chlorophosphine reagent

in the presence of a Lewis acid such as aluminium trichloride is known to lead to a mixture of mono- and disubstituted products[119] which are virtually inseparable by chromatography.[120]

The product DIPPF **7** was isolated as a dark yellow oil, in contrast to its diphenylphosphino-counterpart **6** which forms yellow-orange crystals, however, flash chromatography on silica followed by refrigeration for 18h yielded orange crystals which had only a slight tendency to melt [mp 34-36°C (*n*-hexane)]. The compound was characterised by NMR and IR spectroscopy and by mass spectrometry and gave a satisfactory elemental analysis. All results were in good accordance with the reported literature values.[7]

The ^{1}H NMR spectrum recorded at 250MHz (Fig. 3.9, overleaf) showed the expected pair of doublets of doublets integrating to 24H for the methyl groups. The eight methyl groups are symmetrically equivalent but diastereotopic because of the prochiral C-H group and therefore magnetically inequivalent, giving rise to twice the number of signals as would be expected for non-diastereotopic groups. Each methyl group is then coupled to the adjacent isopropyl C-H proton ($^{3}J_{H,H}$ = 7.0Hz) and to the phosphorus through a three-bond interaction ($^{3}J_{P,H}$ = 13.0Hz). The isopropyl C-H protons each produce a septet (coupling to two equivalent methyl groups, $^{3}J_{H,H}$ = 7.0Hz) of doublets (coupling to phosphorus, $^{2}J_{P,H}$ = 2.3Hz), producing an overall pattern consisting of 14 peaks. For ferrocenylphosphines such as DPPF **6** and DIPPF **7**, the four ferrocenyl protons *alpha* to the phosphines usually give rise to the resonance furthest upfield, while the *β*-protons produce a downfield signal.[121] In the case of DIPPF, the resonance of the α-protons occurs at δ = 4.14ppm and the resonance of the β-protons occurs at δ = 4.24ppm. The ^{31}P-{^{1}H} NMR spectrum of the ligand showed a singlet at δ = -0.39ppm, a considerable downfield shift when compared to DPPF (δ = -17.9ppm).

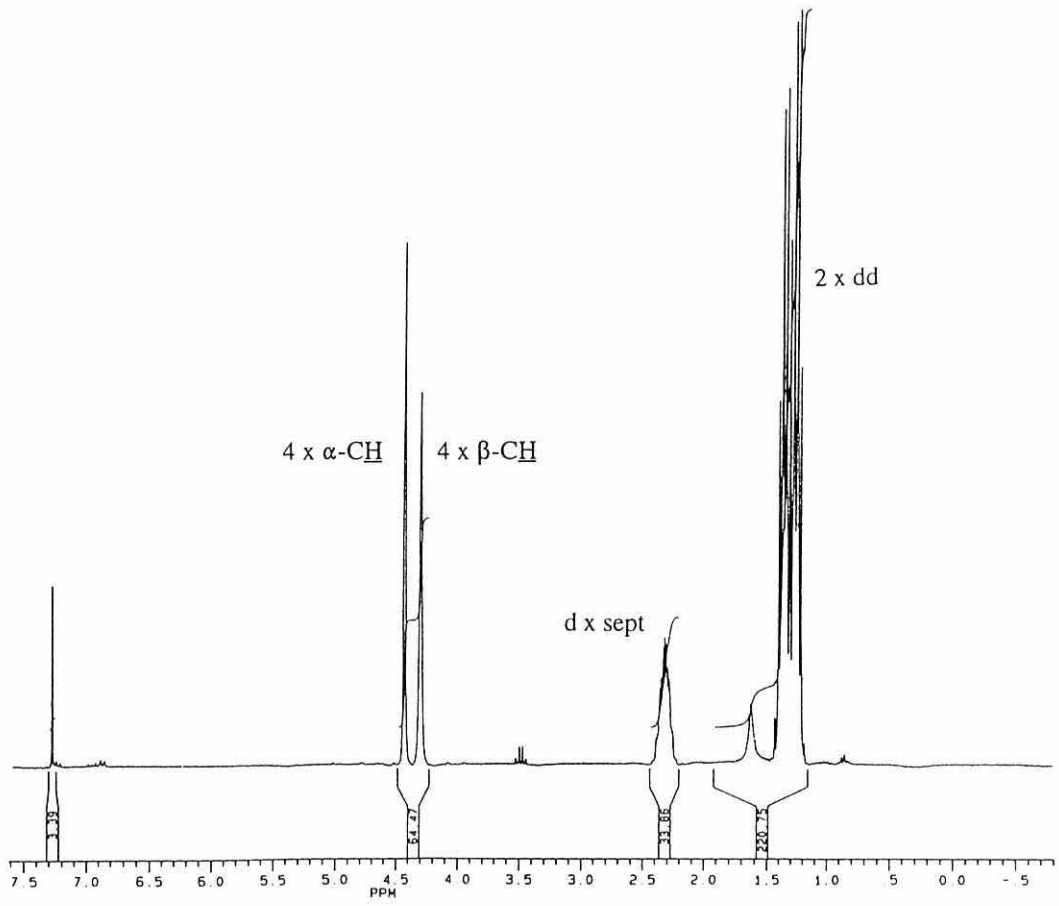

Figure 3.9 ^{1}H NMR spectrum of 1,1'-bis(diisopropylphosphino)ferrocene **7** ($CDCl_3$, 250MHz)

In common with other ferrocenylphosphine ligands, DIPPF **7** was found to be particularly susceptible to aerobic oxidation. Cyclic voltammetry (Fig. 3.10, overleaf) in dichloromethane showed that the ligand had an oxidation potential of $E^{o\prime} = +0.43V$[122] *vs.* SCE (*cf.* ferrocene, $E^{o\prime} = +0.45$).[123] The oxidation peak is partially reversible and its potential, being lower than that of ferrocene, indicates that the corresponding ferrocenium cation is not stable. This explains the air-sensitivity of the free ligand, since the oxidation of the phosphines is facilitated by prior oxidation of the iron (II) to iron (III). The analogous DPPF **6**, on the other hand, has an irreversible oxidation potential of $E^{o\prime} = +0.61V$[122] *vs.* SCE and is, therefore, much more oxidatively stable than DIPPF.

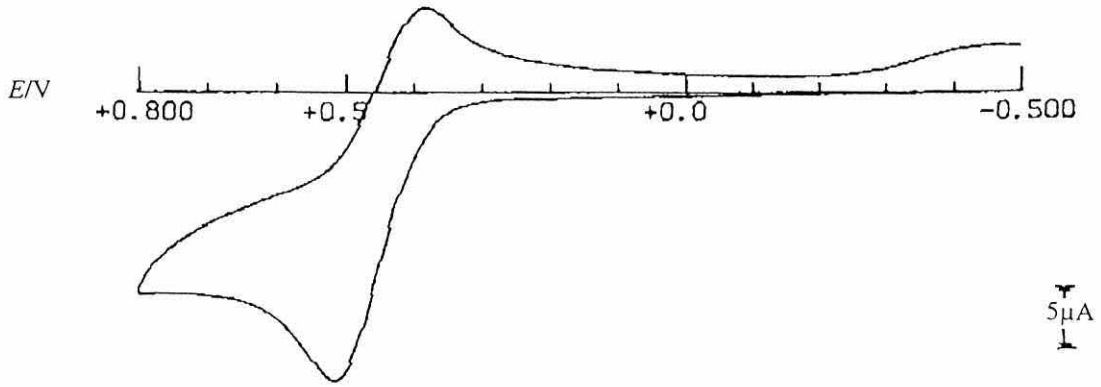

3.2.9 1,1'-Bis(diphenylphosphino)ferrocene

For comparison in catalytic studies, DPPF **6** was also prepared, following the literature procedure.[4] The compound was isolated by precipitation from *n*-hexane/ ether as a yellow powder which was recrystallised from toluene to give orange-yellow crystals in *ca.* 80% yield, characterised by NMR and IR spectroscopy, mass spectrometry and elemental analysis. All results agreed with those previously reported for the compound [mp 178-180°C (dec.) (lit. 181-182°C)].[4] ^{31}P-{ ^{1}H} NMR, for example, showed a singlet at δ = -17.9ppm (lit.-17.2ppm).[124]

3.2.10 1,1'-Bis[diisopropylphosphino(borane)]ferrocene

The preparation of the *P*-borane adduct of DIPPF **7** was examined in order to alleviate the problems of its air-sensitivity, using the commercially available tetrahydrofuran-borane (BH_3.THF) complex, in THF solution.[61] This proved ineffective, possibly on account of the antiquity of the reagent bottle, although TLC of the reaction mixture showed the quantitative conversion of the starting material to a non-polar species, which

was presumably destroyed upon isolation. An alternative synthesis was, therefore, examined using sodium borohydride and iodine as described above for the protection of 1-bromo-1'-aminoferrocene **1**.[116]

In order to test the reaction on an inexpensive phosphine, triphenylphosphine-borane **39** was prepared in virtually quantitative yield according to the literature preparation.[63] A 1,2-dimethoxyethane (DME) solution of triphenylphosphine and sodium borohydride was treated with a solution of iodine in the same solvent and after stirring at room temperature the product was isolated as colourless crystals by solvent exchange to benzene and crystallisation from a benzene/ *n*-hexane mixture. The product was obtained in essentially quantitative yield and was characterised by comparison of its analytical and spectral data with the literature values [mp 186-189°C (lit. 187-189°C)].[63] Compound **39** exhibited a phosphorus-boron coupling of $^{1}J_{P,B}$ = 55Hz (lit. 57Hz)[63] which could be seen in both the ^{31}P-{^{1}H} and ^{11}B-{^{1}H} NMR spectra.

The formation of phosphine-boranes from ferrocenylphosphines also proceeded in high yield. Thus, the boranes of DPPF **6** (compound **40**)[58] and DIPPF **9** (compound **41**) were prepared using sodium borohydride and iodine in DME. Both formed yellow-orange crystals which are air-stable and remain so in a number of solvents. The compounds were characterised by NMR and IR spectroscopy and by mass spectrometry and both gave satisfactory elemental analyses. The ^{31}P-{^{1}H} chemical shifts are compared in Table 3.2 (overleaf) and show in each case a downfield shift of $\Delta \simeq$ +30ppm, in the direction of greater oxidative stability.

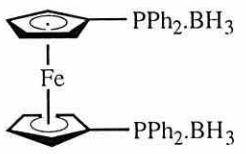

40

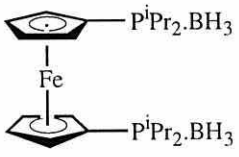

41

LIGAND	$^{31}P-\{^{1}H\}$ δ (ppm) =		
	Phosphine	Phosphine-borane	Δ ($\delta_{PB}-\delta_{P}$)
PPh_3	-6.0	+20.0	+26.0
DIPPF	+0.4	+30.5	+30.1
DPPF	-17.9	+15.0	+32.2

Table 3.2 Comparison of $^{31}P-\{^{1}H\}$ NMR shifts for phosphines and phosphine-boranes

A common feature of the mass spectra is the low abundance of the boranes in the fragmentation patterns, the result of a relatively weak phosphorus-boron bond. In the infra-red spectra, characteristic bands are those at *ca.* 2400cm^{-1} (a boron-hydrogen stretch) and at *ca.* 1100cm^{-1} (an aryl-phosphine stretch typical of four co-ordinate phosphorus).

The ^{1}H-NMR spectrum of DIPPF-borane **41** closely resembles that of the unprotected ligand **7**, except that the coupling of the isopropyl protons to phosphorus is slightly enhanced upon protection. Thus, $^{3}J_{P,H}$ = 14.5Hz (*vs.* 13.0Hz) and $^{2}J_{P,H}$ = 3.0Hz (*vs.* 2.3Hz). This can be explained by the shielding effect of the borane on the phosphorus. The fact that in none of the boranes examined could NMR signals originating from the borane be positively identified appears to be a feature of such systems,[125] although recently Kagan *et al.*[41] reported broad multiplets in the region of δ = 1.0-1.5ppm. These signals, while certainly present in the spectra of the current study (Fig. 3.11, overleaf), do not give measurable integrals and are, therefore, ambiguous: the $^{11}B-\{^{1}H\}$ NMR and IR spectra provide more concrete evidence for successful borane protection.

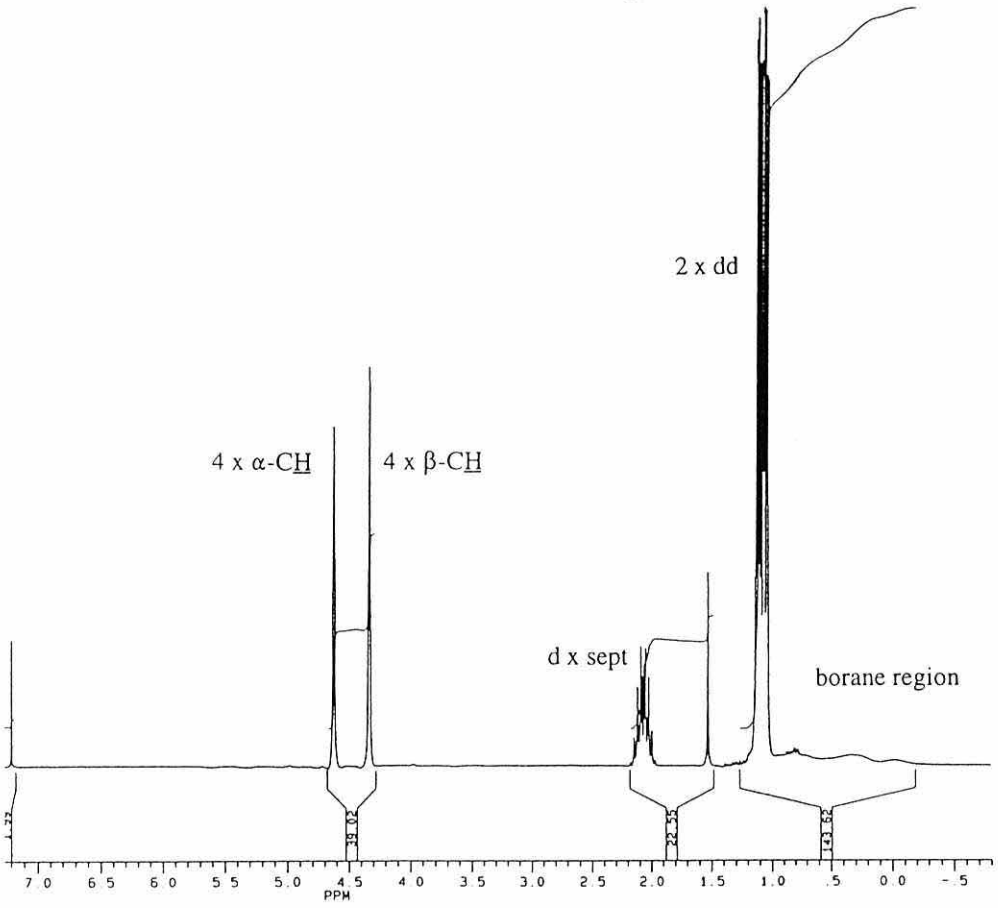

Figure 3.11 Immeasurable integration in the borane region of the ^{1}H NMR spectrum of **41** ($CDCl_3$, 250MHz).

In order to assess the stability of the new phosphine-borane **41**, a sample was treated with an excess of hydrogen peroxide. After 24h the sample remained intact and showed no sign (by $^{31}P-\{^{1}H\}$ NMR) of oxidation or decomposition. Phosphine-boranes have been reported to be stable to the Jones oxidation,[126] but due to the redox properties of ferrocene the 1,1'-bis[diisopropylphosphino(borane)]ferrocene adduct **41** oxidises under such conditions to a blue-green ferrocenium cation.

As a more general approach to the phosphine-borane protection, attempts to protect the phosphine reagents chlorodiphenylphosphine and chlorodiisopropylphosphine were made using the same methodology, but both were unsuccessful, yielding brown oily decomposition products. Analogous protected chlorodiorganophosphine-boranes have previously been prepared using BH_3.THF[127] and organozinc reagents.[128]

3.2.11 (*R,S*)-1,1'-Bis(diisopropylphosphino)-2-[(*N,N*-dimethyl-amino)ethyl]ferrocene

The isopropylphosphino-analogue of the BPPFA ligand **18**, IPPFA **5**, was prepared by the literature method[7] with a view to examining its effectiveness in asymmetric Heck coupling.[83] The product was isolated by careful column chromatography on silica using 5% ether/ petrol, along with a trace of its mono-substituted analogue **42**, and was characterised by elemental analysis, NMR and IR spectroscopy and mass spectrometry. The ^{1}H NMR spectra of the mono- and diphosphine are similar in many respects, both being complicated by the presence of diastereomeric groups and by the large number of methyl proton resonances, however, the $^{31}P-\{^{1}H\}$ NMR spectra show clear resonances at δ = -5.7ppm for the monophosphine **42** and δ = -1.0 and -5.6ppm for the diphosphine **5**. The slight upfield shift of the phosphine resonance in the disubstituted product with respect to its monophosphine counterpart (Δ = 0.1ppm) can be attributed to the shielding effect of the phosphine on the "lower" cyclopentadienyl ring in the former.

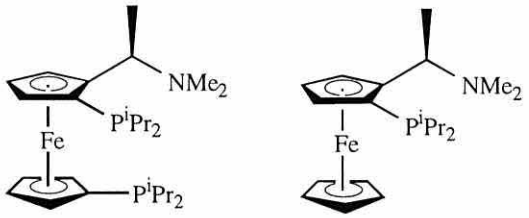

5 **42**

3.2.12 (*S,S*)-1-(*p*-Tolylsulfinyl)-2-[diisopropylphosphino-(borane)]ferrocene

The synthesis of 1,2-heterodisubstituted ferrocenylphosphines was achieved using the method of Kagan *et al.*[41] (Chapter 1.2.3), *via* a chiral sulfoxide, the chirality being introduced by the use of a sulfinate bearing a menthol auxiliary. Thus, ferrocene was mono-lithiated according to the procedure of Müller-Westerhoff,[16] using *tert*-

butyllithium and potassium *tert*-butoxide. The lithioferrocene was added to a THF solution of (1*R*)-menthyl (*S*)-toluene-4-sulfinate to give yellow crystals of (*S*)-ferrocene *p*-tolyl sulfoxide **43** which were characterised by NMR and IR spectroscopy and by mass spectrometry and gave an optical rotation of $[\alpha]^{25}_{D}$ = -4.2 [lit. 4 ± 1 (c = 0.9, $CHCl_3$)].[15] The compound also gave a satisfactory elemental analysis and its melting point was in good agreement with the literature [mp 127-129°C (lit. 127-128°C)].[15]

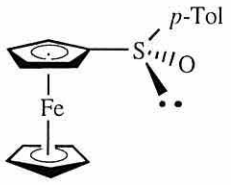

43

(*S*,*S*)-1-(*p*-Tolylsulfinyl)-2-[diisopropylphosphino(borane)]ferrocene **44** was generated from the chiral sulfoxide **43** by *ortho*-lithiation using lithium *N*,*N*-diisopropylamide (LDA) and subsequent reaction of the lithio-intermediate with chlorodiisopropyl-phosphine. To avoid problems of phosphine oxidation, the product phosphine was reacted *in situ* with fresh BH_3.THF (Fig. 3.12).

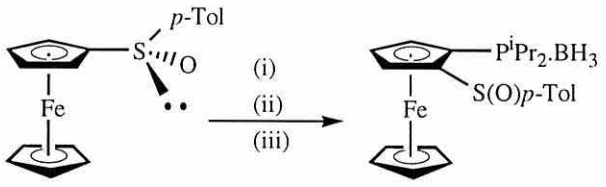

43 **44**

Figure 3.12 Synthesis of (*S*,*S*)-1-(*p*-tolylsulfinyl)-2-[diisopropylphosphino(borane)]ferrocene **44**: (i) LDA, (ii), ClP^iPr_2, (iii) BH_3.THF

The borane-protected product **44** was characterised by NMR and IR spectroscopy and by mass spectrometry and gave a satisfactory elemental analysis. The ^1H NMR spectrum of the product showed three different environments for the four methyl groups of the isopropyl substituents. This suggests that rotation of the phosphorus-ferrocene bond is restricted by the adjacent sulfoxide group: if this were the case, then one isopropyl group

would be directed away from the sulfoxide and would give rise to two equivalent methyl signals, while the other isopropyl group would be directed towards the sulfoxide and its methyl groups would be inequivalent as a result of the chirality about the sulfur. The isopropyl C-H signals are similarly inequivalent, giving resonances at δ = 2.17 and 3.09ppm. Such a theory could be confirmed by X-ray crystallography.

3.2.13 Attempted Synthesis of (*S*)-1-[Diphenylphosphino-(borane)]-2-[diisopropylphosphino(borane)]ferrocene

The capacity of *tert*-butyllithium to selectively cleave the ferrocene-sulfoxide bond was exploited in the attempted synthesis of the novel mixed 1,2-diphosphine-borane, (*S*)-1-[diphenylphosphino(borane)]-2-[diisopropylphosphino(borane)]ferrocene **45**. Thus, (*S*,*S*)-1-(*p*-tolylsulfinyl)-2-[diisopropylphosphino(borane)]ferrocene **44** was cooled and reacted with *tert*-butyllithium. The resultant (*R*)-1-[diisopropylphosphino(borane)]-2-lithioferrocene was reacted with chlorodiphenylphosphine, then BH_3.THF, to afford the mixed phosphine as its protected borane adduct **45** (Fig. 3.13).

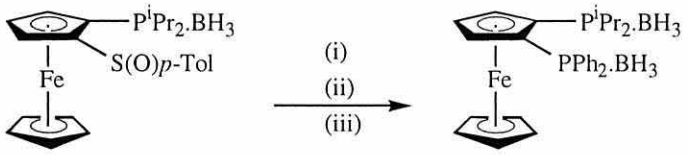

44 **45**

Figure 3.13 Attempted synthesis of (*S*)-1-[diphenylphosphino(borane)]-2-[diisopropylphosphino-(borane)]ferrocene **45**: (i) ^{t}BuLi, (ii) $ClPPh_2$, (iii), BH_3.THF

The yield was found to be surprisingly low, at 14%, and a considerable quantity of [diisopropylphosphino(borane)]ferrocene **46** (20%) was isolated which suggested that the yield was compromised in part by ineffective reaction with the chlorodiphenyl-phosphine. This could be attributable to the antiquity and, therefore, impurity of the phosphine reagent, but considerable steric hindrance is to be expected during the

introduction of two vicinal, bulky, tertiary phosphine groups, and the rate of reaction could perceivably reflect such a limitation.

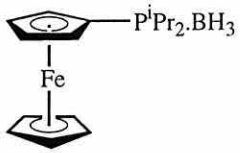

46

Upon examination of the characterisation of the product, however, it became clear that the isolated product was not the desired product **45**. A singlet in the ^{31}P-{^{1}H} NMR at +80ppm with no corresponding resonance in the ^{11}B-{^{1}H} spectrum suggested that a phosphine oxide had been formed, and from the observed distribution of aromatic proton signals in the ^{1}H NMR spectrum it was clearly the phosphine oxide of the diphenylphosphino-group. The diisopropylphosphino-borane produced a doublet in both the ^{31}P-{^{1}H} and ^{11}B-{^{1}H} spectra and so can be concluded to be intact. The oxidation of the diphenyl-substituted phosphorus could perceivably have occurred at any point (i) prior to the reaction, if the reagent were impure; (ii) *in situ*, if the reaction conditions were sufficiently oxidative; or (iii) upon work-up, if the borane protection were unsuccessful.

Further evidence for the product being (*S*)-1-(diphenylphosphoryl)-2-[diisopropyl-phosphino(borane)]ferrocene **47** was to be found in the IR spectrum which showed a phosphorus-oxygen stretch at 1168cm^{-1} and in the mass spectrum which showed a relative intensity of 100% for M^{+}-BH_3, m/z = 502.

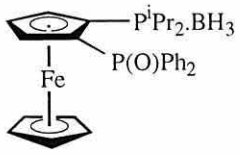

47

3.2.14 1,2-Bis[diisopropylphosphino(borane)]ferrocene

Although for the synthesis of the symmetrically disubstituted isopropylphosphine it was not necessary to use a chiral sulfoxide as starting material, the chiral sulfoxide **44** was readily available and so was chosen nonetheless. Thus, a method similar to that used for the synthesis of the asymmetrically substituted diphosphine was employed using chlorodiisopropylphosphine as the electrophilic quench and red-orange crystals of 1,2-bis[diisopropylphosphino(borane)]ferrocene **9** were obtained. The compound was characterised by NMR and IR spectroscopy and by mass spectrometry and gave a satisfactory elemental analysis.

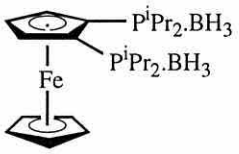

9

The ^{1}H NMR spectrum showed a highly complicated isopropyl region, again suggesting restricted rotation of the phosphine groups leading to inequivalence which may be unexpected in view of the apparent C_2 symmetry of the system. The coupling of phosphorus to the isopropyl protons cannot be seen in the spectrum, presumably as a result of the coincidence of the signals: $^2J_{H,P}$ is typically exactly double the value of $^3J_{H,H}$, so it is possible that the doublet of the $^2J_{H,P}$ is accidentally coincident with the septet peaks of $^3J_{H,H}$. In the ferrocene region of the spectrum, the C_2 symmetry allows both components of the expected *pseudo*-triplets to be resolved to their respective doublets of doublets. Thus, $^3J_{3,4}$ and $^3J_{4,5}$ = 2.5Hz, while $^4J_{3,5}$ =1.4Hz and C4-H, the proton at the "back" of the substituted cyclopentadienyl ring, gives rise to a clean triplet with ^3J = 2.5Hz. In the IR spectrum, the stretching frequency of the B-H bond is 2395.5cm^{-1}.

3.3 Co-ordination Chemistry

2.3.1 Dichloro[1,1'-bis(diisopropylphosphino)ferrocene]nickel (II)

Nickel complexes of DPPF **6** and DIPPF **7** were prepared according to a standard literature procedure by adding 0.95 molar equivalents of a hot methanolic solution of dichloronickel (II) hexahydrate to a refluxing methanolic solution of the ligand.[129] Complexation was instantaneous, and the products were isolated by filtration. The complexes **48** and **49** were dark green in colour, indicating a tetrahedral co-ordination geometry. Despite their being paramagnetic, some NMR data were obtained, and the complexes were characterised by IR spectroscopy, mass spectrometry and elemental analysis. The ^{31}P-{ ^{1}H} spectrum of [$NiCl_2$(DIPPF)] **49** was recorded and showed a singlet at δ = 52ppm, however, the spectroscopy of [$NiCl_2$(DPPF)] **48** proved impossible and so there is no analogue for comparison.

Cyclic voltammetry of the new complex in dichloromethane solution (Fig. 3.14) gave a partially reversible one-electron oxidation arising from the iron (II)/ iron (III) redox system, at a potential of $E^{o\prime}$ = +0.70V *vs.* SCE.[122] The difference between this and the free ligand ($E^{o\prime}$ = +0.43V) is indicative of the increase in stability produced by complexation. No evidence of the redox properties of the nickel moiety was observed.

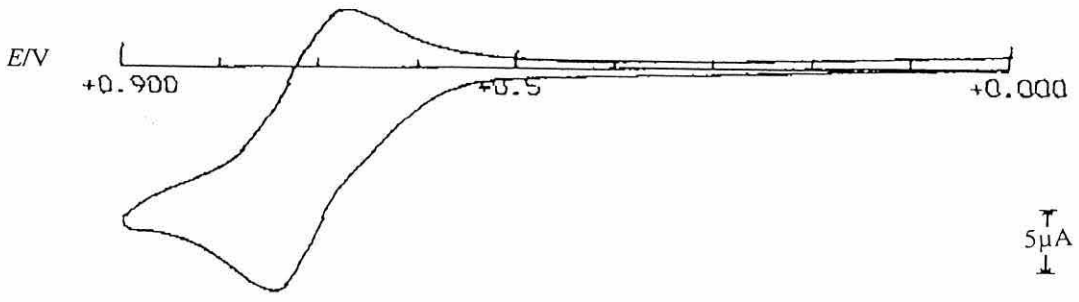

Figure 3.14 Cyclic voltammogram of dichloro[1,1'-bis(diisopropylphosphino)ferrocene]nickel (II): scan rate = 200mVs^{-1}

The single crystal X-ray structure of [$NiCl_2$(DIPPF)] **49** (Fig. 3.15) was obtained from a crystal grown by slow diffusion from dichloromethane into *n*-hexane. The complex is approximately tetrahedral as indicated by its dark green colour, but the nickel and iron are not co-planar with respect to the phosphines: the nickel dichloride sits to one side of the diphosphine rather than directly between the two donor groups. The bite angle about the nickel, P-Ni-P, is 103.0° and the nickel dichloride bond angle Cl-Ni-Cl is 125.4°, thus the distortion from a perfect tetrahedron (109.5°) is considerable. The cyclopentadienyl rings of the ferrocene are parallel and almost eclipsed, assuming a similar geometry to that of the analogous DPPF complex **48**.[130]

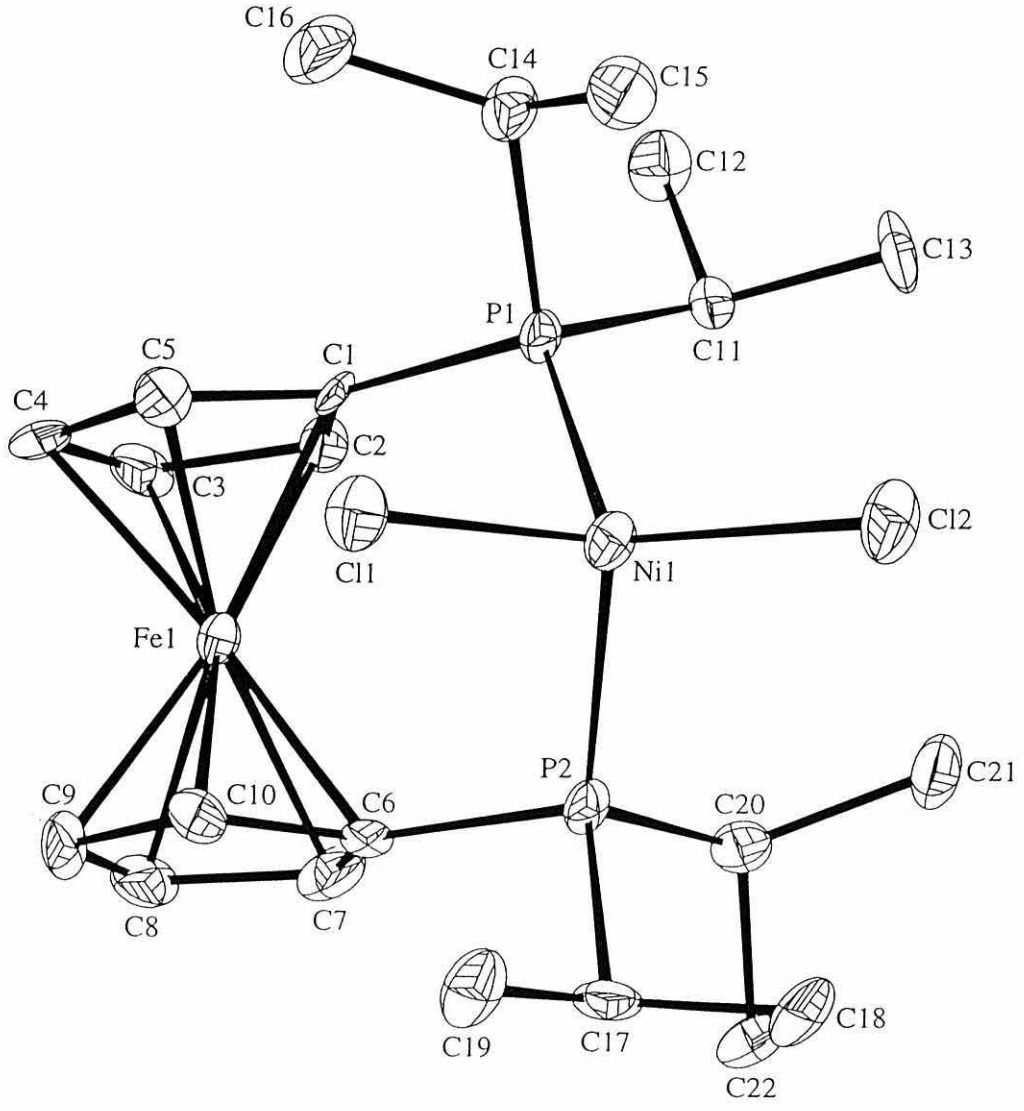

Figure 3.15 Single crystal X-ray structure of [$NiCl_2$(DIPPF)] **49**

Empirical formula	$C_{22}H_{36}Cl_2FeP_2Ni$
Formula weight	547.91
Temperature	150 (2) K
Wavelength	0.71069Å
Crystal system	Orthorhombic
Space group	Pna21
Unit cell dimensions	a = 14.812 (2)Å
	b = 9.769 (2)Å
	c = 17.024 (3)Å
Volume	2463.3 (7)Å^3
Z	4
Density (calculated)	1.477 mg/m^3
Absorption coefficient	1.707 mm^{-1}
F (000)	1144
Crystal size	0.25 x 0.18 x 0.15 mm (RED)
Theta range for data collection	2.39 to 25.02°
Index ranges	-16<=h<=16, -7<=k<=10, -15<=l<=19
Reflections collected	8905
Independent reflections	3664 [R (int) = 0.0956]
Refinement method	Full-matrix least-squares on F^2
Data/restraints/parameters	3664/7/261
Goodness-of-fit on F^2	0.763
R indices [on 1322 data with I>2Σ(I)]	R1 = 0.0376, wR2 = 0.0838
R indices (all data)	R1 = 0.0506, wR2 = 0.0864
Absolute structure parameter	-0.05 (2)
Largest diff. peak and hole	0.472 and -0.323 e.A^{-3}

Table 3.3 Crystal data and structure refinement for [$NiCl_2$(DIPPF)] **49**

3.3.2 *cis*-Dichloro[1,1'-bis(diisopropylphosphino)ferrocene]-palladium (II)

Palladium complexes of DPPF **6** and DIPPF **7** were prepared by mixing the respective ligand with 0.95 equivalents of *cis*-[Pd(COD)Cl_2] in dichloromethane, with subsequent crystallisation from dichloromethane/ *n*-hexane. The complexes were orange-red in colour, typical of a square-planar co-ordination geometry. *cis*-[$PdCl_2$(DPPF)] **50** is dark red and gives a characteristic ^{1}H NMR spectrum with the phenyl resonances refined to a 8H:4H:8H pattern at 250MHz, by removal of electron density from the phosphorus atoms, as opposed to the free ligand in which the phenyl resonances appear as a broad multiplet. Elemental analysis and the measured melting point were consistent with the expected values [mp 266-268°C (toluene), lit. 265°C ($CHCl_3$)].[52] *cis*-[$PdCl_2$(DIPPF)] **51**, also characterised by elemental analysis, NMR and IR spectroscopy and mass spectrometry, is in contrast a much more yellow-orange coloured complex. The pattern of the ^{1}H NMR resonances from the methyl groups in the complex differs greatly from that of the free ligand: in the complex they are divided clearly into two multiplets at δ = 1.25ppm and δ = 1.60ppm, each integrating to 12H. This suggests that there are two distinct chemical environments in the complex in which the eight methyl groups are located, with four being more shielded than the other four. The complex gives a singlet in the ^{31}P-{^{1}H} NMR spectrum at δ = +66ppm, which is considerably downfield of the corresponding DPPF complex **50** (δ = +33ppm). This difference can be attributed to the isopropylphosphine being more electron-rich and therefore tending to donate more electron density through phosphorus to the palladium. Furthermore, such a result bodes well for the catalytic properties of the complex.

Cyclic voltammetry of the new complex **51** in dichloromethane solution (Fig. 3.16, overleaf) gave a partially reversible one-electron oxidation arising from the iron (II)/ iron (III) redox system, at a potential of $E^{o\prime}$ = +0.93V *vs.* SCE.[122] The difference between this potential and that of the free ligand ($E^{o\prime}$ = +0.43V) is indicative of the increase in stability produced by complexation. Clearly the palladium complex is also more

oxidatively stable than its nickel analogue ($E^{o\prime}$ = +0.70V). The complex also displayed an irreversible two-electron reduction at $E^{o\prime}$ = -1.80V which corresponds to the reduction of palladium from oxidation state (II) to (0). This result is also important with respect to the catalytic properties of the complex, since many of the proposed intermediates in the catalytic cycles outlined in Chapter 1 require a two-electron palladium reduction.

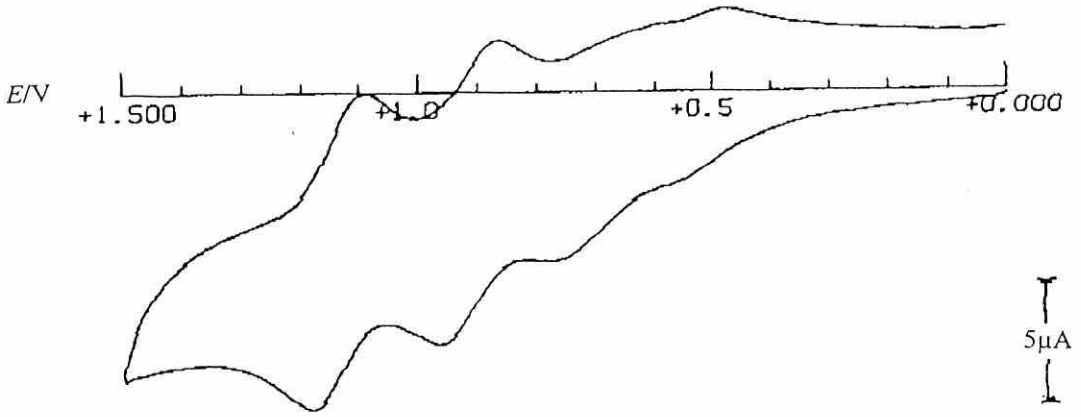

Figure 3.16 Cyclic voltammogram of *cis*-dichloro[1,1'-bis(diisopropylphosphino)ferrocene]palladium (II): scan rate = 200mVs^{-1}

The single crystal X-ray structure of *cis*-[$PdCl_2$(DIPPF)] **51** (Fig. 3.17) was obtained from a crystal grown by slow diffusion from a layer of dichloromethane into a layer of *n*-hexane. The complex has a slightly distorted square-planar geometry, with the palladium lying out of the plane of P-fc-P. Such a geometry explains the observation made on the ^{1}H NMR spectrum, since in the complex four methyl groups are nearer the metal than are the other four, thus there is a distinct difference in the shielding of each set of resonances. The solid state structure includes a bidentate phosphine bite angle about the metal of 103.4°, larger than that of the analogous DPPF complex **50** (99.1°) by some 4.3°. This feature is important from the point of view of catalysis, as described in Chapter 1. The Cl-Pd-Cl angle, at 87.7°, is correspondingly smaller than that of *cis*-[$PdCl_2$(DPPF)] **50**. The mutually *cis* chlorine atoms have slightly longer than normal bond lengths, 2.36Å, reflecting the *trans* effect of the phosphines.[52]

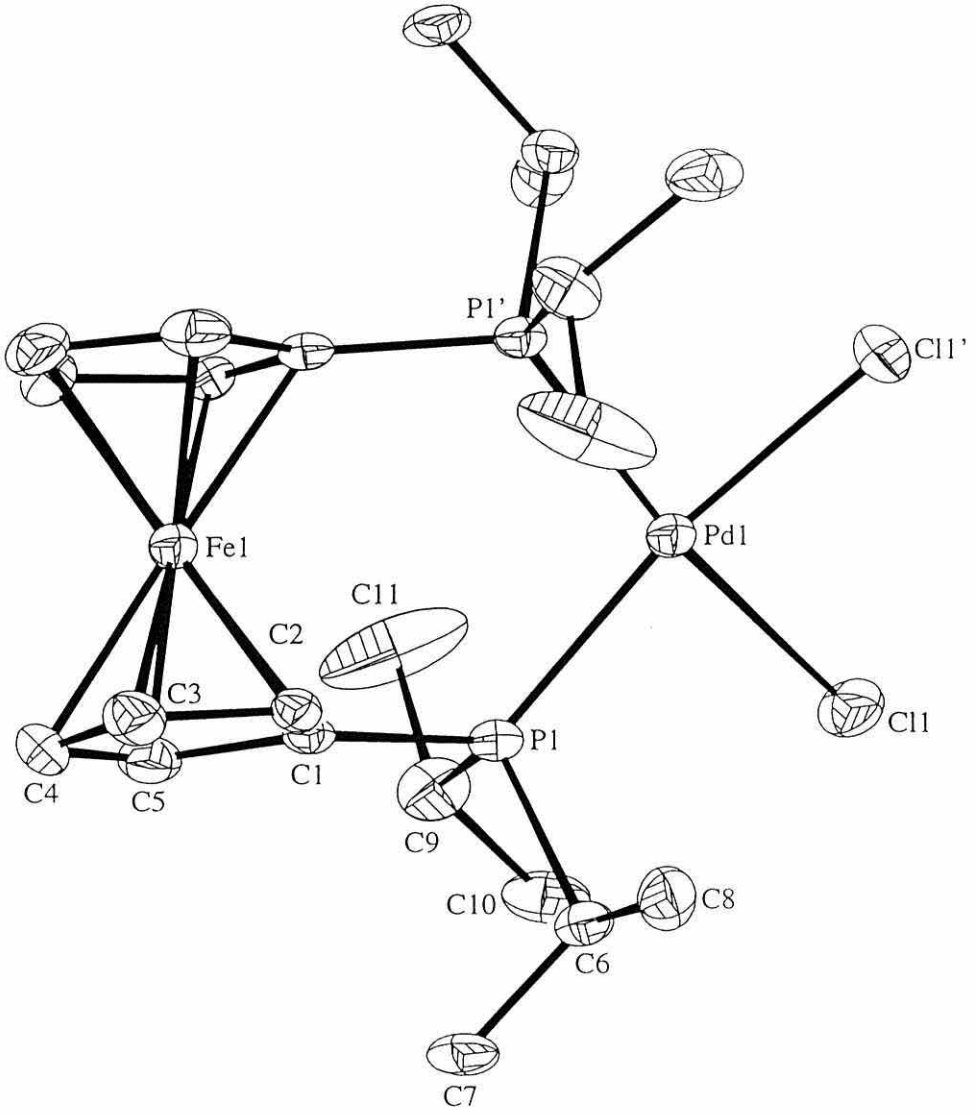

Figure 3.17 Single crystal X-ray structure of *cis*-[$PdCl_2$(DIPPF)] **51**

Empirical formula	$C_{22}H_{36}Cl_2FeP_2Pd$
Formula weight	595.60
Temperature	150 (2) K
Wavelength	0.71069Å
Crystal system	Orthorhombic
Space group	Pnna
Unit cell dimensions	a = 16.028 (3)Å
	b = 16.944 (3)Å
	c = 8.887 (2)Å
Volume	2413.5 (8)Å^3
Z	4
Density (calculated)	1.639 mg/m^3
Absorption coefficient	1.707 mm^{-1}
F (000)	1216
Crystal size	0.20 x 0.16 x 0.12 mm (RED)
Theta range for data collection	2.40 to 24.96°
Index ranges	-18<=h<=11, -14<=k<=20, -10<=l<=10
Reflections collected	6558
Independent reflections	1889 [R (int) = 0.0903]
Refinement method	Full-matrix least-squares on F^2
Data/restraints/parameters	1889/0/132
Goodness-of-fit on F^2	0.821
R indices [on 1322 data with I>2Σ(I)]	R1 = 0.0329, wR2 = 0.0692
R indices (all data)	R1 = 0.0530, wR2 = 0.0720
Largest diff. peak and hole	1.817 and -0.490 e.A^{-3}

Table 3.4 Crystal data and structure refinement for *cis*-[$PdCl_2$(DIPPF)] **51**

3.3.3 *cis*-Dichloro{(*R,S*)-1,1'-bis(diisopropylphosphino)-2-[(*N,N*-dimethylamino)ethyl]ferrocene}palladium (II) - Dichloromethane Solvate

A palladium complex of IPPFA **5** was prepared by mixing the ligand with 0.95 equivalents of *cis*-[Pd(COD)Cl_2] in dichloromethane, with subsequent crystallisation from dichloromethane/ *n*-hexane. The complex **52** was orange-red in colour, typical of a square-planar co-ordination geometry, and was characterised by NMR and IR spectroscopy, mass spectrometry and elemental analysis. The ^{31}P-{^{1}H} spectrum shows two doublets at δ = 75.9 and 57.5ppm, each with a phosphorus-phosphorus coupling constant of $^{2}J_{P\text{-}P}$ = 25Hz, the result of a through-metal interaction which can only be seen in this case by virtue of the chirality of the ligand; the same interaction is not apparent in either of the achiral complexes *cis*-[$PdCl_2$(DIPPF)] **51** and *cis*-[$PdCl_2$(DPPF)] **50**.

Cyclic voltammetry of the new complex **52** in dichloromethane solution (Fig. 3.18, overleaf) gave a partially reversible one-electron oxidation arising from the iron (II)/ iron (III) redox system, at a potential of $E^{o\prime}$ = +0.89V *vs.* SCE.[122] Complex **52** is, therefore, intermediary in oxidative stability between [$NiCl_2$(DIPPF)] **49** ($E^{o\prime}$ = +0.70V) and *cis*-[$PdCl_2$(DIPPF)] **51** ($E^{o\prime}$ = +0.93V), although in this case no reduction potential for the palladium (II)/ (0) reduction was detected.

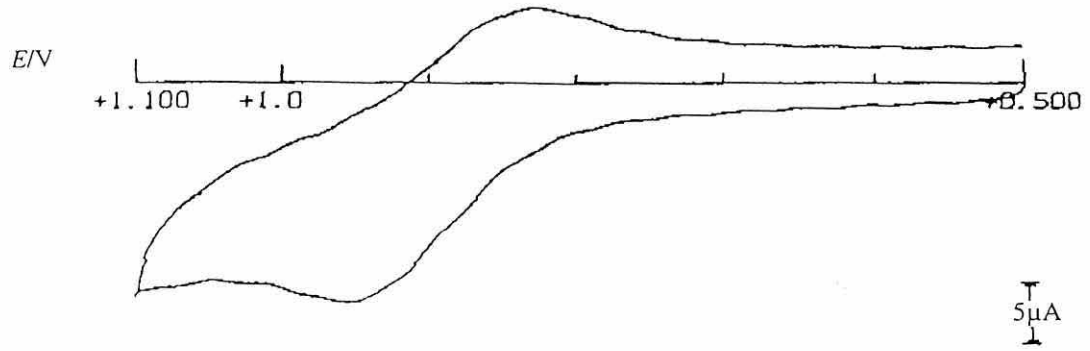

Figure 3.18 Cyclic voltammogram of *cis*-dichloro{(*R,S*)-1,1'-bis(diisopropylphosphino)-2-[(*N,N*-dimethylamino)ethyl]ferrocene}palladium (II): scan rate = 200mVs^{-1}

The single crystal X-ray structure of *cis*-[$PdCl_2$(IPPFA)] **52** (Fig. 3.19) was obtained from a crystal grown by slow diffusion from a layer of dichloromethane into a layer of *n*-hexane. The palladium is co-ordinated to the two phosphine groups and not to the amine. The structure shows the predicted stereochemistry of (*R,S*) and the complex was found to crystallise in a 1:1 molar ratio with dichloromethane. The geometry of the complex is distorted square-planar, with the palladium lying slightly out of the plane of P-fc-P. The solid state structure includes a bite angle about the metal of 103.1°, larger than that of the analogous BPPFA **18** complex (98.8°)[51] by some 4.3°, but very similar to that of the achiral analogue DIPPF **7** (103.4°). This feature is important from the point of view of catalysis, as described in Chapter 1. The Cl-Pd-Cl angle, at 86.6°, is again similar to that of *cis*-[$PdCl_2$(DIPPF)] (87.7°) and *cis*-[$PdCl_2$(BPPFA)] (87.8°).[51] The mutually *cis* chlorine atoms have longer than normal bond lengths, 2.378Å, again reflecting the *trans* effect of the phosphines.

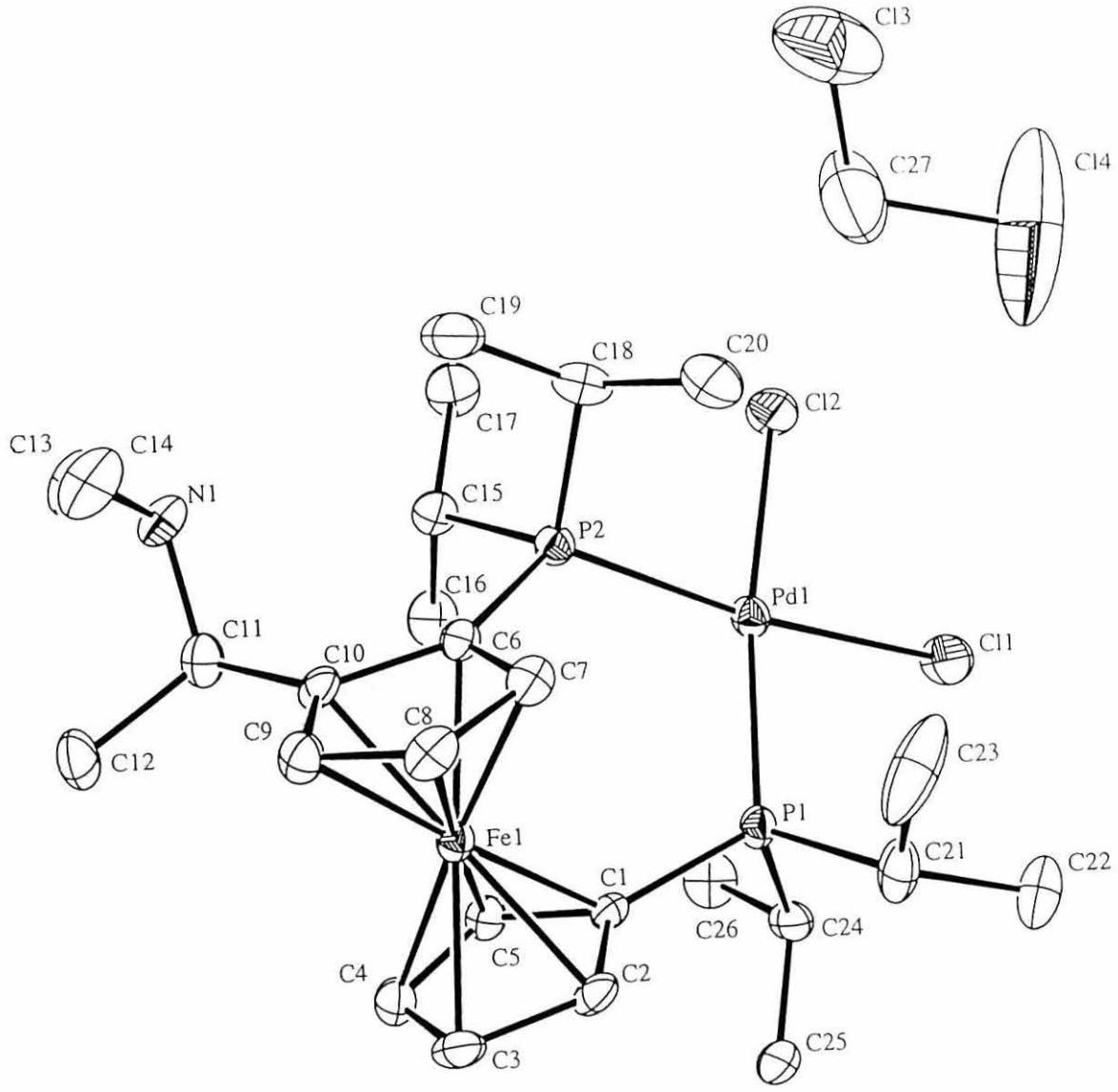

Figure 3.19 Single crystal X-ray structure of *cis*-[$PdCl_2$(IPPFA)].CH_2Cl_2 **52**

Empirical formula	$C_{27}H_{47}Cl_4FeNP_2Pd$
Formula weight	751.65
Temperature	150 (2) K
Wavelength	0.71073Å
Crystal system	Orthorhombic
Space group	P2 (1) 2 (1) 2 (1)
Unit cell dimensions	a = 13.5430 (5)Å
	b = 14.9910 (9)Å
	c = 16.0090 (10)Å
Volume	3250.2 (3)Å^3
Z	4
Density (calculated)	1.536 mg/m^3
Absorption coefficient	1.445 mm^{-1}
F (000)	1544
Crystal size	0.2 x 0.1 x 0.2 mm (RED)
Theta range for data collection	2.96 to 28.30°
Index ranges	-16<=h<=16, -19<=k<=19, -21<=l<=21
Reflections collected	7850
Independent reflections	7850 [R (int) = 0.0000]
Refinement method	Full-matrix least-squares on F^2
Data/restraints/parameters	7850/0/329
Goodness-of-fit on F^2	1.060
R indices [on 1322 data with I>2Σ(I)]	R1 = 0.0538, wR2 = 0.1012
R indices (all data)	R1 = 0.0730, wR2 = 0.1111
Absolute structure parameter	-0.01 (3)
Largest diff. peak and hole	1.331 and -1.037 e.A^{-3}

Table 3.5 Crystal data and structure refinement for *cis*-[$PdCl_2$(IPPFA)].CH_2Cl_2 **52**

3.4 Catalysis

3.4.1 The Heck Reaction

In view of previous testimony as to the efficacy of diisopropylphosphine ligands[82] and the demonstrated difference between the reactivity of DPPF **6** and DIPPF **7**,[99] the palladium-DIPPF complex **51** was expected to be effective in the catalytic Heck coupling. The original Heck reaction mixture comprises palladium (II) acetate, a hindered base, a phosphine, the reagent and substrate and acetonitrile as solvent. These conditions were, therefore, retained with the sole exception that the palladium (II) acetate and phosphine were replaced with *cis*-[$PdCl_2$(DIPPF)] **51**.

Successful coupling of iodobenzene **53** with methyl acrylate **54** (Fig. 3.20) could only be achieved with the addition of a catalytic amount of copper (I) iodide (stoichiometric with respect to palladium): test reactions in the absence of co-catalyst or in the presence of zinc metal as reducing agent led to no observable reaction after 24h. Upon addition of copper (I) iodide, however, the coupling was found to yield 100% conversion (GLC) to methyl cinnamate **55** after 24h, with no evidence of by-product formation. The product was isolated in 96% yield by extraction and chromatography on silica using 5% ether/ petrol and was characterised by comparison of its physical and spectroscopic data with those of an authentic sample. The ^{1}H NMR spectrum showed a characteristic *trans* coupling constant between the two alkenyl protons of $^3J_{H,H}$ = 16Hz: a *cis* coupling constant would be in the region of 7-9Hz.

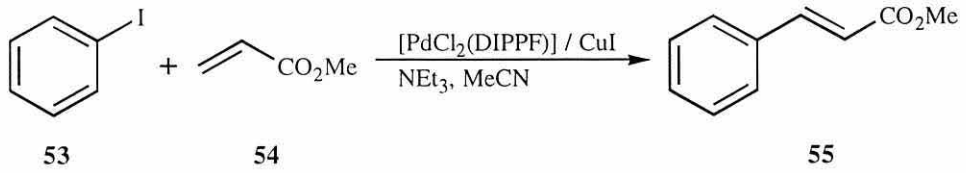

53 **54** **55**

Figure 3.20 Heck coupling of iodobenzene with methyl acrylate

Several reasons for the observed rate increase with copper (I) iodide are possible. The first (**A**) is that the copper (I) iodide undergoes halogen exchange with the catalyst precursor to give an iodo-chloropalladium species which would presumably be more active than the dichloro-precursor (Fig. 3.21). The second (**B**) is that the copper (I) reduces the palladium (II) and is itself oxidised up to copper (II). A third possibility (**C**) is that the introduction of a soft ligand such as iodide produces competition for the co-ordination sites about the palladium and promotes phosphine dissociation to open up an active site, while remaining in a catalytic role. Whichever method is nearer to reality, it is clear that without the employment of the copper (I) iodide co-catalyst the catalysis is ineffective.

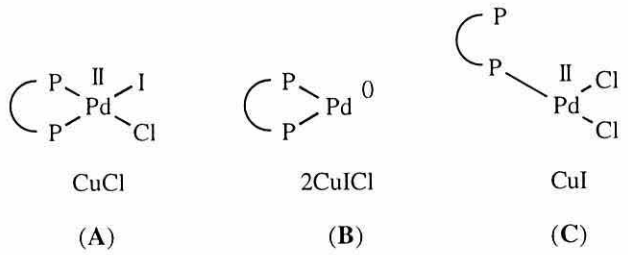

Figure 3.21 Possible explanations for copper (I) iodide rate increase

The new catalyst mixture was used in attempts to couple bromobenzene and chlorobenzene, but in both cases there was no sign of methyl cinnamate in the reaction mixture after 24h. In order to assess the scope of the catalyst mixture, a range of other alkene substrates were coupled with iodobenzene **53**. Thus, methyl methacrylate **56**, vinyl acetate **57**, acrylonitrile **58**, *n*-butyl vinyl ether **59**, styrene **60** and vinylidene chloride **61** were coupled with iodobenzene under analogous conditions. The results varied considerably, so each reaction will be discussed in turn.

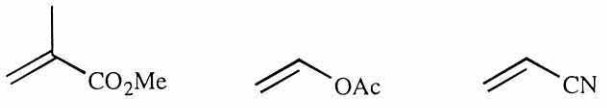

56 **57** **58**

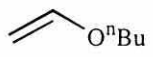

59

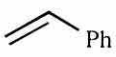

60

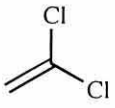

61

Firstly, the coupling of iodobenzene **53** with methyl methacrylate **56** might have been expected to mirror that of methyl acrylate **54**, however, this was found not to be the case. Following the method outlined above for the methyl acrylate coupling, a 3:1 mixture of two coupling products was obtained after the 24h reflux. GLC/MS showed these to be the *trans*-cinnamate **62** and its *gem*-substituted isomer **63**. Work-up of the reaction mixture followed by careful flash chromatography on silica gel (using light petroleum) yielded the mixture as a single fraction which allowed characterisation by ^{1}H NMR and showed the same 3:1 ratio observed by GLC.

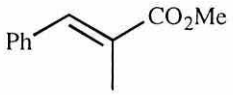

62

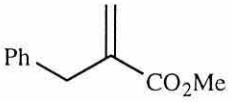

63

The ^{1}H NMR spectrum of the major product **62** showed two methyl group resonances at δ = 2.14 and δ = 3.84ppm. The downfield resonance is clearly that of the methyl ester, while the other methyl group shows allylic coupling of $^4J_{H,H}$ = 1.5Hz across the double bond. However, in the spectrum of the minor product **63** only one methyl group resonance is present, that of the methyl ester: the benzylic methylene group shows allylic coupling of $^4J_{H,H}$ = 1.2Hz to the proton *trans* across the double bond, while this proton is also coupled to its geminal neighbour with a coupling constant of $^2J_{H,H}$ = 2.7Hz (Fig. 3.22, overleaf).

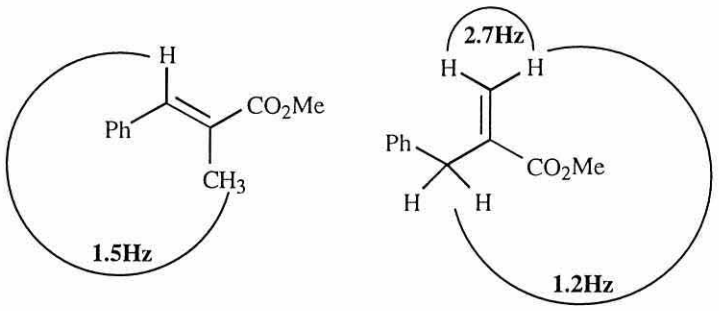

62 **63**

Figure 3.22 Allylic couping in major (LEFT) and minor (RIGHT) products from methyl methacrylate coupling

A possible explanation for the formation of this by-product **63** can be offered by consideration of the reaction mechanism, which by virtue of the isopropenyl group in the starting material can in this case be assumed to proceed under basic conditions *via* a palladium-π-allyl intermediate (Fig. 3.23).

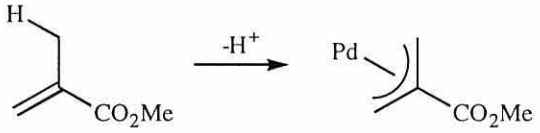

Figure 3.23 Formation of a η^3- allyl intermediate in the reaction of methyl methacrylate

This intermediate could then allow for substitution at either end of the allyl group, yielding the observed product mixture, with the further possibility of *cis*-cinnamate formation. The observed dominance of the *trans*-cinnamate **62** in the mixture can be attributed to the thermodynamic stability of such species being extended conjugated systems, relative to that of the alternative in which the conjugation is interrupted by the benzylic methylene group. In an attempt to prove this further, the products were subjected to a reflux in the presence of the catalyst mixture but in the absence of any further substrate, with the expectation of producing a single thermodynamic *trans*-cinnamate product, however, the initial product ratio was observed to persist.

The coupling of vinyl acetate **57** was found to be among the highest yielding and cleanest of the reactions, yielding the desired *trans*-derivative **64** almost quantitatively (98.5%). A trace of the *cis*-coupled product **65** was detected by GLC/MS (<1%), along with a small quantity of phenyl acetaldehyde **70** (<0.5%), identified by spectral comparison with an authentic sample.

64 **65** **66**

The *trans* coupling constant in this case was $^3J_{H,H}$ = 12.8Hz and the corresponding *cis*-isomer **65** exhibited a coupling constant of $^3J_{H,H}$ = 7.1Hz. The small quantity of phenyl acetaldehyde **66** in the reaction mixture increased considerably upon acid work-up and can be attributed to hydrolytic cleavage of the acetate to produce the enol which then tautomerises to the observed aldehyde (Fig. 3.24).

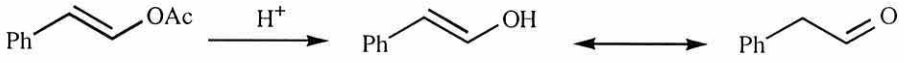

Figure 3.24 Formation of phenyl acetaldehyde by-product

Acrylonitrile **58** gave rise to a 3:1 mixture of diastereomeric products albeit in low yield (27%). The *trans*-isomer **67** exhibited a coupling constant of $^3J_{H,H}$ = 16.4Hz while the *cis*-isomer **68** gave a coupling constant of $^3J_{H,H}$ = 12.1Hz.

67 **68**

n-Butyl vinyl ether **59** produced phenyl acetaldehyde **66** (18%), the required *trans*-

coupling product **69** (8%; $^3J_{H,H}$ = 13.0Hz) and its *cis*-isomer **70** (7%; $^3J_{H,H}$ = 7.0Hz).

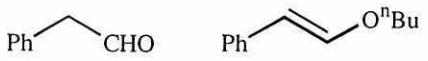

66 **69** **70**

The low yield observed in this reaction can be explained by hydrolytic cleavage of the butyl-oxygen bonds in the products **69** and **70** to generate the enolate tautomer of phenyl acetaldehyde **66**, however, the lack of selectivity in the configuration of **69** and **70** has been observed previously in similar systems.[86]

Styrene **60**, containing no electron-withdrawing substituent, is less reactive than the other substrates tested and this lack of reactivity accounts for the low (13%) yield of *trans*-stilbene **71**. The only by-product observed was the *cis*-isomer **71** (4.5%) and again the two configurations were coincidentally present in the ratio 3:1. Due to the C_2 symmetry of the products no coupling between the alkenyl protons was observed in the ^{1}H NMR spectrum of the isolated *trans*-stilbene **71**: instead both protons coincide as a singlet at δ = 7.27Hz. This singlet is also coincident with that of chloroform in the solvent and required a high concentration of sample to be used in order to prove its existence. On close examination the integration of 2H not only corresponded to the multiplet of 10H expected for the phenyl resonances, but it also matched exactly the integration of the section of the multiplet arising from the two *para*-protons.

71 **72**

The only negative result was the attempted coupling of vinylidene chloride **61** with iodobenzene **53**. A possible explanation for this is that the chlorides are not sufficiently electron-withdrawing, although it is likely that halide scrambling and decomposition are responsible for the lack of recoverable starting material in the reaction mixture.

In order to assess the efficiency of isopropylphosphines compared to their phenylphosphine counterparts in the Heck reaction, the coupling of iodobenzene **53** and methyl acrylate **54** was repeated in the presence of the palladium complexes of a series of previously reported isopropyl- and phenylphosphine ligands **73**,[7] **74**,[119] **75**,[7] **33**[17] and **76**.[17]

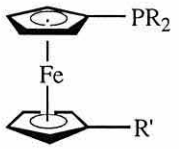

	R	R'
73	Ph	P^iPr_2
74	Ph	H
75	^{i}Pr	H
33	Ph	Br
76	^{i}Pr	Br

Iodoferrocene **77**[131] was chosen as a second substrate, in addition to iodobenzene, since the coupled cinnamate analogue **78** could be of synthetic use in polymer chemistry.[132] The reactions were carried out in the same manner as the above Heck reaction using **51**, with 1 mol% catalyst precursor and an excess of methyl acrylate with respect to the aryl iodide. The results of both sets of reactions are summarised in Table 3.6 (overleaf).

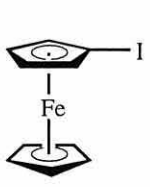

77

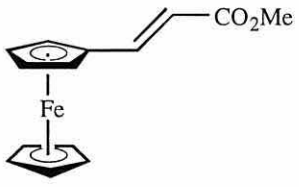

78

$[PdCl_2L_2]$ L =	Recovered PhI (%)	$PhCH=CHCO_2CH_3$ (%)		Recovered FcI (%)	$FcCH=CHCO_2CH_3$ (%)	
		cis	*trans*		*cis*	*trans*
6	(93)	0	(7)	92	0	4
7	0	0	96 (100)	56	0	38
73	(43)	(4)	(53)	74	0	20
74	(72)	(3)	(25)	88	0	12
75	(3)	(1)	(96)	63	0	32
33	(89)	(<1)	(10)	93	0	4
76	0	3 (4)	94 (96)	66	0	30

Table 3.6 Heck coupling of aryl iodides with methyl acrylate in the presence of palladium-ferrocenylphosphines (yields in parentheses are from GLC; others are isolated yields)

The product from the reactions using iodoferrocene **77** had to be isolated in each case as a consequence of its involatility. Aqueous work-up and column chromatography on silica using 5% ether/ petrol then ether yielded red crystals of **78** which were characterised by NMR and IR spectroscopy and mass spectrometry. The ^1H NMR spectrum shows a *trans* coupling constant of 16Hz which is identical to that of the phenyl analogue, methyl cinnamate **55**.

The results shown in Table 3.6 demonstrate a clear advantage in the use of isopropylphosphines over their phenylphosphine counterparts. The difference in reactivity can be attributed directly to the more electron-rich isopropylphosphines in comparison to the phenylphosphines providing greater electronic stabilisation to the catalyst. As expected, the bidentate ligand DIPPF **7** provided the highest regioselectivity because of the flexibility and chelate effect associated with such a system. Furthermore, the bite angle of *cis*-$[PdCl_2(DIPPF)]$ **51** (103.4°) is large relative to other bidentate phosphine complexes {*e.g. cis*-$[PdCl_2(DPPF)]$ **50**, 99.1°}.[52] Interestingly, the hybrid 1-(diisopropylphosphino)-1'-(diphenylphosphino)ferrocene[7] ligand **73** provided a correspondingly intermediate set of results, lying between those of DPPF **6** and DIPPF

7. The similarity in the results using ligands **74** and **33** and ligands **75** and **76** would indicate that the effect of non-participating 1'-substituents on the ferrocene backbone is negligible.

The asymmetric coupling reaction described by Hayashi *et al.*[83] was also examined, under the catalytic conditions successfully employed for the methyl acrylate/ iodobenzene system and using the chiral complex *cis*-[$PdCl_2$(IPPFA)] **52**. One limitation of this reaction is the requirement for aryl triflates, the reaction of aryl iodides producing racemic products. Hayashi *et al.* attributed this difference in selectivity to the relative stability of the leaving group, *viz.* $TfO^- > I^-$.

A similar reaction was studied, that of 2,3-dihydropyran **89** and iodobenzene **77** (Fig. 3.25), since it was hoped that if the triflate leaving group were unnecessary in the presence of a different catalyst, then the coupling might be successfully achieved using iodobenzene as before. However, the conversion observed 24h into the reaction, at <5%, meant that not only was the rate of reaction too low to be synthetically useful, but the quantity of product present in the reaction mixture was too small to measure any asymmetric induction.

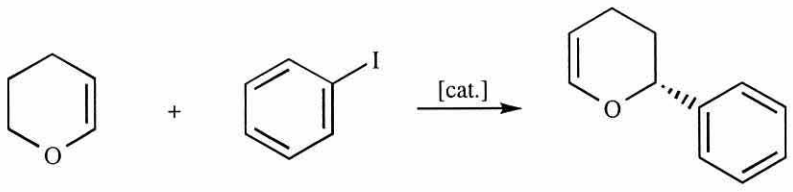

89 **77**

Figure 3.25 Attempted asymmetric Heck reaction

3.4.2 Organomagnesium Cross-Coupling

The cross-coupling reaction of bromobenzene **79** with *sec*-butylmagnesium chloride **80** in the presence of *cis*-[$PdCl_2$(DPPF)] **50** has been reported to yield *sec*-butylbenzene **81** in 95% isolated yield with no observable by-product formation.[52] The Grignard cross-coupling reaction was therefore chosen to test the nickel and palladium DIPPF complexes **49** and **51** in their catalytic activity, as compared with that of *cis*-[$PdCl_2$(DPPF)] **50**.

sec-Butylmagnesium chloride **80** was prepared from 2-chlorobutane and magnesium in ether according to the literature method.[133] The excess magnesium was negligible but the solution was titrated nonetheless, using a standardised solution of hydrochloric acid. The catalysis was achieved also by repeating the literature method (Fig. 3.26), with addition of millimolar quantities of the reagent and substrate at *ca.* -80°C to 1 mol% of the catalyst precursor, under argon.[52]

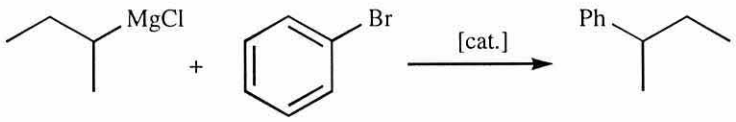

79 **80** **81**

Figure 3.26 Catalytic cross-coupling of bromobenzene and *sec*-butylmagnesium chloride

Aliquots were quenched at intervals with dilute hydrochloric acid and the organic layer of each was analysed directly by gas chromatography. The components of the reaction mixture were identified by GLC/MS so that subsequent reactions could be monitored by comparison alone. The reaction was repeated using each of the nickel and palladium complexes prepared, and the results are presented graphically overleaf (Fig. 3.27).

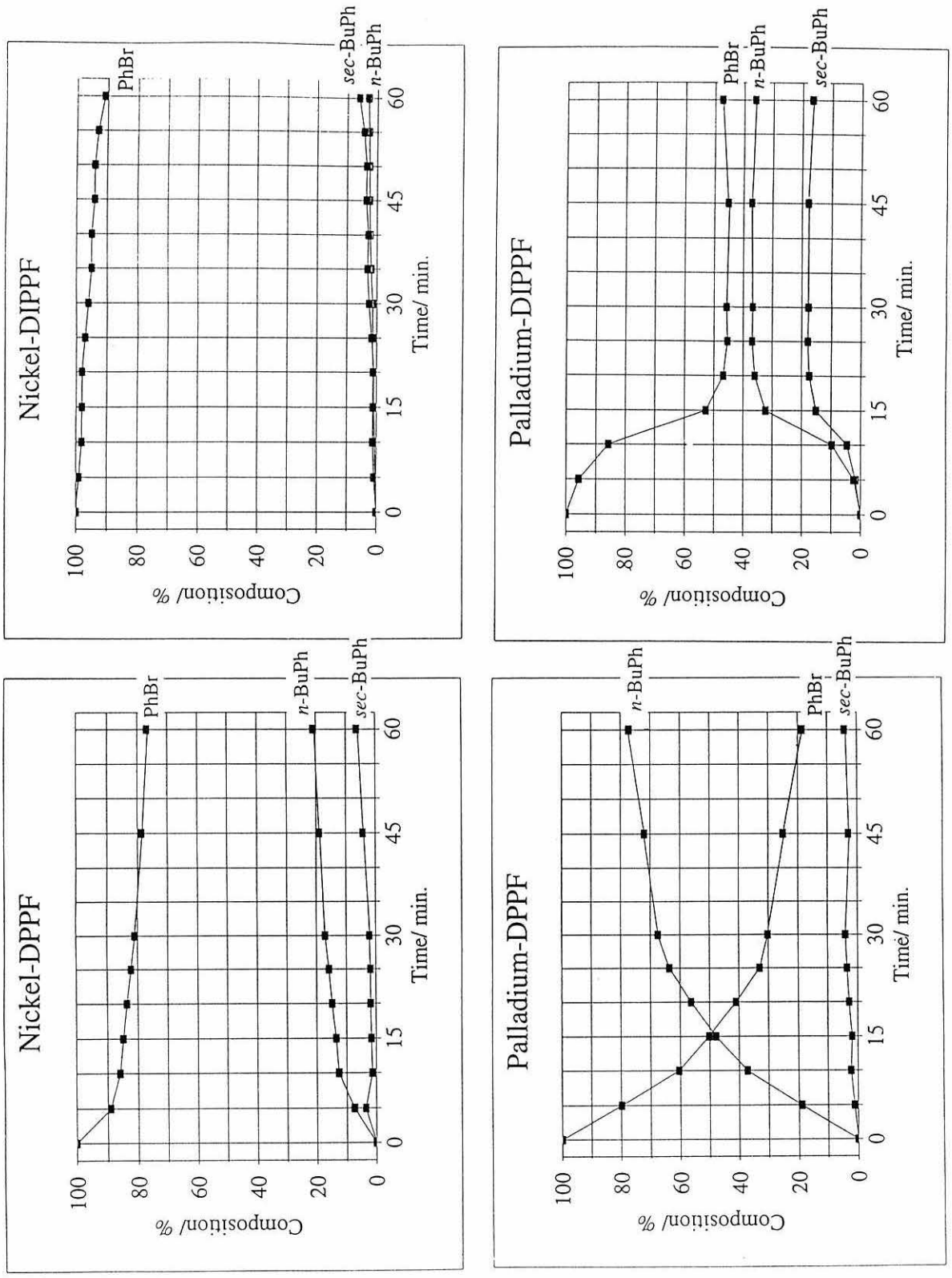

Figure 3.27 Cross-coupling reaction profiles for different catalysts

From the results in Figure 3.27 it is clear that the nickel-phosphine complexes **48** and **49** form less efficient catalysts than do their palladium counterparts **50** and **51**. The nickel-DIPPF catalyst precursor **49** gave no observable reaction over one hour and nickel-DPPF **48** gave only 20% conversion of starting material over the same period. This result could be expected in view of the fact that for the nickel catalysed cross-coupling reaction, Kumada *et al.*[134] concluded that DPPP was the optimal ligand.

The complex *cis*-[$PdCl_2$(DIPPF)] **51** produces the highest rate of reaction and is therefore the best catalyst, in terms of turnover, of the series studied (the reaction effectively reaching completion in a matter of 15 min.), however the product mixture was largely *n*-butylbenzene and not the expected *sec*-butylbenzene **81**. This is most likely to be the result of a β-elimination leading to isomerisation, as proposed again by Kumada *et al.*[134] who studied the nickel catalysed reaction between chlorobenzene and isopropylmagnesium chloride (Fig. 3.28).

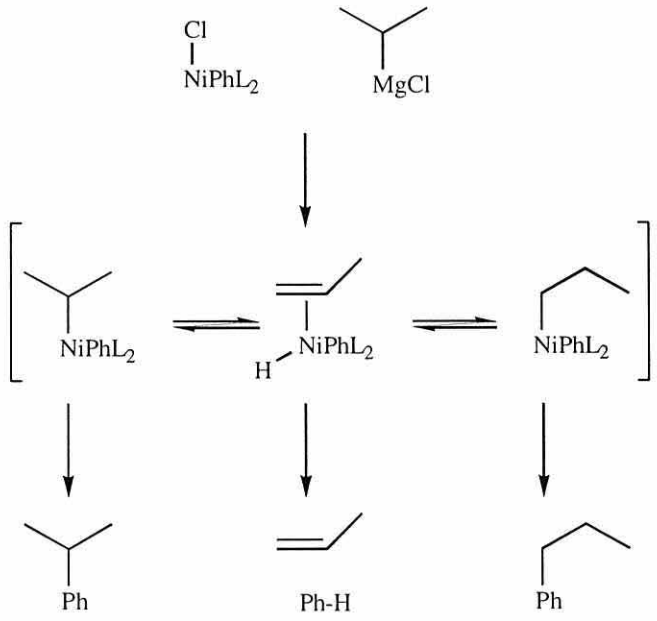

Figure 3.28 Isomerisation of metal-alkenyl intermediate: L = phosphine or diphosphine

Such a mechanism was supported in part by the detection of a trace amount (*ca.* 0.05%) of 2-butenylbenzene by GLC/MS. The lifetime of the intermediate metal-alkenyl

complex shown would be largely dependent upon the strength of the metal-alkenyl co-ordinative bond, which in turn would depend upon the electronic stabilisation about the metal due to the phosphine ligand. Kumada *et al.* suggested that an increase in the electron density about the metal due to the effects of strongly electron-donating ligands would facilitate the σ-π conversion necessary to produce the intermediate metal-alkenyl complex.[134]

The fact that the isomerisation from *sec*- to *n*-butyl-palladium took place in the presence of DIPPF **7** but not DPPF **6** supports the assumption that in common with other alkylphosphines, DIPPF is a much better donor than the arylphosphine DPPF. In order to further illustrate this point, a sample of 1,1'-bis(diisopropylphosphoryl)ferrocene **82**, the dioxide of DIPPF, was deliberately prepared by reaction of the phosphine with an excess of hydrogen peroxide, on an NMR-tube scale. The $^{31}P-\{^{1}H\}$ NMR spectrum was recorded and the shift of δ = 64.5ppm was also identified in the spectrum of a sample of DIPPF left open to the air for several days. The large downfield shift with respect to the phosphine is a result of the electron density being removed from phosphorus (Table 3.7, overleaf). The chemical shift of phosphine oxides has been shown to provide a better measure of the phosphine basicity than the shift of the phosphine itself, because the tetrahedral geometry of the phosphine oxide limits the contribution to basicity of steric effects such as the R-P-R bond angle.[135] Thus, the shift of DIPPF oxide **82**, at δ = +64.5ppm, indicates that DIPPF **7** is indeed a much stronger base than DPPF **6** (for DPPF oxide, δ = +28.3ppm).[136] Since DIPPF is a stronger base, upon co-ordination to a metal it will provide better complex stabilisation, thus explaining the observed difference between the reactivity of complexes of DIPPF and DPPF.

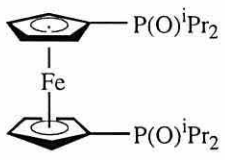

82

LIGAND	$^{31}P-\{^{1}H\}$ δ (ppm) =		
	Phosphine	Phosphine Oxide	Δ ($\delta_{P=O}-\delta_{P}$)
DIPPF	+0.3	+64.5	+64.2
DPPF	-17.2	+28.3	+45.5

Table 3.7 Comparison of $^{31}P-\{^{1}H\}$ NMR shifts for phosphines and phosphine oxides

3.4.4 Other Cross-Couplings

The Suzuki-type cross-coupling of a number of aryl halides with phenylboronic acid **83** was examined using the nickel and palladium complexes of DIPPF, **49** and **51**. The coupling of 4-chlorotoluene **84** and phenylboronic acid has been reported to proceed in high yield using [$NiCl_2$(DPPF)] **49** as catalyst precursor, when the complex is first treated with four molar equivalents of *n*-butyllithium in order to produce a nickel (0) active catalyst.[137]

While the reported reaction in 1,4-dioxane solution was found to be repeatable (Fig. 3.29, overleaf), albeit in greatly reduced yield (36% *vs.* 69%[137]) using freshly distilled 4-chlorotoluene **84**, the reported reaction in THF solution produced no observable product formation. THF can be expected to be less efficacious on two accounts: firstly, the boiling point and therefore reaction temperature (reflux) of THF is some 35 °C lower than that of dioxane and secondly, both the polarity and co-ordinating ability of THF are lower than those of dioxane. Considering the ionic nature of many of the intermediates in the Suzuki catalytic cycle, both of these are important parameters in the choice of solvent. When [$NiCl_2$(DIPPF)] **49** was used as the catalyst precursor, however, no reaction was observed in either solvent.

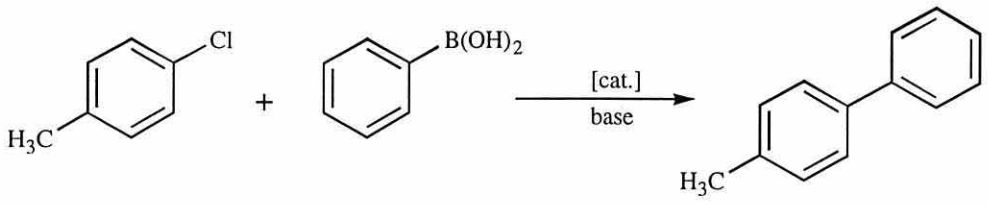

84 83

Figure 3.29 Cross-coupling of 4-chlorotoluene and phenylboronic acid

Indolese[107] recently claimed that aryl chlorides could be coupled using a similar protocol but without the initial deliberate reduction of the nickel. This reaction was found to be unrepeatable using the reported conditions. The same outcome was observed using [$NiCl_2$(DIPPF)] **49** as the catalyst precursor. However, when the aryl chloride was replaced with iodobenzene **53**, some conversion of phenylboronic acid to biphenyl **85** was observed by GLC (9%).

Aryl bromides and iodides were, nevertheless, successfully coupled using *cis*-[$PdCl_2$(DIPPF)] **51**. The reaction of phenylboronic acid **83** with iodobenzene **53** in dioxane using K_3PO_4 as base gave 93% GLC yield of biphenyl **85**, whilst the same coupling with bromobenzene **79** proceeded in 85% GLC yield. In line with concurrent work within the research group using anthracenyl halides, 9-iodoanthracene **86** and 9-bromoanthracene **87** were also coupled with phenylboronic acid **83**, in 38% and 26% GLC yield respectively. Anthracenyl halides are generally less reactive in such reactions compared to their phenyl counterparts, so the lower yields are to be expected. Interestingly, in none of the reactions, whether successful or not, was there any evidence of biphenyl having been formed as a by-product. Where this has been reported previously, the ratio of product to by-product has been *ca.* 50:1,[107] so it is to expected that any by-product generated during the anthracenyl or chlorotolyl couplings would have been beyond the lower limits of detection.

As an alternative to phenylboronic acid **83** and again in line with concurrent work, the

coupling of ferrocenylboronic acid **88** was examined. This bright yellow compound is sensitive to temperature and moisture, and the coupling was unsucessful under various conditions. In each case a considerable quantity of ferrocene was observed by TLC, presumably the result of decomposition of the substrate which has been observed under similar conditions.[138] These results are summarised in Table 3.8.

$[MCl_2L]$ M, L =	^{n}BuLi	$ArB(OH)_2$ Ar =	ArX	SOLVENT	PRODUCT	YIELD GLC, %
Ni, DPPF	4eq.	Ph	4-Tol-Cl	dioxane	4-Tol-Ph	36
Ni, DPPF	4eq.	Ph	4-Tol-Cl	THF	-	0
Ni, DIPPF	4eq.	Ph	4-Tol-Cl	dioxane	-	0
Ni, DIPPF	4eq.	Ph	4-Tol-Cl	THF	-	0
Ni, DPPF	-	Ph	4-Tol-Cl	dioxane	-	0
Ni, DIPPF	-	Ph	4-Tol-Cl	dioxane	-	0
Ni, DIPPF	-	Ph	Ph-I	dioxane	Ph-Ph	9
Pd, DIPPF	-	Ph	Ph-I	dioxane	Ph-Ph	93
Pd, DIPPF	-	Ph	Ph-Br	dioxane	Ph-Ph	85
Pd, DIPPF	-	Ph	An-I	dioxane	9-Ph-An	38
Pd, DIPPF	-	Ph	An-Br	dioxane	9-Ph-An	26
Pd, DIPPF	-	Fc	Ph-I	dioxane	-	0
Ni, DIPPF	-	Fc	Ph-I	dioxane	-	0
Ni, DPPF	4 eq.	Fc	Ph-I	dioxane	-	0

Table 3.8 Cross-coupling of aryl halides with arylboronic acids in the presence of metal-phosphine catalysts

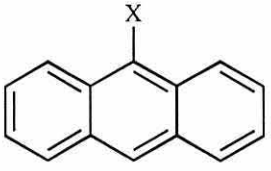

86 X = I

87 X = Br

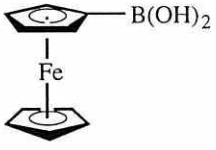

88

The homocoupling of 4-chlorotoluene **84** was also attempted in the presence of the $[NiCl_2(DIPPF)]$ **49** and fresh powdered zinc according to the procedure of Colon and Kelsey.[108] However, no coupling was observed after a 48h reflux in DMF. Interestingly, traces of toluene were detected by GLC, showing that the chloride had been removed and indicating that the rate determining step is the oxidative addition of the aryl fragment. Unfortunately, the small scale of the reaction rendered the isolation of the catalyst remnants impracticable.

Chapter 4

Conclusions and Further Work

4.1 Outline

The content of this chapter will follow the same sequence as is presented in Chapters 2 and 3, namely the synthesis of ferrocenylamines and ferrocenylphosphines and their co-ordination chemistry, followed by the catalytic studies.

4.2 Synthesis

4.2.1 Ferrocenylamines

A convenient and rapid synthesis of heterosubstituted aminoferrocenes has been developed which allows for the preparation of the simple yet important precursor 1-bromo-1'-aminoferrocene **1**. This compound was successfully protected as its *N*-borane **30**. 1-Bromo-1'-aminoferrocene was shown to be a useful synthon for the preparation of a number of derivatives such as 1-amino-1'-ferrocenecarboxylic acid **2** (as its methyl ester **31**) and 1-(diphenylphosphino)-1'-aminoferrocene **3**.

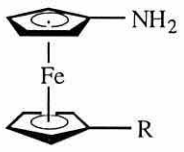

1 R = Br

2 R = CO_2H

31 R = CO_2Me

3 R = PPh_2

As may be expected, most of the derivatives of aminoferrocene are air-sensitive and this may limit their general applicability, as indeed it has their characterisation. Further work is, therefore, required on the protection of these compounds. If, for example, both substituents of 1-(diphenylphosphino)-1'-aminoferrocene **3** could be protected as their

borane adducts, then the ligand could be characterised properly and its co-ordination chemistry could be studied by subsequent deprotection in the presence of a transition metal. Amino acid **2**, meanwhile, could be expected to form complexes wherein the acid proton is lost, to produce a novel *N,O*-donating ligand suitable for chelation to hard metals such as titanium.

The heterosubstitution of the borane-protected 1-bromo-1'-aminoferrocene **30** has yet to be investigated, but this extra protection/ deprotection step may give better access to 1-amino-1'-ferrocenecarboxylic acid **2**.

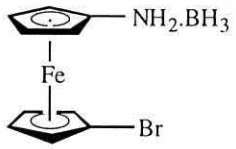

30

Alternatively, the amino acid could be obtained as its hydrochloride salt by bubbling dry hydrogen chloride gas through the reaction mixture, thereby avoiding the introduction of water to the work-up. Although the synthesis of the related 1-amino-2-ferrocene-carboxylic acid **90** is beyond the scope of the current work, some synthetic routes are suggested by this and related work. An efficient synthesis may be to follow the method of Kagan *et al.*,[41] using an *ortho*-lithiated chiral sulfoxide, quenching with *O*-benzylhydroxylamine and protecting with BH_3.THF. The sulfoxide could then be removed and substituted by a carboxylic acid group, thus producing the 1,2-amino acid **90** in optical purity (Fig. 4.1, overleaf).

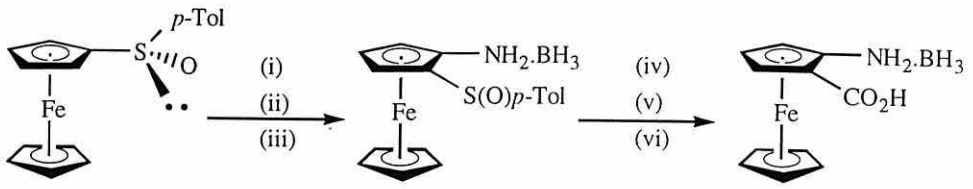

43 **90**

Figure 4.1 Possible synthesis of 1-amino-2-ferrocenecarboxylic acid. (i) LDA, (ii) $BnONH_2$, (iii) BH_3.THF, (iv) ^tBuLi, (v), CO_2, (vi) H_3O^+

Alternatively, if a ferrocenyloxazoline were to be *ortho*-lithiated, reacted with *O*-benzylhydroxylamine, protected with BH_3.THF and treated with acid, then the oxazoline may be cleaved with acid to produce the desired 1,2-amino acid **90**, again in high optical purity (Fig. 4.2).

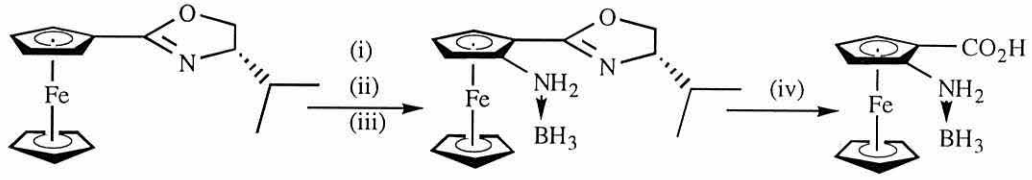

90

Figure 4.2 Alternative possible synthesis of 1-amino-2-ferrocenecarboxylic acid. (i) ^nBuLi, (ii) $BnONH_2$, (iii) BH_3.THF, (iv), H_3O^+

1,1'-Diaminoferrocene **28** has not hitherto been used in co-ordination chemistry. By virtue of the anomalous electrochemical properties of aminoferrocenes,[115] 1,1'-diaminoferrocene could be expected to exhibit behaviour very different from that of the diphosphinoferrocenes and could be an important ligand for electrochemically-controlled catalysis. In view of the stability of 1-bromo-1'-amino(borane)ferrocene **30**, a satisfactory synthetic route to the ligand could be devised starting from this precursor, and the co-ordination chemistry and catalytic properties of the new ligand could then be studied. The strategy for the heterosubstitution of aminoferrocenes described herein has, therefore, opened up the possibility for much further work in the field.

The selective lithiation of (*R,S*)-1,1'-dibromo-2-[(*N,N*-dimethylamino)ethyl]ferrocene **4** proved unsuccessful under the conditions examined. It is possible that effects of solvent and temperature limited the outcome of the reaction and these could be examined in greater depth, however, it is more than likely that the rate of lithium-bromine exchange is too high to allow for the initiation of any electronic or steric directing effects, in which case the current methodology involving ring-opening of a chiral [1]-ferrocenophane[7] will remain the most efficient route to 1,1'-heterodisubstituted chiral amines.

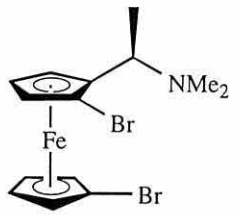

4

The single crystal X-ray structure of *cis*-dichloro-[(*R,S*)-1,1'-bis(diisopropylphosphino)-2-(*N,N*-dimethylamino)ethylferrocene], *cis*-[$PdCl_2$(IPPFA)] **52**, illustrates the structural differences between this and other chiral amine-based ligands such as BPPFA **18**. Unfortunately, the consequences of these differences with regard to catalysis were not demonstrated successfully. Nevertheless, similar complexes of (*tert*-butylphosphino)-ferrocenes have previously been shown to be efficient catalyst precursors for catalytic homogeneous hydrogenation and comparable results may be expected with the electron-rich IPPFA complex.[6] Related reactions such as hydrosilylation and hydroboration should also be catalysed by complexes of IPPFA.

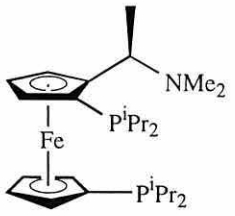

5

4.2.2 Ferrocenylphosphines

The synthesis of a number of ferrocenylphosphine ligands was achieved, some of which are novel and others such as 1,1'-bis(diisopropylphosphino)ferrocene (DIPPF) **7** were prepared for comparative catalytic studies. The nickel and palladium (II) chloride complexes of DIPPF, **49** and **51**, were characterised by single crystal X-ray crystallography and compared with their diphenylphosphino-counterparts. Many structural similarities were found, although the different electronic properties of DIPPF and DPPF **6** were illustrated by comparison of their respective oxides: DIPPF was shown to be much more electron-rich than DPPF.

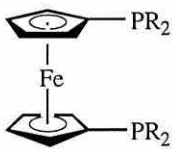

6 R = Ph

7 R = ^{i}Pr

The protection of ferrocenylphosphines as their phosphine-borane adducts was investigated, with the successful employment of BH_3.THF and sodium borohydride/ iodine. The former method was used for *in situ* phosphine protection, while the latter was used to protect previously isolated phosphines in order to prevent their aerobic oxidation. The borane adduct of DIPPF, **41** was synthesised and fully characterised, although the available protocols for deprotection have not yet been applied to this compound. However, it was shown to be oxidatively stable and easily manipulated, two advantages it has over the free phosphine **7**.

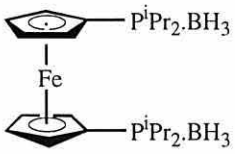

41

The chiral sulfoxide method of Kagan *et al.*[41] was used to produce (*S*)-1-(diphenylphosphoryl)-2-[diisopropylphosphino(borane)]ferrocene **47** and 1,2-bis[diisopropylphosphino(borane)]ferrocene **9**, two novel vicinal diphosphine-boranes. The deprotection of these compounds should produce bidentate ligands with rigid interannular angles and bond-lengths and should, therefore, provide an interesting comparison with the flexible 1,1'-diphosphines. Such a comparison would focus on the dependence of bite angle and other structural constraints rather than on the electronic effects of the ligands, since the 1,1'- and 1,2-diphosphines should be similar with regard to electronic influences.

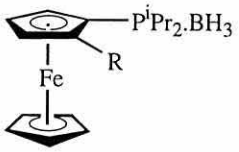

47 R = P(O)Ph$_2$

9 R = P^{i}Pr$_2$.BH$_3$

4.3 Catalysis

4.3.1 The Heck Reaction

The palladium (II) chloride complex of DIPPF, **51** proved to be an efficient catalyst precursor for the Heck arylation of alkenes and a range of alkenes were arylated with varying degrees of success. The efficacy of the ligand is believed to be the result of its electron-donating capacity combined with structural flexibility. Further research is required in order to determine the mechanism of the reaction, as the only species to be isolated from the reaction mixtures were those originating from the reaction itself: no effort was made to isolate catalytic intermediates or catalyst remnants. The range of substrates coupled suggests that the catalyst is capable of effecting the coupling of various types of alkene, from acrylates to styrenes. However, the attempted coupling of bromobenzene and chlorobenzene with methyl acrylate was unsuccessful, showing that while the new catalyst is efficient for the coupling of aryl iodides, it is no competition for other catalysts such as DIPPB/$Pd(OAc)_2$, which are capable even of coupling aryl chlorides.[82]

The comparison of (diisopropylphosphino)ferrocenes with (diphenylphosphino)ferrocenes proved conclusively that for the reactions studied the former produce far more efficient palladium catalysts than do the latter. Thus, while *cis*-[$PdCl_2$(DPPF)] **50** gave a yield of just 7% for the coupling of iodobenzene with methyl acrylate, *cis*-[$PdCl_2$(DIPPF)] **51** gave quantitative conversion. Furthermore, the hybrid ligand [$Fe(\eta^5\text{-}C_5H_4P^iPr_2)(\eta^5\text{-}C_5H_4PPh_2)$] **73** gave intermediate results for the couplings, showing a direct relationship between the donor group rather than solely the geometry. The unidentate ligands bearing a bromine substituent on their "lower" cyclopentadienyl rings gave similar results to those with no such substituent. It would have been of interest to have isolated the remnants of these catalysts, because in some related coupling reactions using similar catalysts halogen scrambling has been observed in the catalyst fragments at the end of the reaction.[139]

The asymmetric Heck reaction, following the procedure of Hayashi *et al.*[83] did not prove successful, possibly on account of the different substrate used. In order to test this theory, the reaction should be performed using the symmetric catalyst *cis*-[$PdCl_2$(DIPPF)] **51** to assess whether or not the reaction is actually feasible. It is possible that the difference in ring size between 2,3-dihydrofuran and 2,3-dihydropyran would affect the resultant e.e., but the actual catalysis ought to be similar in both cases.

4.3.2 Organomagnesium Cross-Coupling

A comparison of the nickel and palladium complexes of DPPF and DIPPF showed that the increased electron-donating ability of DIPPF **7** compromised its usefulness in the Grignard cross-coupling reaction. Instead of the expected product, a stereoisomer was identified, despite the rate of reaction being considerably greater with DIPPF than with DPPF **6**. Both nickel complexes **48** and **49** were shown to produce less efficient catalysts than their palladium counterparts **50** and **51**, returning much lower rates of reaction.

4.3.3 Other Cross-Couplings

The suitability of DIPPF **7** for use in the Suzuki cross-coupling was found to be limited, however, some of the more reactive substrates were efficiently coupled using the palladium (II) complex **51**. The choice of solvent was found to be of critical importance, with all successful couplings taking place in 1,4-dioxane but not in THF. Ferrocene-boronic acid, despite being an important precursor for the synthesis of substituted ferrocenes, gave no reaction under the conditions examined. This is assumed to be the result of its greater sensitivity to air and moisture than phenylboronic acid.[138] A broader range of substrates is required for further work, since the number of organoborons which have been coupled using different catalysts is considerable.

4.3 Summary

In conclusion, the synthesis of a number of novel ferrocenylamines and ferrocenylphosphines has been achieved, notably a series of heterosubstituted aminoferrocenes and a series of (diisopropylphosphino)ferrocenes. The co-ordination of some (isopropylphosphino)ferrocenes to Group 10 metals has provided novel complexes which have been applied successfully in catalytic cross-coupling reactions.

Chapter 5

Experimental

5.1 General

5.1.1 Techniques

All experiments were run under a dry nitrogen or argon atmosphere using standard oven-dried Schlenk glassware, unless otherwise indicated. NMR spectra were recorded on a Bruker AC250 instrument operating at 250MHz for ^{1}H, 62.5MHz for ^{13}C, 101.25MHz for ^{31}P and 80.25MHz for ^{11}B nuclei. Chemical shifts (δ) are given in ppm and are relative to tetramethylsilane (for ^{1}H and ^{13}C), triphenylphosphine (for ^{31}P) and boron trifluoride diethyl etherate (for ^{11}B). J values are given in Hz and refer to $J_{H,H}$ unless otherwise indicated. Mass spectra were recorded using a variety of techniques including electron impact, chemical ionisation (NH_3), fast atom bombardment (NOBA matrix) and electrospray at the EPSRC National Laboratory Service at the University of Wales, Swansea and at Bangor. GLC/MS was conducted on a Finnigan 4500 spectrometer using a 30m, 0.25mm internal diameter DBS liquid phase column, helium carrier gas and 70eV ionisation. GLC was performed using a Perkin-Elmer 8410 gas chromatograph fitted with a cross-bonded RTX-1701 column. Infra-red spectra were recorded on a Perkin-Elmer 1600 series FTIR spectrometer, using between 1 and 4 scans. Elemental analysis was conducted on a Carlo Erba EA1108 elemental analyser. Melting points are uncorrected and were measured on a Gallerkamp melting point apparatus. Optical rotations were measured on a Polaar 2001 automatic polarimeter. Electrochemistry was carried out by Zanello and co-workers at the University of Siena according to a previously published procedure.[140]

5.1.2 Materials

Column chromatography was performed using a neutral alumina (150 mesh, 158Å, Brockmann Grade 1) or silica gel (Kieselgel 230-400 mesh) support, as specified. Thin layer chromatography was conducted on precoated Kieselgel 60 F254 (Art. 5554; Merck) plates. Tetrahydrofuran (THF) and diethyl ether (referred to as "ether") were distilled from sodium benzophenone ketyl and dichloromethane was distilled from calcium hydride. *N,N*-Dimethylformamide (DMF) was dried over phosphorus pentoxide and distilled from calcium carbonate prior to use. Acetonitrile, *n*-hexane and triethylamine were distilled and stored under nitrogen over 4Å molecular sieves. 1,4-Dioxane was used as received and stored under nitrogen in a Sure/Seal™ bottle. "Petrol" refers to the fraction of light petroleum boiling between 40 and 60°C and was used without purification.

5.1.3 Chemicals

All chemicals were purchased from Lancaster Synthesis Ltd., Aldrich Chemical Co. Ltd. or Fluorochem Ltd. and were either used as received or purified by standard methods. Butyllithium was routinely titrated against diphenylacetic acid.

5.2 Synthesis

5.2.1 Preparation of 1,1'-Dibromoferrocene

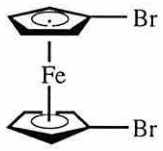

11

Ferrocene (37.2g, 0.2 mol) was dissolved in *n*-hexane (300ml) and to the rapidly stirred solution was added *n*-butyllithium (160ml of a 2.5M solution in hexanes, 0.4 mol) and TMEDA (30ml, 0.2 mol). The mixture was stirred for 18h at room temperature and was then cooled using an external acetone/ liquid nitrogen bath. To the cooled mixture was added 1,2-dibromotetrafluoroethane (47.8ml, 0.4 mol). The resulting mixture was allowed to warm slowly to room temperature and then to stir for 2h before being quenched with water (100ml). The product was extracted with ether (5 x 100ml). The combined extracts were washed with water (2 x 100ml) and brine (2 x 100ml), dried over anhydrous magnesium sulfate and evaporated to a volume of *ca.* 50ml to yield dark orange crystals, 63.1g, 92%, mp 51-52°C (*n*-hexane) [lit. 50-51° (EtOH)].[9]

^{1}H NMR ($CDCl_3$): δ = 4.08 (pt, 4H, *J* = 1.8; 4 x β-CH), 4.42 (pt, 4H, *J* = 1.8; 4 x α-CH)
^{13}C-{^{1}H} NMR ($CDCl_3$): δ = 69.9 (4 x β-CH), 72.7 (4 x α-CH), 78.3 (2 x CBr)
IR $\nu_{max}(CHCl_3)/cm^{-1}$: 3096.3 (s), 1403.8 (s), 1374.5 (s), 1147.7 (m), 1102.1 (m), 998.7 (w), 862.3 (s), 804.6 (s)
MS (EI) m/z (rel. int.): 346 M^+(49), 344 M^+ (100), 342 M^+ (48), 265 (20), 263 (20), 184 (13)
Calc. %: C 34.93 H 2.35 ($C_{10}H_8Br_2Fe$)
Found %: C 34.81 H 2.33

5.2.2 Preparation of 1-Bromo-1'-(*N*-phthalimido)ferrocene

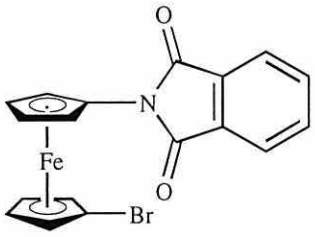

24

A mixture of 1,1'-dibromoferrocene (4.5g, 15.0 mmol) and copper (I) phthalimide (3.6g, 10.0 mmol) was ground to a fine powder and heated for 3h at 140°C using an external oil bath. The mixture was allowed to cool to room temperature and was extracted using ether (3 x 50ml). The organic extracts were combined, washed with brine (2 x 20ml) and water (2 x 20ml), dried over anhydrous magnesium sulfate and evaporated to dryness. Flash chromatography on silica using 15% ether/ petrol yielded unreacted 1,1'-dibromoferrocene (1.84g, 20%) and dark red crystals of 1-bromo-1'-(*N*-phthalimido)ferrocene (1.20g, 28%), mp 123-125°C (*n*-hexane).

^{1}H NMR ($CDCl_3$): δ = 4.17 (pt, 2H, *J* = 1.8; 2 x β-C<u>H</u>), 4.22 (pt, 2H, *J* = 1.3; 2 x β'-C<u>H</u>), 4.49 (pt, 2H, *J* = 1.8; 2 x α-C<u>H</u>), 5.21 (pt, 2H, *J* = 1.3; 2 x α'-C<u>H</u>)

^{13}C-{^{1}H} NMR ($CDCl_3$): δ = 64.1 (2 x β-<u>C</u>H), 67.8 (2 x β'-<u>C</u>H), 68.3 (2 x α-<u>C</u>H), 71.3 (2 x α'-<u>C</u>H), 88.6 (<u>C</u>N), 123.2 (2 x <u>C</u>H), 134.2 (2 x <u>C</u>H), 167.0 (2 x <u>C</u>O)

IR ν_{max}($CHCl_3$)/cm^{-1}: 3018.3 (s), 1779.0 (s), 1483.5 (s), 1371.9 (bs), 1105.9 (m), 1079.0 (s), 1033.1 (m)

MS (EI) m/z (rel. int.): 411 M^+ (13), 409 M^+ (14), 331 (100), 266 (39), 147 (12)

Calc. %: C 52.72 H 2.95 N 3.42 ($C_{18}H_{12}BrFeNO_2$)

Found %: C 52.81 H 2.67 N 3.44

5.2.3 Preparation of 1-Bromo-1'-aminoferrocene

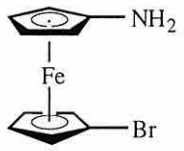

1

A solution of 1,1'-dibromoferrocene (3.44g, 10 mmol) in THF (25ml) was cooled using an external acetone/ dry ice bath. To this solution was added *n*-butyllithium (4ml of a 2.5M solution in *n*-hexane). The mixture was allowed to stir for 10 min. A solution of *O*-benzylhydroxylamine (0.49g, 4 mmol) in THF (10ml) was then added and the mixture was allowed to warm to room temperature with stirring over 1h. The mixture was quenched with water (10ml) before extraction of the product into dilute hydrochloric acid (20ml). The aqueous layer was washed with ether (20ml). Fresh ether (20ml) was added and the mixture was slowly made basic with dilute sodium bicarbonate solution. The yellow product transferred to the organic layer which was separated and a further extraction was performed with the same volume of ether. The combined organic fractions were dried over anhydrous magnesium sulfate and the solvent was removed *in vacuo*. Purification was achieved by flash chromatography on a basic alumina support [yield 0.61g, 53%, mp 90-92°C (*n*-hexane)], which also afforded the faster eluting *n*-butyl-substituted aminoferrocene **26** (14%) and the dibutylated derivative **27** (6%).

^{1}H NMR ($CDCl_3$): δ = 2.71 (bs, 2H; N$\underline{H}_2$), 3.94 (pt, 2H, *J* = 1.6; 2 x α'-C$\underline{H}$), 3.95 (pt, 2H, *J* = 1.6; 2 x β'-C$\underline{H}$), 4.05 (pt, 2H, *J* = 1.8; 2 x β-C$\underline{H}$), 4.32 (pt, 2H, *J* = 1.8; 2 x α-C$\underline{H}$)

^{13}C-{^{1}H} NMR ($CDCl_3$): δ = 60.4 (2 x α'-$\underline{C}$H), 63.7 (2 x β'-$\underline{C}$H), 67.3 (2 x β-$\underline{C}$H), 70.7 (2 x α-$\underline{C}$H), 79.3 ($\underline{C}$Br), 106.4 ($\underline{C}NH_2$)

MS (EI) m/z (rel. int.): 281 M^+ (45), 279 M^+ (47), 257 (100), 201 (81), 108 (26)

Calc. %: C 42.91 H 3.60 N 5.00 ($C_{10}H_{10}BrFeN$)

Found %: C 42.98 H 3.89 N 5.15

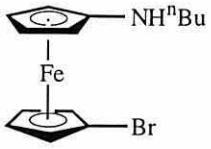

26

^{1}H NMR ($CDCl_3$): δ = 0.95 (t, 3H, *J* = 6.8; C<u>H</u>$_3$), 1.41 (*pseudo*-sxt, 2H, *J* = 6.8; $CH_3C\underline{H}_2$), 1.55 (m, 2H; C<u>H</u>$_2$), 2.24 (bs, 1H; N<u>H</u>), 2.92 (t, 2H, *J* = 6.8; NC<u>H</u>$_2$), 3.83 (pt, 2H, *J* = 1.8; 2 x α'-C<u>H</u>), 3.90 (pt, 2H, *J* = 1.8; 2 x β'-C<u>H</u>), 4.00 (pt, 2H, *J* = 1.9; 2 x β-C<u>H</u>), 4.32 (pt, 2H, *J* = 1.9; 2 x α-C<u>H</u>)

^{13}C-{^{1}H} NMR ($CDCl_3$): δ = 14.1 (<u>C</u>H$_3$), 20.5 (<u>C</u>H$_2$), 32.1 (<u>C</u>H$_2$), 46.7 (<u>C</u>H$_2$), 57.5 (2 x α'-<u>C</u>H), 65.3 (2 x β'-<u>C</u>H), 66.8 (2 x β-<u>C</u>H), 70.1 (2 x α-<u>C</u>H), 78.9 (<u>C</u>Br), 112.5 (<u>C</u>NHBu)

MS (EI) m/z (rel. int.): 337 M^+ (88), 335 M^+ (93), 257 (100)

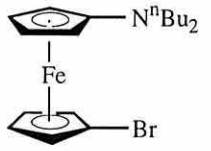

27

^{1}H NMR ($CDCl_3$): δ = 0.94 (t, 6H, *J* = 6.8; 2 x C<u>H</u>$_3$), 1.34 (*pseudo*-sxt, 4H, *J* = 6.8; 2 x $CH_3C\underline{H}_2$), 1.56 (*pseudo*-sxt, 4H, *J* = 6.8; 2 x C<u>H</u>$_2$), 2.92 (t, 4H, *J* = 6.8; 2 x NC<u>H</u>$_2$), 3.67 (pt, 2H, *J* = 1.8; 2 x α'-C<u>H</u>), 3.94 (pt, 2H, *J* = 1.8; 2 x β'-C<u>H</u>), 4.03 (pt, 2H, *J* = 1.9; 2 x β-C<u>H</u>), 4.32 (pt, 2H, *J* = 1.9; 2 x α-C<u>H</u>)

MS (EI) m/z (rel. int.): 393 M^+ (98), 391 M^+ (100), 312 (28), 256 (18), 184 (15)

5.2.4 Preparation of (*N*,*N*-Dicarboethoxyl)aminoferrocene

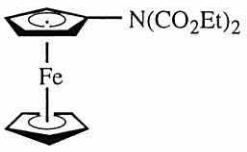

29

1-Bromo-1'-aminoferrocene (1.05g, 3.75 mmol) was dissolved in THF (50ml) and the solution was cooled using an external acetone/ dry ice bath. To the rapidly stirred solution was added *n*-butyllithium (4.5ml of a 2.5M solution in hexanes, 11.25 mmol) and the resulting mixture was stirred for 10 min. To the mixture was added ethyl chloroformate (2.0g, 18 mmol) and the resulting mixture was allowed to warm to room temperature and stir for a further 18h. The reaction was quenched with water (100ml) and extracted with ethyl acetate (3 x 50ml). The combined organic fractions were washed with brine (2 x 50ml) and water (50ml), dried over anhydrous magnesium sulfate and concentrated *in vacuo*. Flash chromatography on silica using 20% ether/ petrol gave the product as bright yellow crystals in 0.59g (46%) yield, mp 58-60°C (hexane).

^{1}H NMR ($CDCl_3$): δ = 1.40 (t, 6H, *J* = 7.1; 2 x C<u>H</u>$_3$), 4.13 (pt, 2H, *J* = 2.0; 2 x β-C<u>H</u>), 4.22 (s, 5H; Cp), 4.35 (q, 4H, *J* = 7.1; 2 x C<u>H</u>$_2$), 4.52 (pt, 2H, *J* = 2.0; 2 x α-C<u>H</u>)

^{13}C-{^{1}H} NMR ($CDCl_3$): δ = 14.1 (2 x C<u>H</u>$_3$), 63.4 (2 x β-<u>C</u>H), 65.0 (2 x <u>C</u>H$_2$), 65.3 (2 x α-<u>C</u>H), 69.3 (Cp), 94.6 (<u>C</u>N)

IR ν_{max}($CHCl_3$)/cm^{-1}: 3018.6 (s), 2400.6 (w), 1722.4 (bs), 1463.1 (s), 1372.8 (s), 1201.9 (bs), 1101.8 (s), 1028.6 (s), 1002.5 (s)

MS (EI) m/z (rel. int.): 345 M^+ (12), 344 (100), 272 (10), 226 (72), 200 (9)

Calc. %: C 55.67 H 5.55 N 4.06 ($C_{16}H_{19}FeNO_2$)

Found %: C 56.24 H 5.42 N 4.28

5.2.5 Preparation of 1-Bromo-1'-[amino(borane)]ferrocene

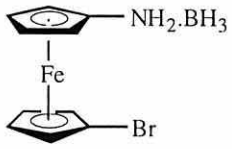

30

1-Bromo-1'-aminoferrocene (1.0g, 3.6 mmol) and sodium borohydride (0.21g, 5.76 mmol) were dissolved in DME (50ml). To the rapidly stirred solution was added dropwise a solution of iodine (0.3g, 1.2 mmol) in DME (50ml). After 1h stirring, the solvent was removed and the residue was taken up in dichloromethane and filtered. The filtrate was evaporated to dryness and the residual solid was washed with *n*-hexane. The solid was then dissolved in the minimum volume of benzene (*ca.* 10ml) and was precipitated with *n*-hexane to give yellow crystals in a yield of 0.87g (82%), mp 131-132°C (benzene).

^{1}H NMR ($CDCl_3$): δ = 4.17 (pt, 2H, *J* = 1.9; 2 x α'-C<u>H</u>), 4.22 (pt, 2H, *J* = 1.9; 2 x β'-C<u>H</u>), 4.50 (pt, 4H, *J* = 1.9; 2 x α-C<u>H</u> + 2 x β-C<u>H</u>), 5.08 (bs, 2H; N<u>H</u>$_2$)

^{13}C-{^{1}H} NMR ($CDCl_3$): δ = 65.2 (2 x α'-<u>C</u>H), 68.3 (2 x β'-<u>C</u>H), 68.6 (2 x β-<u>C</u>H), 71.3 (2 x α-<u>C</u>H)

IR ν_{max}($CHCl_3$)/cm^{-1}: 3211.7 (m), 2333.4 (s), 1597.5 (bm), 1499.6 (s), 1407.4 (m), 1149.8 (m), 753.3 (bs)

MS (EI) m/z (rel. int.): 295 M^+ (10), 293 M^+ (11), 281 (30), 279 (31), 162 (55), 131 (100)

Calc. %: C 40.88 H 4.46 N 4.77 ($C_{10}H_{13}BBrFeN$)

Found %: C 40.59 H 4.50 N 4.81

5.2.6 Preparation of 1-Amino-1'-ferrocenecarboxylic Acid

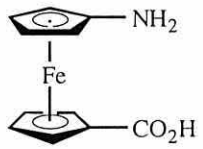

2

1-Bromo-1'-aminoferrocene (2.8g, 10 mmol) was dissolved in ether (30ml) and the solution was cooled by means of an external acetone/ dry ice bath. To the stirred solution was added *n*-butyllithium (12ml of a 2.5M solution in hexanes, 30 mmol). The mixture was allowed to warm to -50°C over 10 min. and was treated with excess carbon dioxide gas before being allowed to warm to room temperature. The resultant mixture was stirred for a further 2h, after which the bright yellow-orange suspension was filtered and the residue was washed with ether (3 x 30ml). The product was obtained as a yellow-orange powder in 0.76g (31%) yield. The powder decomposed rapidly to a black solid.

^{1}H NMR (D_2O, HOD-suppressed): δ = 3.92 (bm, 2H; 2 x α-C<u>H</u>), 4.14 (bm, 2H; 2 x β-C<u>H</u>), 4.40 (bm, 2H; 2 x β'-C<u>H</u>), 4.65 (bm, 2H; 2 x α'-C<u>H</u>)

^{13}C-{^{1}H} NMR (D_2O): δ = 72.3 (2 x α-<u>C</u>H + 2 x β-<u>C</u>H), 72.8 (2 x β'-<u>C</u>H), 73.5 (2 x α'-<u>C</u>H), 73.6 (<u>C</u>CO_2H), 75.8 (<u>C</u>NH_2), 169.4 (<u>C</u>=O)

IR ν_{max}($CHCl_3$)/cm^{-1}: 3426.5 (bs), 2942.0 (s), 1620.1 (s), 1087.9 (s), 871.9 (s), 594.0 (bs)

MS (electrospray) m/z (rel. int.): 245 M^+ (8), 244 (100), 200 (22)

5.2.7 Preparation of Methyl 1-Amino-1'-ferrocenecarboxylate

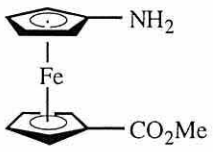

31

1-Bromo-1'-aminoferrocene (2.8g, 10 mmol) in a mixture of ether and THF (50:50, 30ml) was treated with 2.5 equivalents of *n*-butyllithium (10ml of a 2.5M solution in hexanes) at -70°C. The mixture was allowed to warm to -50°C over 10 min. and was treated with excess dry carbon dioxide before being allowed to warm to room temperature. The mixture was then quenched with water (20ml) and the aqueous product-containing fraction was separated and dried *in vacuo* to give a pale yellow powder. This product was then redissolved in methanol before being treated slowly with a solution of methanolic HCl (prepared by the careful addition of acetyl chloride to methanol). After stirring overnight the reaction mixture was brought to pH8 by the dropwise addition of dilute sodium hydroxide solution. The product mixture was extracted into ether (3 x 20ml) and the extracts were combined, dried over anhydrous magnesium sulfate and concentrated *in vacuo*. Flash chromatography on neutral alumina afforded methyl 1-(*N*-butylamino)-1'-ferrocenecarboxylate **32** (24%), aminoferrocene **25** (9%) and the major product **31** (1.6g, 62%) as a deep orange-red solid from the third orange band.

^{1}H NMR ($CDCl_3$): δ = 1.59 (bs, 2H; N$\underline{H}_2$), 3.81 (s, 3H; C$\underline{H}_3$), 3.88 (pt, 2H, *J* = 1.8; 2 x α-C$\underline{H}$), 3.98 (pt, 2H, *J* = 1.8; 2 x β-C$\underline{H}$), 4.35 (pt, 2H, *J* = 1.9; 2 x β'-C$\underline{H}$), 4.77 (pt, 2H, *J* = 1.9; 2 x α'-C$\underline{H}$)

^{13}C-{^{1}H} NMR ($CDCl_3$): δ = 59.3 ($\underline{C}H_3$), 65.1 (2 x α-$\underline{C}$H), 65.8 (2 x β-$\underline{C}$H), 70.9 (2 x β'-$\underline{C}$H), 71.7 (2 x α'-$\underline{C}$H), 72.3 ($\underline{C}CO_2Me$), 106.9 ($\underline{C}NH_2$), 156.3 ($\underline{C}$=O)

MS (EI) m/z (rel. int.): 259 M^+ (100), 228 (4), 167 (12), 143 (3), 137 (8)

Accurate mass: 259.02731, Δ = 10ppm

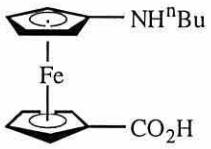

32

^{1}H NMR ($CDCl_3$): δ = 0.94 (t, 3H, *J* = 6.8; C$\underline{H}_3$), 1.21 (m, 2H; $CH_3C\underline{H}_2$), 1.52 (m, 2H; C$\underline{H}_2$), 1.61 (bs, 1H; N$\underline{H}$), 2.94 (t, 2H, *J* = 6.8; NHC$\underline{H}_2$), 3.74 (s, 3H; OC$\underline{H}_3$), 3.83 (pt, 2H, *J* = 1.8; 2 x α-C$\underline{H}$), 3.86 (pt, 2H, *J* = 1.8; 2 x β-C$\underline{H}$), 4.32 (pt, 2H, *J* = 1.9; 2 x β'-C$\underline{H}$), 4.72 (pt, 2H, *J* = 1.9; 2 x α'-C$\underline{H}$)

^{13}C-{^{1}H} NMR ($CDCl_3$): δ = 13.9 ($\underline{C}H_3$), 20.4 ($CH_3\underline{C}H_2$), 29.7 ($\underline{C}H_2$), 32.0 (NH$\underline{C}H_2$), 56.4 (2 x α-$\underline{C}$H), 64.7 (2 x β-$\underline{C}$H), 65.8 (2 x β'-$\underline{C}$H), 70.2 (2 x α'-$\underline{C}$H), 71.2 ($\underline{C}CO_2Me$), 107.1 ($\underline{C}$NHBu), 156.6 ($\underline{C}$=O)

MS (EI) m/z (rel. int.): 315 M^+ (100), 284 (3), 259 (6), 240 (7), 223 (19), 189 (22)

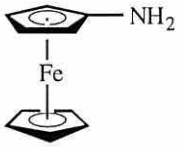

25

^{1}H NMR ($CDCl_3$): δ = 2.54 (bs, 2H, N$\underline{H}_2$), 3.89 (pt, 2H, *J* = 1.8, 2 x α-C$\underline{H}$), 3.96 (pt, 2H, *J* = 1.8, 2 x β-C$\underline{H}$), 4.07 (s, 5H, Cp); identified by spectral comparison with an authentic sample prepared by the direct water quenching of 1-amino-1'-lithioferrocene.

5.2.8 Preparation of 1-Diphenylphosphino-1'-aminoferrocene

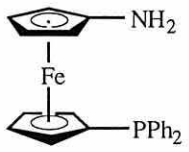

4

To a solution of 1-bromo-1'-(diphenylphosphino)ferrocene (4.49g, 10 mmol) in THF (25ml) at -10°C was added 1 equivalent of *n*-butyllithium (4ml of a 2.5M solution in hexanes) over 10 min., followed by a solution of *O*-benzylhydroxylamine (4.9g, 4 mmol) in THF (10ml). The mixture was allowed to warm to room temperature over 1h and was then quenched with water (20ml). The product was extracted in a manner similar to that outlined above for 1-bromo-1'-aminoferrocene. The combined organic extracts were dried over anhydrous magnesium sulfate and reduced to an oil *in vacuo*. The yellow product was dissolved in the minimum volume of hot *n*-hexane and allowed to cool and crystallise, giving dark yellow crystals in a yield (based on added amine) of 0.59g, 38% which were found to decompose rapidly upon standing.

^{1}H NMR ($CDCl_3$): δ = 2.30 (bs, 2H; $N\underline{H}_2$), 3.74 (m, 2H; 2 x α'-C$\underline{H}$) 3.87 (m, 2H; 2 x β'-CH), 3.98 (m, 2H; 2 x α-C$\underline{H}$), 4.27 (m, 2H; 2 x β-C$\underline{H}$), 7.15-7.45 (bm, 10H; 2 x Ph)

^{31}P-{^{1}H} NMR ($CDCl_3$): δ = -17.57(s)

MS (EI) m/z (rel. int.): 385 M^+ (100), 369 (10), 308 (19), 231 (12), 200 (32)

5.2.9 Preparation of (±)-1,1'-Dibromo-2-[(*N,N*-dimethyl)methyl-amino]ferrocene

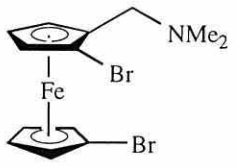

37

Ferrocenyl(*N,N*-dimethyl)methylamine (6.14g, 25.3 mmol) in ether (50ml) was cooled by means of an external acetone/ dry ice bath and to the cooled solution was added TMEDA (1.9ml, 25.3 mmol) and 2.1 equivalents of *n*-butyllithium (21ml of a 2.5M solution in hexanes, 53 mmol). The mixture was allowed to warm to room temperature and was stirred for 18h before being cooled once again using the same bath and treated with 1,2-dibromotetrafluoroethane (6.4ml, 53 mmol). After warming to room temperature and stirring for a further 2h, the reaction was quenched with water (100ml) and the mixture was extracted with ether (5 x 100ml). The combined organic extracts were dried over anhydrous magnesium sulfate and evaporated to dryness. The resultant dark orange oil was purified by flash chromatography on basic alumina using 3:1 ether/ dichloromethane as eluent, to give the product 1,1'-dibromo-2-[(*N,N*-dimethylamino)methyl]ferrocene **37**, as a dark yellow oil (3.4g, 36%).

^{1}H NMR ($CDCl_3$): δ = 2.24 [s, 6H; N($C\underline{H}_3$)$_2$], 3.42 (ABq, 2H, *J* = 13.1; $C\underline{H}_2$), 4.09 (m, 2H; 2 x β'-C<u>H</u>), 4.20 (pt, 1H, *J* = 1.8; C3-<u>H</u>), 4.24 (pt, 1H, *J* = 1.8; C4-<u>H</u>), 4.28 (m, 2H; 2 x α'-C<u>H</u>), 4.45 (pt, 1H, *J* = 1.8; C5-<u>H</u>)

^{13}C-{^{1}H} NMR ($CDCl_3$): δ = 45.0 (2 x $\underline{C}H_3$), 56.1 ($\underline{C}H_2$), 69.2 (2 x β'-<u>C</u>H), 70.3 (<u>C</u>3), 70.7 (<u>C</u>4), 72.7 (<u>C</u>5), 73.2 (2 x α'-<u>C</u>H), 78.7 ($\underline{C}CH_2$), 81.1 (<u>C</u>Br), 83.7 (<u>C</u>Br)

IR ν_{max} ($CHCl_3$)/cm^{-1}: 3096.6 (m), 2973.5 (s), 2938.9 (s), 2860.2 (s), 2776.9 (s), 2177.4 (bm), 1472.6 (s), 1411.5 (s), 1389.9 (s)

MS (EI) m/z (rel. int.): 403 M^+ (49), 401 M^+ (100), 399 M^+ (50), 321 (14), 323 (14), 241 (25), 184 (15)

5.2.10 Preparation of (*R*)-1-Ferrocenyl(*N,N*-dimethyl)ethylamine

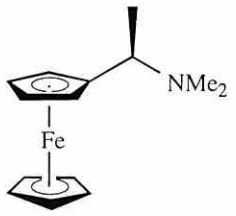

16

1-Ferrocenyl(*N,N*-dimethyl)ethylamine was prepared in 89% yield according to the method of Hauser and Lindsay[29] and resolved according to the procedure of Ugi *et al.*,[33] on a 39 mmol scale. [bp 115-7°C/5mm (lit. 120-1°C/7mm)].[33]

^{1}H NMR ($CDCl_3$): δ = 1.46 (d, 3H, *J* = 6.9; C<u>H</u>$_3$), 2.09 {s, 6H; [N(C<u>H</u>$_3$)$_2$]}, 3.62 (q, 1H, *J* = 6.9; C<u>H</u>), 4.13 (m, 9H, Cp + 2 x α-C<u>H</u> + 2 x β-C<u>H</u>)

^{13}C-{^{1}H} NMR ($CDCl_3$): δ = 16.1 (<u>C</u>H$_3$), 40.7 [N(<u>C</u>H$_3$)$_2$], 58.6 (<u>C</u>HCH$_3$), 66.9 (<u>C</u>5), 67.2 (<u>C</u>4), 67.3 (<u>C</u>3), 68.6 (Cp), 69.3 (<u>C</u>2), 87.2 (<u>C</u>1)

IR ν_{max}($CHCl_3$)/cm^{-1}: 3092.3 (s), 2970.9 (s), 2855.0 (s), 2775.7 (s), 1679.3 (bs), 1471.8 (s), 1454.0 (s), 1366.2 (s)

MS (EI) m/z (rel. int.): 257 M^+ (100), 242 (35), 227 (22), 212 (18), 198 (56), 185 (34)

$[\alpha]^{25}_D$ = -12.8, c = 1.5, EtOH (lit. -14.1, c = 1.5, EtOH)[33] and +12.6

Calc. %: C 65.30 H 7.45 N 5.45 ($C_{14}H_{19}FeN$)

Found %: C 65.06 H 7.66 N 5.72

5.2.11 Preparation of (*R,S*)-1,1'-Dibromo-2-[(*N,N*-dimethyl-amino)ethyl]ferrocene

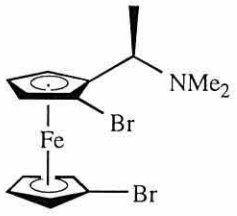

38

(*R,S*)-1,1'-Dibromo-2-[(*N,N*-dimethylamino)ethyl]ferrocene was prepared from (*R*)-1-ferrocenyl(*N,N*-dimethyl)ethylamine on a 57 mmol scale using a method similar to that outlined for the preparation of 1,1'-dibromo-2-[(*N,N*-dimethylamino)methyl]ferrocene. The product was obtained a dark yellow oil in a yield of 9.85 g (42%).

^{1}H NMR ($CDCl_3$): δ = 1.54 (d, 3H, *J* = 6.9; C$\underline{H}_3$), 2.15 [s, 6H; N(C$\underline{H}_3$)$_2$], 3.78 (q, 1H, *J* = 6.9; C$\underline{H}$CH$_3$), 4.08 (m, 2H; 2 x β'-C$\underline{H}$), 4.15 (pt, 1H, *J* = 2.5; C3-$\underline{H}$), 4.20 (pt, 1H, *J* = 2.5; C4-$\underline{H}$), 4.38 (m, 2H; 2 x α'-C$\underline{H}$), 4.48 (m, 1H; C5-$\underline{H}$)

^{13}C-{^{1}H} NMR ($CDCl_3$): δ = 16.2 (C$\underline{H}_3$), 40.9 [2 x N(C$\underline{H}_3$)$_2$], 55.4 (C$\underline{H}$), 65.0 (C$\underline{3}$), 67.5 (2 x β'-C$\underline{H}$), 68.7 (C$\underline{4}$), 69.7 (C$\underline{5}$), 70.7 (2 x α'-C$\underline{H}$), 79.6 (C$\underline{C}$H), 80.0 (C$\underline{C}$Br), 88.5 (C$\underline{C}$Br)

IR ν_{max} ($CHCl_3$)/cm^{-1}: 3097.2 (m), 2978.4 (s), 2939.2 (s), 2860.4 (s), 2777.0 (s), 2176.8 (bm), 1473.5 (s), 1411.0 (s), 1389.7 (s)

MS (EI) m/z (rel. int.): 417 M$^+$ (49), 415 M$^+$ (100), 413 M$^+$ (51), 402 (19), 400 (48), 398 (16), 373 (16), 371 (32), 369 (20), 346 (19), 344 (25), 342 (21)

5.2.12 Lithiation of (*R,S*)-1,1'-Dibromo-2-[(*N,N*-dimethylamino)-ethyl]ferrocene

(*R,S*)-1,1'-Dibromo-2-[(*N,N*-dimethylamino)ethyl]ferrocene (200mg, 0.48 mmol) was dissolved in the specified solvent (10ml). The THF solutions were cooled to the temperature shown by means of an external ice (*ca.* 0°C), 1:3 salt/ ice (*ca.* -20°C), acetonitrile/ dry ice (*ca.* -40°C), chloroform/ dry ice (*ca.* -60°C) or acetone/ dry ice (*ca.* -80°C) bath. The ether and *n*-hexane solutions were cooled by means of an external acetone/ dry ice bath. THF, ether and *n*-hexane solutions were additionally reacted at room temperature. Each solution was treated with *n*-butyllithium (0.19ml of a 2.5M solution in hexanes, 0.48 mmol) and the mixture was stirred at the requisite temperature for 5 min. before being quenched with water (5ml) and extracted using ether (3 x 30ml). The combined organic fractions were washed with brine (2 x 10ml) and water (10ml), dried over anhydrous magnesium sulfate and evaporated to dryness before being examined by NMR spectroscopy. The results are summarised in Table 3.1 (Chapter 3).

5.2.13 Preparation of (*R*,*S*)-1,1'-Bis(diisopropylphosphino)-2-[(*N*,*N*-dimethylamino)ethyl]ferrocene

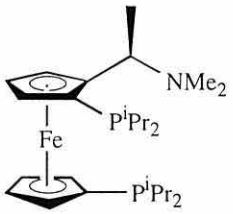

5

(*R*,*S*)-1,1'-Bis(diisopropylphosphino)-2-[(*N*,*N*-dimethylamino)ethyl]ferrocene **5** was prepared according to the procedure of Cullen *et al.*,[7] on a 20 mmol scale. The product was obtained as an orange oil in a yield of 56% along with a trace of the monophosphine **42** (4%).

^{1}H NMR ($CDCl_3$): δ = 1.02 (m, 24H; 8 x C$\underline{H}_3$), 1.29 (d, 3H, *J* = 6.8; C$\underline{H}_3$), 1.89 (m, 4H; 4 x C$\underline{H}$), 2.10 [s, 6H; N(C$\underline{H}_3$)$_2$], 4.00 (pt, 1H, *J* = 1.8; C3-$\underline{H}$), 4.06 (pt, 2H, *J* = 2.0; 2 x α'-C$\underline{H}$), 4.09 (pt, 2H, *J* = 2.0; 2 x β'-C$\underline{H}$), 4.15 (pt, 1H, *J* = 1.8; C4-$\underline{H}$), 4.24 (pt, 1H, *J* = 1.8; C5-$\underline{H}$)

^{13}C-{^{1}H} NMR ($CDCl_3$): δ = 8.3 (NCH-$\underline{C}H_3$), 18.2 (d, $J_{C,P}$ = 6.0; $\underline{C}H_3$), 19.3 (d, $J_{C,P}$ = 9.0; $\underline{C}H_3$), 20.1, (d, $J_{C,P}$ = 10.0; $\underline{C}H_3$), 20.8 (d, $J_{C,P}$ = 11.6; $\underline{C}H_3$), 21.7 (d, $J_{C,P}$ = 17.9; $\underline{C}H_3$), 22.8 (d, $J_{C,P}$ = 13.4; $\underline{C}H_3$), 23.3 (d, $J_{C,P}$ = 5.4; $\underline{C}H_3$), 23.5 (d, $J_{C,P}$ = 11.6; $\underline{C}H_3$), 39.2 [N($\underline{C}H_3$)$_2$], 56.5 (d, $J_{C,P}$ = 7.5; 4 x $\underline{C}$H), 70.1 ($\underline{C}$3), 71.0 ($\underline{C}$4), 71.8 (d, $J_{C,P}$ = 7.5; 2 x α-$\underline{C}$H), 72.1 (d, $J_{C,P}$ = 12.1; $\underline{C}$5), 73.4 (2 x β-$\underline{C}$H), 79.7 (2 x $\underline{C}$P), 95.7 ($\underline{C}$H-NMe$_2$)

^{31}P-{^{1}H} NMR ($CDCl_3$): δ = -1.05 (s), -5.59 (s)

IR ν_{max}($CHCl_3$)/cm^{-1}: 2928.0 (s), 2865.3 (s), 1457.4 (m), 1363.2 (m), 1093.9 (m), 1001.4 (m), 927.8 (m)

MS (EI) m/z (rel. int.): 489 M^+ (5), 471 (10), 443 (68), 398 (100), 271 (9), 243 (9)

$[\alpha]^{25}_D$ = -265.5 (c = 0.5, $CHCl_3$)

Calc. %: C 63.80 H 9.27 N 2.86 ($C_{26}H_{45}FeNP_2$)

Found %: C 64.09 H 9.54 N 2.87

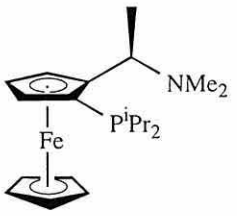

42

^{1}H NMR ($CDCl_3$): δ = 1.02 (m, 12H; 4 x C$\underline{H}_3$), 1.29 (d, 3H, J = 6.8; C$\underline{H}_3$), 2.09 [s, 6H; N(C$\underline{H}_3$)$_2$], 2.21 (dq, 2H, $J_{H,P}$ = 7.4, $J_{H,H}$ = 7.1; 2 x C$\underline{H}$), 4.00 (q, 1H, J = 6.8; C$\underline{H}$), 4.07 (s, 5H; Cp), 4.12 (pt, 1H, J = 2.0; C3-$\underline{H}$), 4.24 (pt, 1H, J = 2.0; C4-$\underline{H}$), 4.28 (pt, 1H, J = 2.0; C5-$\underline{H}$)

^{13}C-{^{1}H} NMR ($CDCl_3$): δ = 9.1 (NCH-$\underline{C}H_3$), 18.2 (d, $J_{C,P}$ = 6.5; $\underline{C}H_3$), 20.7 (d, $J_{C,P}$ = 11.8; $\underline{C}H_3$), 21.7 (d, $J_{C,P}$ = 18.1; $\underline{C}H_3$), 23.0 (d, $J_{C,P}$ = 11.0; $\underline{C}H_3$), 39.4 [N($\underline{C}H_3$)$_2$], 56.5 (d, $J_{C,P}$ = 7.8; 2 x $\underline{C}$H), 67.3 ($\underline{C}$3), 68.4 (d, $J_{C,P}$ = 2.5; $\underline{C}$4), 69.8 (Cp), 73.4 ($\underline{C}$5), 79.6 (d, $J_{C,P}$ = 18.6, $\underline{C}$P), 95.5 ($\underline{C}$HNMe$_2$)

^{31}P-{^{1}H} NMR ($CDCl_3$): δ = -5.69 (s)

MS (EI) m/z (rel. int.): 373 M^+ (12), 355 (21), 256 (100), 212 (38)

5.2.14 Preparation of 1,1'-Bis(diisopropylphosphino)ferrocene

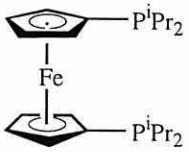

7

1,1'-Bis(diisopropylphosphino)ferrocene was prepared on a 27 mmol scale according to the procedure of Cullen *et al.*[7] The product was obtained in 86% yield as a dark orange oil which crystallised upon refrigeration, mp = 34-36°C (*n*-hexane).

^{1}H NMR ($CDCl_3$): δ = 1.06 (2 x dd, 24H, $J_{H,H}$ = 7.0, $J_{H,P}$ = 13.0; 8 x C$\underline{H}_3$), 1.90 (sept x d, 4H, $J_{H,H}$ = 7.0, $J_{H,P}$ = 2.3; 4 x C$\underline{H}$), 4.18 (pt, 4H, J = 1.6; 4 x α-C$\underline{H}$), 4.27 (pt, 4H, J = 1.7; 4 x β-C$\underline{H}$)

^{13}C-{^{1}H} NMR ($CDCl_3$): δ = 19.8 (d, $J_{C,P}$ = 6.7; 8 x $\underline{C}H_3$), 23.3 (d, $J_{C,P}$ = 11.2; 4 x $\underline{C}$H), 69.1 (4 x β-$\underline{C}$H), 71.1 (d, $J_{C,P}$ = 16.9; 4 x α-$\underline{C}$H), 76.3 (d, $J_{C,P}$ = 17.9; 2 x $\underline{C}$P)

^{31}P-{^{1}H} NMR ($CDCl_3$): δ = -0.39 (s)

IR ν_{max}($CHCl_3$)/cm^{-1}: 3095.1 (m), 2948.8 (bs), 2864.8 (s), 1460.5 (s), 1381.5 (s), 1243.1 (s), 1157.2 (s), 1029.1 (s)

MS (EI) m/z (rel. int.): 418 M^+ (5), 375 (10), 302 (12), 217 (100)

Calc. %: C 63.16 H 8.67 ($C_{22}H_{36}FeP_2$)

Found %: C 63.41 H 8.82

5.2.15 Preparation of 1,1'-Bis(diphenylphosphino)ferrocene

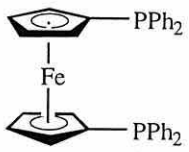

6

1,1'-Bis(diphenylphosphino)ferrocene was prepared according to the procedure of Davison *et al.*,[4] on a 50 mmol scale. The product was obtained as yellow crystals in a yield of (84%), mp 178-180°C (dec.) [lit. 181-182°C].[4]

^{1}H NMR ($CDCl_3$): δ = 3.96 (pt, 4H, J = 1.9; 4 x α-C<u>H</u>), 4.20 (pt, 4H, J = 1.9; 4 x β-C<u>H</u>), 7.22 (m, 20H; 4 x Ph)

^{13}C-{^{1}H} NMR ($CDCl_3$): δ = 72 .4 (4 x β-<u>C</u>H), 73.7 (d, $J_{C,P}$ = 14.5; 4 x α-<u>C</u>H), 76.6 (d, $J_{C,P}$ = 12.6; 2 x <u>C</u>P), 128.1 (d, $J_{C,P}$ = 18.7; 8 x *o*-<u>C</u>H), 128.3 (4 x *p*-CH), 133.4 (d, $J_{C,P}$ = 19.5; 8 x *m*-<u>C</u>H), 138.9 (d, $J_{C,P}$ = 9.7; 4 x <u>C</u>P)

^{31}P-{^{1}H} NMR ($CDCl_3$): δ = -17.9 (s)

IR ν_{max}($CHCl_3$)/cm^{-1}: 3017.8 (bs), 2950.0 (w), 1476.9 (m), 1433.4 (s), 1162.0 (s), 1092.5 (w), 1027.0 (m), 697.5 (s)

MS (EI) m/z (rel. int.): 554 M^+ (100), 477 (14), 369 (12), 292 (9)

Calc. %: C 73.66 H 5.09 ($C_{34}H_{28}FeP_2$)

Found %: C 73.29 H 5.20

5.2.16 Preparation of Triphenylphosphine-borane

$PPh_3.BH_3$

39

Triphenylphosphine-borane was prepared according to the procedure of Nainan and Ryschkewitsch,[64] on a 35 mmol scale. The product was obtained in 93% yield as colourless crystals, mp 186-189°C (lit. 187-189°C).[64]

^{1}H NMR ($CDCl_3$): δ = 7.4-7.7 (m, 15H; 3 x Ph)

^{13}C-{^{1}H} NMR ($CDCl_3$): δ = 128.8 (d, $J_{C,P}$ = 10.3; 6 x *o*-CH), 129.6 (3 x CP), 131.3 (3 x *p*-CH), 133.2 (d, $J_{C,P}$ = 9.6; 6 x *m*-CH)

^{31}P-{^{1}H} NMR ($CDCl_3$): δ = +20.1, (d, $J_{P,B}$ = 59.5)

^{11}B-{^{1}H} NMR ($CDCl_3$): δ = -38.4, (d, $J_{B,P}$ = 59.5)

IR ν_{max} ($CHCl_3$)/cm^{-1}: 3060.6 (w), 2395.8 (s), 2259.7 (w), 1483.0 (m), 1437.1 (s), 1105.4 (s), 1058.0 (m)

MS (EI) m/z (rel. int.): 276 M^+ (15), 262 (100), 185 (20), 108 (15), 77 (35)

Calc. %: C 78.29 H 6.57 ($C_{18}H_{18}BP$)

Found %: C 78.59 H 6.78

5.2.17 Preparation of 1,1'-Bis[diphenylphosphino(borane)]-ferrocene

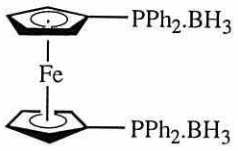

40

1,1'-Bis(diphenylphosphino)ferrocene (2.0g, 3.62 mmol) and sodium borohydride (0.32g, 8.66 mmol) were dissolved in DME (40ml). To the rapidly stirred solution was added, dropwise, a solution of iodine (0.92g, 3.62 mmol) in DME (40ml). After 1h stirring the solvent was removed to give a yellow-orange powder in a yield of 1.93g (92%), mp 188-190°C (benzene).

^{1}H NMR ($CDCl_3$): δ = 4.25 (pt, 4H, *J* = 1.6; 4 x α-C<u>H</u>), 4.54 (pt, 4H, *J* = 1.6; 4 x β-C<u>H</u>), 7.4-7.5 (m, 20H; 4 x Ph)

^{13}C-{^{1}H} NMR ($CDCl_3$): δ = 73.8 (d, $J_{C,P}$ = 9.6; 4 x β-<u>C</u>H), 74.5 (d, $J_{C,P}$ = 7.5; 4 x α-<u>C</u>H), 128.3 (4 x *p*-<u>C</u>H), 128.5 (d, *J* = 10.0; 8 x *o*-<u>C</u>H), 131.1 (4 x <u>C</u>P), 132.5 (d, $J_{C,P}$ = 9.6; 8 x *m*-<u>C</u>H)

^{31}P-{^{1}H} NMR ($CDCl_3$): δ = +15.0, (d, $J_{P,B}$ = 55.7)

^{11}B-{^{1}H} NMR ($CDCl_3$): δ = -38.8, (d, $J_{B,P}$ = 55.7)

IR ν_{max}($CHCl_3$)/cm^{-1}: 3059.5 (w), 2395.1 (s), 1436.5 (s), 1107.5 (s), 1061.9 (m), 1032.4 (m), 699.7 (s)

MS (EI) m/z (rel. int.): 572 M^+ (12), 568 (20), 554 (100), 477 (15), 369 (15), 292 (10)

Calc. %: C 70.16 H 5.89 ($C_{34}H_{34}B_2FeP_2$)

Found %: C 70.15 H 6.04

5.2.18 Preparation of 1,1'-Bis[diisopropylphosphino(borane)]-ferrocene

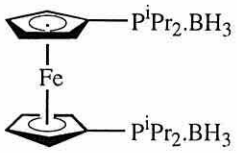

41

1,1'-Bis[diisopropylphosphino(borane)]ferrocene was prepared using a method similar to that outlined for 1,1'-bis[diphenylphosphino(borane)]ferrocene, but using 1,1'-bis(diisopropylphosphino)ferrocene (1.0g, 2.4 mmol). The product was obtained as orange-red crystals, 0.96g (89%), mp 150-152°C (benzene).

^{1}H NMR ($CDCl_3$): δ = 1.10 (2 x dd, 24H, $J_{H,H}$ = 7.1, $J_{H,P}$ = 14.5; 8 x C$\underline{H}_3$), 2.09 (d x sept, 4H, $J_{H,H}$ = 7.1, $J_{H,P}$ = 3.0; 4 x C$\underline{H}$), 4.35 (pt, 4H, J = 1.8; 4 x α-C$\underline{H}$), 4.65 (pt, 4H, J = 1.8; 4 x β-C$\underline{H}$)

^{13}C-{^{1}H} NMR ($CDCl_3$): δ = 17.2 (d, $J_{C,P}$ = 16.2; 8 x $\underline{C}H_3$), 22.5 (d, $J_{C,P}$ = 34.8; 4 x $\underline{C}$H), 60.0 (d, $J_{C,P}$ = 54.6; 2 x $\underline{C}$P), 72.8 (d, $J_{C,P}$ = 7.1; 4 x α-$\underline{C}$H), 73.5 (d, $J_{C,P}$ = 6.1; 4 x β-$\underline{C}$H)

^{31}P-{^{1}H} NMR ($CDCl_3$): δ = +30.5, (d, $J_{P,B}$ = 60.5)

^{11}B-{^{1}H} NMR ($CDCl_3$): δ = -43.7, (d, $J_{B,P}$ = 60.5)

IR ν_{max}($CHCl_3$)/cm^{-1}: 2396.3 (s), 1435.5 (s), 1108.5 (s), 1062.2 (m), 1032.3 (m)

MS (EI) m/z (rel. int.): 446 M^+ (10), 432 (12), 418 (15), 375 (20), 315 (22), 279 (20)

Calc. %: C 59.25 H 9.49 ($C_{22}H_{42}B_2FeP_2$)

Found %: C 59.43 H 9.60

5.2.19 Preparation of (*S*)-Ferrocenyl *p*-Tolyl Sulfoxide

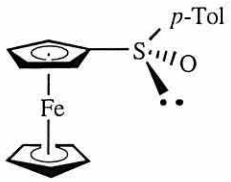

43

(*S*)-Ferrocenyl *p*-tolyl sulfoxide was prepared according to the procedure of Kagan *et al.*,[41] on a 68 mmol scale. The product was obtained as a yellow powder in 66% yield, mp 127-129°C (lit. 127-128°C).[15]

^{1}H NMR ($CDCl_3$): δ = 2.39 (s, 3H; C<u>H</u>$_3$), 4.34 (pt, 1H, *J* = 1.4; C2-<u>H</u>), 4.38 (m, 7H; 2 x β-C<u>H</u> + Cp), 4.62 (pt, 1H, *J* = 1.4; C5-<u>H</u>), 7.26 (d, 2H, *J* = 7.8; 2 x *m*-CH), 7.53 (*J* = 7.8; 2 x *o*-C<u>H</u>)

^{13}C-{^{1}H} NMR ($CDCl_3$): δ = 20.3 (<u>C</u>H$_3$), 65.3 (2 x α-<u>C</u>H), 67.8 (2 x β-<u>C</u>H), 70.0 (Cp), 124.4 (2 x *o*-<u>C</u>H), 129.6 (2 x *m*-<u>C</u>H), 141.0 (<u>C</u>SO)

IR ν_{max}($CHCl_3$)/cm^{-1}: 2922.6 (w), 2237.0 (m), 1083.7 (w), 1039.6 (bm), 911.9 (s), 745.1 (s), 722.4 (s)

MS (EI) m/z (rel. int.): 324 M^+ (100), 308 (8), 276 (9), 244 (43), 233 (10)

$[\alpha]^{25}_D$ = -4.2 [lit. 4 ± 1 (c = 0.9, $CHCl_3$)][15]

Calc. %: C 62.98 H 4.97 ($C_{17}H_{16}FeSO$)

Found %: C 62.78 H 4.97

5.2.20 Preparation of (*S*,*S*)-1-(*p*-Tolylsulfinyl)-2-[diisopropyl-phosphino(borane)]ferrocene

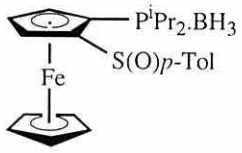

44

To a stirred suspension of (*S*)-ferrocenyl *p*-tolyl sulfoxide (6.4g, 20 mmol) in THF (100ml) cooled by means of an external acetone/ dry ice bath was added LDA (11ml of a 2M solution in THF, *n*-hexane and ethylbenzene, 22 mmol). The sulfoxide dissolved during the addition and the resulting red solution was stirred at -78°C for 20 min. before the addition of chlorodiisopropylphosphine (3.5ml, 22 mmol). After stirring at the same temperature for a further 1h, the mixture was treated with BH_3.THF (24ml of a 1M solution in THF, 24 mmol) and allowed to warm to room temperature. The mixture was stirred at room temperature for 90 min. before being quenched with dilute sodium hydroxide solution (50ml). The mixture was extracted with ether (3 x 50ml) and the combined organic extracts were washed with brine (2 x 50ml) and water (3 x 50ml), dried over anhydrous magnesium sulfate and concentrated *in vacuo*. Flash chromatography on silica using ether as eluent gave a yellow crystalline solid in a yield of 6.7g (74%), mp 149-151°C (*n*-hexane).

^{1}H NMR ($CDCl_3$): δ = 1.07 (2 x dd, 6H, $J_{H,H}$ = 7.0, $J_{H,P}$ = 15.7; 2 x C$\underline{H}_3$), 1.34 (dd, 3H, $J_{H,H}$ = 7.0, $J_{H,P}$ = 15.7; C$\underline{H}_3$), 1.73 (dd, 3H, $J_{H,H}$ = 7.0, $J_{H,P}$ = 15.7; C$\underline{H}_3$), 2.17 (sept x d, 1H, $J_{H,H}$ = 7.0, $J_{H,P}$ = 4.2; C$\underline{H}$), 2.49 (s, 3H; C$\underline{H}_3$), 3.09 (sept x d, 1H, $J_{H,H}$ = 7.0, $J_{H,P}$ = 4.2; C$\underline{H}$), 4.02 (pt, 1H, *J* = 1.8; C5-$\underline{H}$), 4.23 (s, 5H; Cp), 4.57 (pt, 1H, *J* = 1.8; C4-$\underline{H}$), 4.84 (pt, 1H, *J* = 1.8; C3-$\underline{H}$), 7.42 (d, 2H, *J* = 8.1; 2 x *m*-C$\underline{H}$), 7.80 (d, 2H, *J* = 8.1; 2 x *o*-C$\underline{H}$)

^{13}C-{^{1}H} NMR ($CDCl_3$): δ = 17.4 (d, $J_{C,P}$ = 26.6; 4 x $\underline{C}H_3$), 19.2 ($C_6H_4\underline{C}H_3$), 21.5 (d, $J_{C,P}$

= 34.7; CH), 24.5 (d, $J_{C,P}$ = 33.7; CH), 70.8 (C5), 70.9 (C3), 71.9 (Cp), 72.1 (C4), 78.2 (d, $J_{C,P}$ = 12.7; CP), 125.8 (2 x *m*-CH), 129.5 (2 x *o*-CH), 139.3 (CCH_3), 142.2 (CSO)

$^{31}P-\{^{1}H\}$ NMR ($CDCl_3$): δ = +37.1 (d, $J_{P,B}$ = 27.2)

$^{11}B-\{^{1}H\}$ NMR ($CDCl_3$): δ = -42.8 (d, $J_{B,P}$ = 27.2)

IR $\nu_{max}(CHCl_3)/cm^{-1}$: 3002.9 (s), 2933.6 (m), 2385.4 (s), 1492.2 (m), 1462.2 (m), 1253.6 (m), 1034.2 (s), 770.5 (s)

MS (EI) m/z (rel. int.): 454 M^+ (18), 440 (100), 424 (5), 308 (15), 284 (100), 242 (22)

$[\alpha]^{25}_D$ = -184.6° (c = 1.5, $CHCl_3$)

Calc. %: C 60.82 H 7.10 ($C_{23}H_{32}BFeOPS$)

Found %: C 60.88 H 6.88

5.2.21 Preparation of (*S*)-1-(Diphenylphosphoryl)-2-[diisopropylphosphino(borane)]ferrocene

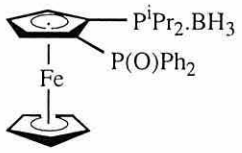

47

(*S*,*S*)-1-(*p*-Tolylsulfinyl)-2-[diisopropylphosphino(borane)]ferrocene (0.5g, 1.1 mmol) was dissolved in THF (50ml) and cooled by means of an external acetone/ dry ice bath. To the stirred solution was added *tert*-butyllithium (0.78ml of a 1.6M solution in hexanes, 1.2 mmol). After stirring for 5 min., the mixture was treated with chloro-diphenylphosphine (0.22ml, 1.2 mmol) and allowed to stir for a further 1h. To the mixture was added BH_3.THF (5ml of a 1M solution in THF, 5 mmol) and the resulting mixture was stirred for 1h before being allowed to warm to room temperature. Stirring was continued for 18h after which the reaction was quenched with water (50ml) and extracted using ether (3 x 100ml). The combined organic extracts were washed with brine (2 x 50ml) and water (2 x 50ml), dried over anhydrous magnesium sulfate and concentrated *in vacuo*. Flash chromatography on silica using 50% ether/ *n*-hexane afforded the product **47** in a yield of 80mg (14%) as a yellow-orange oil and [diisopropylphosphino(borane)]ferrocene **46** as impurity in a yield of 69mg (20%), as dark orange crystals, mp 171-173°C (*n*-hexane).

^{1}H NMR ($CDCl_3$): δ = 1.18 (dd, 12H, $J_{H,H}$ = 7.0, $J_{H,P}$ = 13.8; 4 x C$\underline{H}_3$), 2.12 (*pseudo*-sept, 2H, *J* = 7.0; 2 x C$\underline{H}$), 4.31 (m, 6H, Cp + C4-$\underline{H}$), 4.36 (m, 1H, C5-$\underline{H}$), 4.45 (m, 1H, C3-$\underline{H}$), 7.48 (m, 6H; 4 x *m*-C$\underline{H}$ + 2 x *p*-C$\underline{H}$), 7.80 (m, 4H; 4 x *o*-C$\underline{H}$)

^{13}C-{^{1}H} NMR ($CDCl_3$): δ = 17.3 (d, $J_{C,P}$ = 15.9; 4 x $\underline{C}H_3$), 22.5 (d, $J_{C,P}$ = 35.1; 2 x $\underline{C}$H), 69.9 (Cp), 70.5 (d, $J_{C,P}$ = 6.5; $\underline{C}$5), 71.7 (d, $J_{C,P}$ = 7.5; $\underline{C}$3+ $\underline{C}$4), 129.1 (d, $J_{C,P}$ = 10.3; 4 x *m*-$\underline{C}$H), 133.0 (d, $J_{C,P}$ = 9.4; 4 x *o*-$\underline{C}$H), 134.0 (d, $J_{C,P}$ = 7.8, 2 x *p*-$\underline{C}$H)

$^{31}P-\{^{1}H\}$ NMR ($CDCl_3$): δ = +30.7 (d, $J_{P,B}$ = 60.0), +80.2 (s)

$^{11}B-\{^{1}H\}$ NMR ($CDCl_3$): δ = -43.4 (d, $J_{B,P}$ = 60.0)

IR $\nu_{max}(CHCl_3)/cm^{-1}$: 2967.2 (s), 2935.5 (s), 2874.5 (s), 2395.9 (bs), 1641.0 (bm), 1464.3 (m), 1386.6 (w), 1167.9 (s)

MS (EI) m/z (rel. int.): 516 M^+ (5), 502 (100), 385 (16), 370 (55), 302 (100), 217 (100)

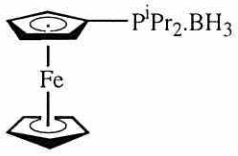

46

^{1}H NMR ($CDCl_3$): δ = 1.20-1.37 (m, 12H; 4 x C<u>H</u>$_3$), 2.10-2.35 (m, 2H; 2 x C<u>H</u>), 4.29 (s, 5H; Cp), 4.35 (m, 2H; 2 x α-C<u>H</u>), 4.45 (m, 2H; 2 x β-C<u>H</u>)

$^{13}C-\{^{1}H\}$ NMR ($CDCl_3$): δ = 16.2 (d, $J_{C,P}$ = 27.7; 4 x <u>C</u>H$_3$), 22.5 (d, $J_{C,P}$ = 35.1; 2 x <u>C</u>H), 69.9 (Cp), 70.5 (d, $J_{C,P}$ = 6.3; 2 x α-<u>C</u>H), 71.7 (d, $J_{C,P}$ = 7.5; 2 x β-<u>C</u>H)

$^{31}P-\{^{1}H\}$ NMR ($CDCl_3$): δ = +30.3 (d, $J_{P,B}$ = 57.2)

$^{11}B-\{^{1}H\}$ NMR ($CDCl_3$): δ = -45.6 (d, $J_{B,P}$ = 57.2)

IR $\nu_{max}(CHCl_3)/cm^{-1}$: 3002.9 (bs), 2933.6 (m), 2872.2 (m), 2385.4 (bs), 1492.2 (m), 1253.6 (m), 1082.3 (m), 1034.2 (bs)

MS (EI) m/z (rel. int.): 316 M^+ (15), 302 (84), 259 (53), 217 (100), 197 (15)

Calc. %: C 60.81 H 8.29 ($C_{16}H_{26}BFeP$)

Found %: C 60.58 H 8.41

5.2.22 Preparation of 1,2-Bis[diisopropylphosphino(borane)]-ferrocene

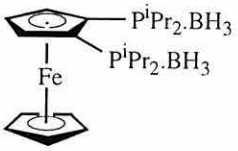

9

(*S*,*S*)-1-(*p*-Tolylsulfinyl)-2-[diisopropylphosphino(borane)]ferrocene (0.5g, 1.1 mmol) was dissolved in THF (50ml) and cooled by means of an external acetone/ dry ice bath. To the stirred solution was added *tert*-butyllithium (0.78ml of a 1.6M solution in hexanes). After stirring for 5 min., the mixture was treated with chlorodiisopropyl-phosphine (0.19ml, 1.2 mmol) and allowed to stir for a further 1h. To the mixture was added BH_3.THF (5ml of a 1M solution in THF, 5 mmol) and the resulting mixture was stirred for 1h before being allowed to warm to room temperature. Stirring was continued for 18h after which the reaction was quenched with water (50ml) and extracted using ether (3 x 100ml). The combined organic extracts were washed with brine (2 x 50ml) and water (2 x 50ml), dried over anhydrous magnesium sulfate and concentrated *in vacuo*. Flash chromatography on silica using 50% ether/ *n*-hexane afforded the product in a yield of 108mg (22%) as orange-red crystals, mp 182-184°C (*n*-hexane), along with orange crystals of [diisopropylphosphino(borane)]ferrocene as impurity in a yield of 51mg (15%), mp 171-173°C (*n*-hexane).

^{1}H NMR ($CDCl_3$): δ = 1.01-1.34 (m, 24H; 8 x C$\underline{H}_3$), 2.18 (*pseudo*-sept, 2H, *J* = 7.0; 2 x C$\underline{H}$), 2.57 (*pseudo*-sept, 2H, *J* = 7.0; 2 x CH), 4.35 (s, 5H; Cp), 4.72 (t, 1H, *J* = 2.5; C4-$\underline{H}$), 4.81 (dd, 2H, $J_{3,4}$ = 2.5, $J_{3,5}$ = 1.4; C3-$\underline{H}$ + C5-$\underline{H}$)

^{13}C-{^{1}H} NMR ($CDCl_3$): δ = 15.5 (d, $J_{C,P}$ = 45.9, 4 x $\underline{C}H_3$), 24.9 (d, $J_{C,P}$ = 18.8; 2 x $\underline{C}$H), 25.4 (d, $J_{C,P}$ = 17.2; 2 x $\underline{C}$H), 72.0 (Cp), 72.1 ($\underline{C}$4), 78.8 (d, $J_{C,P}$ = 10.1, 2 x $\underline{C}$P)

^{31}P-{^{1}H} NMR ($CDCl_3$): δ = +33.8 (d, $J_{P,B}$ = 57.1)

^{11}B-{^{1}H} NMR ($CDCl_3$): δ = -43.5 (d, $J_{B,P}$ = 57.1)

IR $\nu_{max}(CHCl_3)/cm^{-1}$: 2967.2 (s), 2935.5 (s), 2874.5 (s), 2395.9 (bs), 1641.0 (bm), 1464.3 (m), 1386.6 (w), 1367.2 (w)

MS (EI) m/z (rel. int.): 446 M^+ (2), 432 (29), 431 (100), 418 (5), 389 (7), 375 (32)

Calc. %: C 59.25 H 9.49 ($C_{22}H_{42}B_2FeP_2$)

Found %: C 58.98 H 9.52

5.3 Co-ordination Chemistry

5.3.1 Preparation of $[NiCl_2(DIPPF)]$

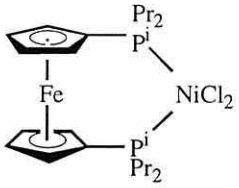

49

1,1'-Bis(diisopropylphosphino)ferrocene (1.0g, 2.39 mmol) and $NiCl_2.6H_2O$ (0.52g, 2.2 mmol) were each dissolved in boiling methanol (10ml). The metal salt solution was added dropwise to that of the ligand and the resulting mixture was stirred with continued reflux for 10 min. The product was filtered off while the mixture was still hot and was washed with cold methanol (2 x 15ml) to yield 1.20g (92%) of dark green crystals, mp 191-193°C (dec.).

^1H NMR ($CDCl_3$): δ = 1.28 (m, 12H; 4 x C<u>H</u>$_3$), 1.60 (m, 12H; 4 x C<u>H</u>$_3$), 3.07 (m, 4H; 4 x C<u>H</u>), 4.54 (m, 4H; 4 x α-C<u>H</u>), 4.79 (m, 4H; 4 x β-C<u>H</u>)

^{31}P-{^1H} NMR ($CDCl_3$): δ = 52.2 (s)

IR $\nu_{max}(CHCl_3)/cm^{-1}$: 2994.6 (bs), 1460.1 (bm), 1391.2 (m), 1370.9 (m), 1164.4 (s), 1037.7 (s), 929.5 (w), 881.3 (w)

MS (FAB) m/z (rel. int.): 571 M^++Na^+ (32), 548 M^+ (62), 418 (100), 375 (28), 302 (18)

Calc. %: C 48.23 H 6.62 ($C_{22}H_{36}Cl_2FeNiP_2$)

Found %: C 48.08 H 6.64

5.3.2 Preparation of $[NiCl_2(DPPF)]$

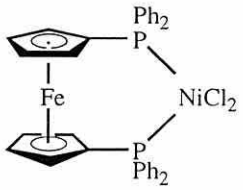

48

A similar procedure to that described for $[NiCl_2(DIPPF)]$ was employed, using 1,1'-bis(diphenylphosphino)ferrocene (1.0g, 1.81 mmol) and $NiCl_2.6H_2O$ (0.42g, 1.75 mmol). The product was isolated as a dark green powder in a yield of 1.18g (96%), mp 278-280°C (dec.).

IR $\nu_{max}(CHCl_3)/cm^{-1}$: 3398.1 (bs), 1641.6 (bm), 1480.3 (m), 1433.7 (m), 1165.5 (m), 1096.5 (m), 1029.7 (m), 797.1 (s)

MS (FAB) m/z (rel. int.): 707 M^++Na^+ (12), 684 M^+ (15), 554 (100), 477(13), 399 (16)

Calc. %: C 59.71 H 4.13 ($C_{34}H_{28}Cl_2FeNiP_2$)

Found %: C 59.80 H 3.97

5.3.3 Preparation of *cis*-[$PdCl_2$(DIPPF)]

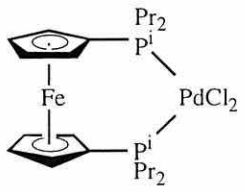

51

1,1'-Bis(diisopropylphosphino)ferrocene (0.81g, 1.93 mmol) was dissolved in dichloromethane (10ml). To the stirred solution was added dropwise a solution of *cis*-[Pd(COD)Cl_2] (0.5g, 1.75 mmol) in dichloromethane (10ml). The mixture was stirred at room temperature for 10 min., and the product was precipitated by the addition of *n*-hexane (20ml). The product was washed with ether (3 x 10ml) to yield an orange solid (0.93g, 89%), mp 232-234°C (toluene).

^{1}H NMR ($CDCl_3$): δ = 1.25 (m, 12H; 4 x C$\underline{H}_3$), 1.60 (m, 12H; 4 x C$\underline{H}_3$), 3.05 (m, 4H; 4 x C$\underline{H}$), 4.50 (m, 4H; 4 x α-C$\underline{H}$), 4.58 (m, 4H; 4 x β-C$\underline{H}$)

^{13}C-{^{1}H} NMR ($CDCl_3$): δ = 19.7 (4 x $\underline{C}H_3$), 20.3 (4 x $\underline{C}H_3$), 28.6 (d, $J_{C,P}$ = 14.3; 4 x $\underline{C}$H), 71.1 (2 x $\underline{C}$P), 72.3 (4 x α-$\underline{C}$H), 74.0, (4 x β-$\underline{C}$H)

^{31}P-{^{1}H} NMR ($CDCl_3$): δ = 62.2 (s)

IR ν_{max}($CHCl_3$)/cm^{-1}: 2971.9 (bs), 1460.5 (bs), 1387.8 (m), 1163.8 (s), 1037.4 (s), 929.8 (w), 882.0 (w)

MS (FAB) m/z (rel. int.): 561 M^+-Cl^- (66), 559 M^+-Cl^- (70), 525 (100), 375 (25), 302 (20)

Calc. %: C 44.36 H 6.09 ($C_{22}H_{36}Cl_2FeP_2Pd$)

Found %: C 44.33 H 6.14

5.3.4 Preparation of *cis*-[$PdCl_2$(DPPF)]

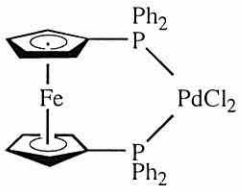

50

A similar procedure to that outlined for *cis*-[$PdCl_2$(DIPPF)] was employed, using 1,1'-bis(diphenylphosphino)ferrocene (1.1g, 1.93 mmol) and *cis*-[Pd(COD)Cl_2] (0.5g, 1.75 mmol). The product was obtained as a dark red solid in a yield of 1.16g (91%), mp 275-280°C (toluene).

^{1}H NMR ($CDCl_3$): δ = 4.21 (m, 4H; 4 x α-C<u>H</u>), 4.41 (m, 4H; 4 x β-C<u>H</u>), 7.35-7.55 (m, 12H; 8 x *m*- + 4 x *p*-C<u>H</u>), 7.91 (m, 8H; 8 x *o*-C<u>H</u>)

^{13}C-{^{1}H} NMR ($CDCl_3$): δ = 74.0 (4 x β-<u>C</u>H), 76.5 (4 x α-<u>C</u>H), 77.8 (2 x <u>C</u>P), 128.1 (8 x *o*-<u>C</u>H), 128.2 (4 x *p*-<u>C</u>H), 131.4 (8 x *m*-<u>C</u>H), 135.1 (4 x <u>C</u>P)

^{31}P-{^{1}H} NMR ($CDCl_3$): δ = 33.4 (s)

IR ν_{max}($CHCl_3$)/cm^{-1}: 3415.8 (bs), 1641.3 (bm), 1479.9 (w), 1435.9 (m), 1095.5 (w), 762.1 (bs)

MS (FAB) m/z (rel. int.): 695 M^+-Cl^- (48), 693 M^+-Cl^- (52), 659 (100), 554 (25), 477 (10), 369 (8)

Calc. %: C 55.81 H 3.86 ($C_{34}H_{28}Cl_2FePdP_2$)

Found %: C 55.58 H 3.92

5.3.5 Preparation of *cis*-[$PdCl_2$(IPPFA)].CH_2Cl_2

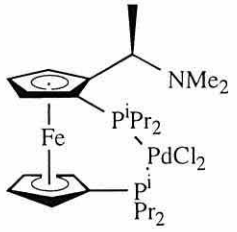

52

A similar procedure to that outlined for *cis*-[$PdCl_2$(DIPPF)] was employed, using (*R,S*)-1,1'-bis(diisopropylphosphino)-2-[(*N,N*-dimethylamino)ethyl]ferrocene (0.94g, 1.92 mmol) and *cis*-[Pd(COD)Cl_2] (0.50g, 1.75 mmol). The product was obtained as an orange-yellow solid (0.93g, 89%), mp 205-208°C (toluene).

^{1}H NMR ($CDCl_3$): δ = 1.27 (d, 3H, *J* = 6.9; C$\underline{H}_3$), 1.51-1.76 (m, 24H; 8 x C$\underline{H}_3$), 2.03 [s, 6H; N(C$\underline{H}_3$)$_2$], 3.32-3.62 (m, 4H; 4 x C$\underline{H}$), 3.58 (q, 1H, *J* = 6.9; C$\underline{H}$), 4.28 (m, 1H; C4-$\underline{H}$), 4.37 (m, 1H; C5-$\underline{H}$), 4.43 (m, 2H; 2 x β-C$\underline{H}$), 4.53 (m, 2H; 2 x α-C$\underline{H}$), 4.69 (m, 1H; C3-$\underline{H}$)

^{13}C-{^{1}H} NMR ($CDCl_3$): δ = 7.8 (C$\underline{H}_3$), 21.0 (8 x C$\underline{H}_3$), 29.4 [N(C$\underline{H}_3$)$_2$], 39.0 (4 x C$\underline{H}$), 56.5 (C$\underline{H}$), 70.7 (2 x α-C$\underline{H}$), 73.6 (2 x β-C$\underline{H}$)

^{31}P-{^{1}H} NMR ($CDCl_3$): δ = 75.9, (d, $J_{P\text{-}P}$ = 25.0), 57.5 (d, $J_{P\text{-}P}$ = 25.0)

IR ν_{max}($CHCl_3$)/cm^{-1}: 4213.0 (m), 2986.4 (s), 2782.4 (w), 2399.5 (m), 1460.4 (bm), 1365.3 (w), 1045.9 (bw), 928.6 (m)

MS (FAB) m/z (rel. int.): 690 M^++Na^+ (18), 667 M^+ (13), 632 (100), 595 (13), 494 (17)

Calc. %: C 44.10 H 6.21 N 1.87 ($C_{27}H_{47}Cl_4FeNP_2Pd$)

Found %: C 43.94 H 6.32 N 2.01

5.4 Catalysis

5.4.1 The Heck Reaction - General Method for *cis*-[$PdCl_2$(DIPPF)] Catalysis

cis-[$PdCl_2$(DIPPF)] **51** (59.5mg, 0.1 mmol) and copper (I) iodide (38.1mg, 0.2 mmol) were suspended in acetonitrile (10ml) to which was added triethylamine (7ml, 50 mmol). The mixture was heated to reflux for 10 min., during which time the colour changed from orange to black. Iodobenzene (1.11ml, 10 mmol) and alkene (10 mmol) were added and the mixture was refluxed for a further 24h. A sample of the reaction mixture was removed for GLC analysis; the remainder was quenched with dilute hydrochloric acid (10ml) and extracted with ether (3 x 20ml). The combined organic fractions were washed with saturated ammonium chloride solution (20ml) and water (2 x 20ml), dried over anhydrous magnesium sulfate, reduced in volume to *ca.*1ml, then chromatographed on silica using 5% ether in petrol.

The experimental results and NMR data are reported in Table 5.1.

SUBSTRATE	PRODUCT	YIELD GLC %	^{1}H NMR ($CDCl_3$) δ (ppm) =
Methyl acrylate	(*E*)-PhCH=CHCO$_2$CH$_3$	100	3.77 (s, 3H), 6.40 (d, 1H, *J* = 16.0), 7.32-7.37 (m, 3H), 7.45-7.51 (m, 2H), 7.66 (d, 1H, *J* = 16.0)
Methyl methacrylate	(*E*)-PhC(CH$_3$)=CHCO$_2$CH$_3$	66.7	2.14 (d, 3H, *J* = 1.5), 3.84 (s, 3H), 7.40 (m, 5H), 7.71 (d, 1H, *J* = 1.5)
	PhCH$_2$C(=CH$_2$)CO$_2$CH$_3$	23.8	3.66 (d, 2H, *J* = 2.7), 3.75 (s, 3H), 5.47 (dd, 1H, *J* = 1.2, 2.7), 6.25 (d, 1H, *J* = 1.2), 7.42 (m, 5H)

SUBSTRATE	PRODUCT	YIELD GLC %	^{1}H NMR ($CDCl_3$) δ (ppm) =
Vinyl acetate	(*E*)-PhCH=CHOAc	98.5	2.21 (s, 3H), 6.40 (d, 1H, *J* = 12.8), 7.29-7.79 (m, 5H), 7.85 (d, 1H, *J* = 12.8)
	(*Z*)-PhCH=CHOAc	0.9	2.06 (s, 3H), 5.72 (d, 1H, *J* = 7.1), 7.29-7.36 (m, 5H), 7.59 (d, 1H, *J* = 7.4)
	$PhCH_2CHO$	0.6	4.13 (q, 2H, *J* = 7.1), 7.29 (m, 5H), 9.98 (s, 1H)
Acrylonitrile	(*Z*)-PhCH=CHCN	20.3	5.85 (d, 1H, *J* = 16.4), 7.34-7.41 (m, 5H), 7.40 (d, 1H, *J* = 16.4)
	(*E*)-PhCH=CHCN	6.7	5.42 (d, 1H, *J* = 12.1), 7.10 (d, 1H, *J* = 12.1), 7.34-7.41 (m, 5H)
n-Butyl vinyl ether	(*Z*)-PhCH=CHO^{n}Bu	6.9	0.98 (t, 3H, *J* = 7.0), 1.44-1.76 (m, 4H), 3.85 (t, 2H, *J* = 7.0), 5.21 (d, 1H, *J* = 7.0), 6.22 (d, 1H, *J* = 7.0), 7.11-7.40 (m, 5H)
	(*E*)-PhCH=CHO^{n}Bu	8.2	0.98 (t, 3H, *J* = 7.0), 1.44-1.76 (m, 4H), 3.94 (t, 2H, *J* = 7.0), 5.85 (d, 1H, *J* = 13.0), 7.01 (d, 1H, *J* = 13.0), 7.12-7.39 (m, 5H)
	$PhCH_2CHO$	18	Identified by GLC/MS comparison
Stryrene	(*E*)-PhCH=CHPh	12.9	7.27 (s, 2H), 7.37-7.68 (m, 10H)
	(*Z*)-PhCH=CHPh	4.5	Identified by GLC/MS comparison
Vinylidene chloride	No observed reaction	0	

Table 5.1 Heck reaction of iodobenzene with alkene substrates

5.4.2 The Heck Reaction - General Method for Reaction of Aryl Iodides and Methyl Acrylate

The palladium-phosphine (0.1 mmol) and copper (I) iodide (38.1mg, 0.2 mmol) were suspended in a mixture of acetonitrile (10ml) and triethylamine (2ml). The mixture was heated to reflux under nitrogen for 5 min., during which time the colour changed from orange to black. Iodobenzene (1.11ml, 10 mmol) and methyl acrylate (1.08ml, 12 mmol) were added and the mixture was refluxed for a further 24h. A sample of the reaction mixture was removed for GLC analysis, and the reaction was quenched by the addition of dilute hydrochloric acid (20ml). The products were extracted using ether (3 x 20ml), washed with brine (2 x 10ml) and water (2 x 10ml), dried over anhydrous magnesium sulfate and evaporated to dryness. Purification was achieved by flash chromatography on silica using 5% ether/ petrol then pure ether.

The experimental results are reported in Chapter 3.

(*E*)-FcCH=CHCO$_2$CH$_3$, mp 84-86°C (*n*-hexane)

^{1}H NMR ($CDCl_3$): δ = 3.78 (s, 3H; C<u>H</u>$_3$), 4.17, (s, 5H; Cp), 4.42 (pt, 2H, *J* = 1.8; 2 x β-C<u>H</u>), 4.50 (pt, 2H, *J* = 1.8; 2 x α-C<u>H</u>), 6.04 (d, 1H, *J* = 16.0; C<u>H</u>=CHCO), 7.59 (d, 1H, *J* = 16.0; CH=C<u>H</u>CO)

^{13}C-{^{1}H} NMR ($CDCl_3$): δ = 51.4 (<u>C</u>H$_3$), 68.6 (2 x β-<u>C</u>H), 69.6 (Cp), 70.8 (2 x α-<u>C</u>H), 78.6 (<u>C</u>1), 114.4 (<u>C</u>H=CHCO), 145.9 (CH=<u>C</u>HCO), 167.6 (<u>C</u>=O)

IR ν_{max} ($CHCl_3$)/cm^{-1}: 2950.9 (w), 1696.5 (bs), 1629.9 (s), 1435.0 (m), 1308.3 (m), 1164.5 (m), 1043.7 (w)

MS (EI) m/z (rel. int.): 270 M$^+$ (100), 204 (90), 174 (32), 120 (19)

5.4.3 Organomagnesium Cross-Coupling - General Method

sec-Butylmagnesium chloride (53.0ml, 0.5 mol) was dissolved in ether (200ml) and added dropwise to magnesium turnings (12.2g, 0.5 mol) in ether (100ml). A single crystal of iodine was added to the mixture which began to exotherm after *ca.* 10% addition of the alkyl halide. When the addition was complete the mixture was refluxed for 30 min., then allowed to return to room temperature before being filtered through a sinter and stored under argon. The Grignard solution was titrated against a standard solution of hydrochloric acid before each of the subsequent catalyses and was found to be 1.6M on each occasion.

Nickel- or palladium-phosphine (DPPF or DIPPF) (0.04 mmol) was placed in an argon-filled flask and cooled using an external acetone/ dry ice bath. Bromobenzene (0.42ml, 4 mmol) and *sec*-butylmagnesium chloride (4.9ml of the 1.6M solution in ether, 3.1 mmol) were added to the cooled complex, which was then allowed to warm to room temperature. The mixture was stirred for 1h, during which samples were taken for GLC analysis at 5 min. intervals.

The experimental results are reported in Chapter 3.

5.4.4 Suzuki Cross-Coupling - General Method

Suzuki cross-coupling was carried out according to the procedure of Miyaura[137] (with nickel reduction) or Indolese[107] (without), as specified in Table 3.8.

To a stirred solution of nickel-phosphine (0.1 mmol) in 1,4-dioxane or THF (10ml) was added *n*-butyllithium (0.16ml of a 2.5M solution in hexanes, 4 mmol) at room temperature. The mixture was stirred for 10 min. to give a red solution of nickel (0). To this solution was added phenylboronic acid (0.13g, 1.1 mmol), tripotassium phosphate (0.64g, 3 mmol) and 4-chlorotoluene (0.12ml, 1 mmol). The mixture was refluxed for 18h. After cooling to room temperature, a sample of the mixture was analysed by GLC. The remainder was evaporated to dryness and chromatographed on silica gel using 5% ether/ petrol.

The experimental results are reported in Chapter 3.

Chapter 6

References

1. R. S. Cahn, C. K. Ingold, V. Prelog, *Angew. Chem. Int. Ed. Engl.*, 1966, **5**, 385-415
2. K. Schlögl, *Top. Stereochem.*, 1967, **1**, 39-91
3. *Ferrocenes: Homogeneous Catalysis, Organic Synthesis, Materials Science*, Ed. A. Togni and T. Hayashi, VCH, Weinheim, 1995
4. J. J. Bishop, A. Davison, M. L. Katcher, D. W. Lichtenberg, R. E. Merrill, J. C. Smart, *J. Organomet. Chem.*, 1971, **27**, 241-249
5. A. Togni, C. Breutel, M. C. Soares, N. Zanetti, T. Gerfin, V. Gramlich, F. Spindler and G. Rihs, *Inorg. Chim. Acta*, 1994, **222**, 213-224
6. I. R. Butler, W. R. Cullen, T.-J. Kim, S. J. Rettig and J. Trotter, *Organometallics*, 1985, **4**, 972-980
7. I. R. Butler, W. R. Cullen and T.-J. Kim, *Synth. React. Inorg. Met.-Org. Chem.*, 1985, **15**, 109-116
8. B. McCulloch, D. L. Ward, J. D. Woolins and C. H. Brubaker, Jr., *Organometallics*, 1985, **4**, 1425-1432
9. (a) L. L. Lai and T.-Y. Dong, *J. Chem. Soc. Chem. Commun.*, 1994, 2347-2348
   (b) L. L. Lai and T.-Y. Dong, *Synthesis*, 1995, 1231-1232
   (c) L. L. Lai and T.-Y. Dong, *J. Organomet. Chem.*, 1996, **509**, 131-134
10. M. E. Wright, *Organometallics*, 1990, **9**, 853-856
11. D. Seyferth and H. P. Withers, *J. Organomet. Chem.*, 1980, **185**, C1-C5
12. I. R. Butler, *Polyhedron*, 1992, **11**, 3117-3121
13. I. R. Butler, W. R. Cullen, S. J. Rettig and A. S. C. White, *J. Organomet. Chem.*, 1995, **492**, 157-164
14. I. R. Butler, W. R. Cullen, J. Ni and S. J. Rettig, *Organometallics*, 1985, **4**, 2196-2201
15. F. Rebière, O. Samuel and H. B. Kagan, *Tetrahedron Lett.*, 1990, **31**, 3121-3124
16. R. Sanders and U. T. Müller-Westerhoff, *J. Organomet. Chem.*, 1996, **512**, 219-224
17. I. R. Butler and R. L. Davies, *Synthesis*, 1996, 1350-1354

18. D. Guillaneux and H. B. Kagan, *J. Org. Chem.*, 1995, **60**, 2502-2505

19. F. L. Hedberg and H. Rosenberg, *Tetrahedron Lett.*, 1969, 4011-4012

20. I. R. Butler, W. R. Cullen, F. W. B. Einstein, S. J. Rettig and A. J. Willis, *Organometallics*, 1983, **2**, 128-135

21. I. R. Butler and W. R. Cullen, *Can. J. Chem.*, 1983, **61**, 147-153

22. J. Podlaha, P. Štěpnička, J. Ludvík and I. Císařová, *Organometallics*, 1996, **15**, 543-550

23. I. R. Butler, M. Kalaji, L. Nehrlich and D. J. Williams, *Polyhedron*, 1993, **12**, 1003-1006

24. I. R. Butler, M. Kalaji, L. Nehrlich, M. Hursthouse, A. I. Karaulov and K. M. Abdul Malik, *J. Chem. Soc. Chem. Commun.*, 1995, 459-460

25. I. R. Butler, W. R. Cullen, S. J. Rettig and A. S. C. White, *J. Organomet. Chem.*, 1995, **492**, 157-164

26. I. Manners, *Polyhedron*, 1996, **15**, 4311-4329

27. A. Togni, *Angew. Chem. Int. Ed. Engl.*, 1996, **35**, 1475-1477

28. H. B. Kagan, P. Diter, A. Gref., D. Guillaneux, A. Masson-Szymczak, F. Rebière, O. Samuel, O. Riant and S. Taudien, *Pure Appl. Chem.*, 1996, **68**, 29-36

29. C. R. Hauser and J. K. Lindsay, *J. Org. Chem.*, 1957, **22**, 906-908

30. D. Marquarding, H. Klusacek, G. K. Gokel, P. Hoffmann and I. K. Ugi, *J. Am. Chem. Soc.*, 1970, **92**, 5389-5393

31. G. W. Gokel, P. Hoffmann, H. Klusacek, D. Marquarding, E. Ruch and I. K. Ugi, *Angew. Chem. Int. Ed. Engl.*, 1970, **9**, 64-65

32. G. W. Gokel, D. Marquarding and I. K. Ugi, *J. Org. Chem.*, 1972, **37**, 3052-3058

33. G. W. Gokel and I. K. Ugi, *J. Chem. Educ.*, 1972, **49**, 294-296

34. S. Bhattacharyya, *J. Chem. Res. (S)*, 1995, 36-37

35. R. Herrmann and I. K. Ugi, *Angew. Chem. Int. Ed. Engl.*, 1979, **18**, 956-957

36. I. R. Butler, W. R. Cullen, F. G. Herring and N. R. Jagannathan, *Can. J. Chem.*, 1986, **64**, 667-669

37. T. Sammakia, H. A. Latham and D. R. Schaad, *J. Org. Chem.*, 1995, **60**, 10-11

38. C. J. Richards, T. Damalidis, D. E. Hibbs and M. Hursthouse, *Synlett*, 1995, 74-76

39. K. H. Ahn, C.-W. Cho, H.-H. Baek, J. Park and S. Lee, *J. Org. Chem.*, 1996, **61**, 4937-4943

40. T. Sammakia and H. A. Latham, *J. Org. Chem.*, 1996, **61**, 1629-1635

41. O. Riant, G. Arouarch, D. Guillaneux, O. Samuel and H. B. Kagan, *J. Org. Chem.*, 1998, **63**, 3511-3514

42. F. Rebière, O. Riant, L. Ricard and H. B. Kagan, *Angew. Chem. Int. Ed. Engl.*, 1993, **32**, 568-570

43. Y. Nishibayashi, Y. Arikawa, K. Ohe and S. Uemura, *J. Org. Chem.*, 1996, **61**, 1172-1174

44. C. Ganter and T. Wagner, *Chem. Ber.*, 1995, **128**, 1157-1161

45. M. Tsukazaki, M. Tiknl, A. Roglans, B. J. Chapell, N. J. Taylor and V. Snieckus, *J. Am. Chem. Soc.*, 1996, **118**, 685-686

46. O. Riant, O. Samuel and H. B. Kagan, *J. Am. Chem. Soc.*, 1993, **115**, 5835-5836

47. T. Hayashi, T. Mise, M. Fukushima, M. Kagotani, N. Nagashima, Y. Hamada, A. Matsumoto, S. Kawakami, M. Konishi, K. Yamamoto and M. Kumada, *Bull. Chem. Soc. Jpn.*, 1980, **53**, 1138-1151

48. T. Hayashi and M. Kumada, *Acc. Chem. Res.*, 1982, **15**, 395-401

49. T. Hayashi, *Pure Appl. Chem.*, 1988, **60**, 7-12

50. F. H. van der Steen and J. A. Kanters, *Acta Cryst.*, 1986, C**42**, 547-550

51. T. Hayashi, M. Kumada, T. Higuchi and K. Hirotsu, *J. Organomet. Chem.*, 1987, **334**, 195-203

52. T. Hayashi, M. Konishi, Y. Kobori, M. Kumada, T. Higuchi and K. Hirotsu, *J. Am. Chem. Soc.*, 1984, **106**, 158-163

53. G. M. Whitesides, J. F. Gaasch and E. R. Stedronsky, *J. Am. Chem. Soc.*, 1972, **94**, 5258-5270

54. A. G. Avent, R. B. Bedford, P. A. Chaloner, S. Z. Dewa and P. B. Hitchcock, *J. Chem. Soc. Dalton Trans.*, 1996, 4633-4638

55. N. J. Goodwin, W. Henderson and J. K. Sarfo, *Chem. Commun.*, 1996, 1551-

1552

56. K. Naumann, G. Zon and K. Mislow, *J. Am. Chem. Soc.*, 1969, **91**, 7012-7023
57. S. Griffin, L. Heath and P. Wyatt, *Tetrahedron Lett.*, 1998, **39**, 4405-4406
58. L. McKinstry and T. Livinghouse, *Tetrahedron Lett.*, 1994, **35**, 9319-9322
59. H. Schmidbaur, *J. Organomet. Chem.*, 1980, **200**, 287-306
60. F. Langer and P. Knockel, *Tetrahedron Lett.*, 1995, **36**, 4591-4594
61. E. Soulier, J.-C. Clément, J.-J. Yaouanc and H. des Abbayes, *Tetrahedron Lett.*, 1998, **39**, 4291-4294
62. A. Longeau, F. Langer and P. Knockel, *Tetrahedron Lett.*, 1996, **37**, 2209-2212
63. K. C. Nainan and G. E. Ryschkewitsch, *Inorg. Chem.*, 1969, **8**, 2671-2674
64. T. Imamoto, T. Kusumoto, N. Suzuki and K. Sato, *J. Am. Chem. Soc.*, 1985, **107**, 5301-5303
65. H. Brisset, Y. Gourdel, P. Pellon and M. Le Corre, *Tetrahedron Lett.*, 1993, **34**, 4523-4526
66. M. S. Kharasch and E. K. Fields, *J. Am. Chem. Soc.*, 1941, **63**, 2316-2320
67. M. Tamura and J. K. Kochi, *J. Am. Chem. Soc.*, 1971, **93**, 1487-1489
68. K. Tamao, K. Sumitani and M. Kumada, *J. Am. Chem. Soc.*, 1972, **94**, 4374-4376
69. R. J. P. Corriu and J. P. Masse, *J. Chem. Soc. Chem. Commun.*, 1972, 144
70. R. F. Heck and J. P. Nolly, *J. Org. Chem.*, 1972, **37**, 2320-2322
71. M. Yamamura, I. Moritani and S. I. Murahashi, *J. Organomet. Chem.*, 1975, **91**, C39-C42
72. *Comprehensive Organometallic Chemistry II*, **12**, Ed. E. W. Abel, F. G. A. Stone and G. Wilkinson, Pergamon, Oxford, 1995
73. C. A. Merlic and M. F. Semmelhack, *J. Organomet. Chem.*, 1990, **391**, C23-C27
74. Y. Fujiwara, *Tetrahedron Lett.*, 1967, 1119-1122
75. T. Mizoroki, K. Mori and A. Ozaki, *Bull. Chem. Soc. Jpn.*, 1971, **44**, 581
76. R. F. Heck, *Pure Appl. Chem.*, 1981, **53**, 2323-2332
77. L. F. Tietze and W. Buhr, *Angew. Chem. Int. Ed. Engl.*, 1995, **34**, 1366-1368

78. *Organometallics in Synthesis: a Manual,* Ed. M. Schlosser, Wiley, New York, 1994

79. A. Spencer, *J. Organomet. Chem.*, 1984, **258**, 101-118

80. T. Jeffery, *J. Chem. Soc. Chem. Commun.*, 1984, 1287-1289

81. W. A. Herrmann, C. Brossmer, K. Öfele, C.-P. Reisinger, T. Priermeier, M. Beller and H. Fischer, *Angew. Chem. Int. Ed. Engl.*, 1995, **34**, 1844-1848

82. Y. Ben-David, M. Portnoy, M. Gozin and D. Milstein, *Organometallics*, 1992, **11**, 1995-1996

83. (a) F. Ozawa, A. Kubo and T. Hayashi, *Tetrahedron Lett.*, 1992, **33**, 1485-1488

(b) T. Hayashi, A. Kubo and F. Ozawa, *Pure Appl. Chem.*, 1992, **64**, 421-427

(c) F. Ozawa, Y. Kobatake and T. Hayashi, *Tetrahedron Lett.*, 1993, **34**, 2505-2508

84. F. Ozawa, A. Kubo, Y. Matsumoto and T. Hayashi, *Organometallics*, 1993, **12**, 4188-4196

85. Y. Sato, M. Sodeoka and M. Shibasaki, *J. Org. Chem.*, 1989, **54**, 4738-4739

86. W. Cabri, I. Candiani, A. Bedeschi, S. Penco and R. Santi, *J. Org. Chem.*, 1992, **57**, 1481-1486

87. R. F. Heck, *Acc. Chem. Res.*, 1979, **12**, 146-151

88. F. Ozawa, A. Kubo and T. Hayashi, *Chem. Lett.*, 1992, 2177-2180

89. A. Canty, *Acc. Chem. Res.*, 1992, **25**, 83-90

90. Lancaster Synthesis Ltd. Catalogue, 1997-1999 Edition

91. G. Consiglio and C. Botteghi, *Helv. Chim. Acta.*, 1973, **56**, 460-463

92. Y. Kiso, K. Tamao, N. Miyake, K. Yamamoto and M. Kumada, *Tetrahedron Lett.*, 1974, 3-6

93. (a) T. Hayashi, M. Tajika, K. Tamao and M. Kumada, *J. Am. Chem. Soc.*, 1976, **98**, 3718-3719

(b) T. Hayashi, M. Konishi, M. Fukushima, T. Mise, M. Kagotani, M. Tajika and M. Kumada, *J. Am. Chem. Soc.*, 1982, **104**, 180-186

94. T. Hayashi, M. Konishi and M. Kumada, *Tetrahedron Lett.*, 1979, 1871-1874

95. T. Hayashi, M. Konishi and M. Kumada, *J. Organomet. Chem.*, 1980, **186**,

C1-C4

96. K. Tamao, Y. Kiso, K. Sumitani and M. Kumada, *J. Am. Chem. Soc.*, 1972, **94**, 9268-9269

97. W. L. Steffan and G. J. Palenik, *Inorg. Chem.*, 1976, **15**, 2432-2439

98. T. Hayashi, M. Konishi, K.-I. Yokota and M. Kumada, *J. Organomet. Chem.* 1985, **285**, 359-373

99. M. J. Burk, T. G. P. Harper, J. R. Lee and C. Kalberg, *Tetrahedron Lett.*, 1994, **35**, 4963-4966

100. I. R. Butler, W. R. Cullen, T.-J. Kim., F. W. B. Einstein and T. Jones, *J. Chem. Soc., Chem. Commun.*, 1984, 719-721

101. M. J. Calhorda, J. M. Brown and N. A. Cooley, *Organometallics*, 1991, **10**, 1431-1438

102. J. M. Brown and P. J. Guiry, *Inorg. Chim. Acta.*, 1994, **220**, 249-259

103. A. Gillie and J. K. Stille, *J. Am. Chem. Soc.*, 1980, **102**, 4933-4941

104. A. Moriavsky and J. K. Stille, *J. Am. Chem. Soc.*, 1981, **103**, 4182-4186

105. A. Suzuki, *Acc. Chem. Res.*, 1982, **15**, 178-184

106. N. Miyaura, K. Yamada, H. Suginome and A. Suzuki, *J. Am. Chem. Soc.*, 1985, **107**, 972-980

107. A. F. Indolese, *Tetrahedron Lett.*, 1997, **38**, 3515-3516

108. I. Colon and D. R. Kelsey, *J. Org. Chem.*, 1986, **51**, 2627-2637

109. I. R. Butler, *Organometallics*, 1992, **11**, 74-83

110. I. R. Butler, D. S. Brassington, R. A. Bromley, P. Licence and J. Wrench, *Polyhedron*, 1996, **15**, 4087-4092

111. V. Percec, J.-Y. Bae and D. H. Hill, *J. Org. Chem.*, 1995, **60**, 1060-1065

112. M. Herberhold, M. Ellinger and W. Kremnitz, *J. Organomet. Chem.*, 1983, **241**, 227-240

113. A. N. Nesmejanow, W. A. Ssasonowa and V. N. Drosd, *Chem. Ber.*, 1960, **93**, 2717-2729

114. G. R. Knox, P. L. Pauson, D. Willinson, E. Solcaniova and S. Toma, *Organometallics*, 1990, **9**, 301-306

115. W. E. Britton, R. Kashyap, M. El-Hashash and M. El-Kady, *Organometallics*,

1986, **5**, 1029-1031

116. M. A. Mathur, W. H. Myers, H. H. Sisler and G. E. Ryschkewitsch, *Inorganic Syntheses*, Wiley, New York, 128-133

117. R. V. Stevens, N. Beaulieu, W. H. Chean, A. R. Daniewski, T. Takeda, A. Waldner, P. G. Williard and U. Zutter, *J. Am. Chem. Soc.*, 1986, **108**, 1039-1049

118. L. J. Hobson, PhD Thesis, University of Wales, Bangor, 1995

119. G. P. Sollot, H. E. Mertwoy, S. Portnoy and S. L. Snead, *J. Org. Chem.*, 1963, **28**, 1090-1092

120. S. Macan, MSc Thesis, University of Wales, Bangor, 1994

121. D.T. Hill, G. R. Girard, F. L. McCabe, R. K. Johnson, P. D. Stupik, J. H. Zhang, W. M. Reiff and D. S. Eggleston, *Inorg. Chem.*, 1989, **28**, 3529-3533

122. M. Fontani and P. Zanello, unpublished results

123. P. Seiler and J. D. Dunitz, *Acta Cryst.*, 1979, **B35**, 1068-1074

124. A. L. Bandini, G. Banditelli, M. A. Cinellu, G. Sanna, G. Minghetti, F. Demartin and M. Manassero, *Inorg. Chem.*, 1989, **28**, 404-410

125. M. A. Frisch, H. G. Heal, H. Mackle and I. O. Madden, *J. Chem. Soc.*, 1965, 899-907

126. P. Pellon, *Tetrahedron Lett.*, 1992, **33**, 4451-4452

127. H. Schmidbaur, *J. Organomet. Chem.*, 1980, **200**, 287-306

128. A. Longeau, F. Langer and P. Knochel, *Tetrahedron Lett.*, 1996, **37**, 2209-2212

129. A.W. Rudie, D.W. Lichtenberg, M.L. Katcher and A. Davison, *Inorg. Chem.*, 1978, **17**, 2859

130. U. Castellato, D. Ajó, G. Valle, B. Corain, B. Longato and R. Graziani, *J. Cryst. Spectr. Res.*, 1988, **18**, 583-590

131. I. R. Butler, S. B. Wilkes, S. J. McDonald, L. J. Hobson, A. Taralp and C. P. Wilde, *Polyhedron*, 1993, **12**, 1003-1006

132. D. Albagli, G. Bazan, M.S. Wrighton and R.R. Schrock, *J. Am. Chem. Soc.*, 1992, **114**, 4150-4158

133. M. Kumada, K. Tamao and K. Sumitani, *Org. Synth.*, 1988, **50-9**, 407-411

134. K. Tamao, T. Hayashi, H. Matsumoto, H. Yamamoto and M. Kumada, *Tetrahedron Lett.*, 1979, **23**, 2155-2156

135. T. T. Derencsényi, *Inorg. Chem.*, 1981, 20, 665-670

136. T. S. A. Hor, H. S. O. Chan, K.-L. Tan, L.-T. Phang, Y. K. Yan, L.-K. Liu, and Y.-S. Wen, *Polyhedron*, 1991, **10**, 2437-2450

137. S. Saito, M. Sakai and N. Miyaura, *Tetrahedron Lett.*, 1996, **37**, 2993-2996

138. B. Floris and G. Illuminati, *J. Organomet. Chem.*, 1978, **150**, 101-113

139. I. R. Butler, L. J. Hobson, S. J. Coles, M. B. Hursthouse and K. M. Abdul Malik, *J. Organomet. Chem.*, 1997, **540**, 27-40

140. A. Togni, M. Hobi, G. Rihs, G. Rist, A. Albinati, D. Zech, H. Keller, *Organometallics*, 1994, **13**, 1224-1234

Appendix

Table 2.

Atomic coordinates (x 10^4) and equivalent isotropic displacement parameters (A^2 x 10^3) for 98SRC119.

U(eq) is defined as one third of the trace of the orthogonalized Uij tensor.

	x	y	z	U(eq)
Ni(1)	4100(1)	2008(1)	1937(1)	18(1)
Fe(1)	2983(1)	3952(1)	49(1)	16(1)
Cl(1)	5300(1)	2563(2)	1200(1)	26(1)
Cl(2)	4155(1)	1015(2)	3109(1)	31(1)
P(1)	3329(1)	810(2)	984(1)	15(1)
P(2)	3267(1)	3984(2)	2058(1)	16(1)
C(1)	3063(4)	1859(7)	109(3)	11(2)
C(2)	2192(5)	2278(7)	-138(3)	19(2)
C(3)	2300(5)	3027(8)	-842(4)	23(2)
C(4)	3254(6)	3089(8)	-1005(4)	26(2)
C(5)	3735(5)	2398(7)	-399(4)	20(2)
C(6)	3134(5)	4894(6)	1121(4)	13(2)
C(7)	2300(5)	5277(8)	751(4)	24(2)
C(8)	2512(6)	5910(8)	29(4)	27(2)
C(9)	3452(5)	5871(8)	-62(4)	26(2)
C(10)	3861(5)	5239(7)	598(4)	21(2)
C(11)	2239(5)	82(7)	1285(3)	18(2)
C(12)	1730(5)	-708(8)	624(4)	25(2)
C(13)	2354(5)	-849(8)	2014(4)	28(2)
C(14)	3994(5)	-717(8)	646(4)	23(2)
C(15)	4624(6)	-1196(8)	1314(4)	34(2)
C(16)	4517(5)	-555(8)	-114(4)	35(2)
C(17)	3818(5)	5272(8)	2706(4)	23(2)
C(18)	3803(6)	4758(9)	3548(4)	34(2)
C(19)	4812(5)	5558(9)	2446(4)	30(2)
C(20)	2112(5)	3833(7)	2400(3)	18(2)
C(21)	1957(5)	2716(8)	3026(3)	28(2)
C(22)	1662(5)	5179(8)	2658(4)	27(2)

Table 3.

Selected bond lengths [A] and angles [deg] for 98SRC119.

Ni(1)-Cl(2)	2.221(2)	Ni(1)-Cl(1)	2.243(2)
Ni(1)-P(2)	2.300(2)	Ni(1)-P(1)	2.303(2)
Fe(1)-C(9)	2.008(8)	Fe(1)-C(4)	2.024(6)
Fe(1)-C(7)	2.031(7)	Fe(1)-C(5)	2.032(7)
Fe(1)-C(3)	2.036(7)	Fe(1)-C(10)	2.036(7)
Fe(1)-C(8)	2.037(8)	Fe(1)-C(2)	2.037(7)
Fe(1)-C(1)	2.050(7)	Fe(1)-C(6)	2.056(6)
P(1)-C(11)	1.837(7)	P(1)-C(1)	1.850(6)
P(1)-C(14)	1.878(7)	P(2)-C(20)	1.814(7)
P(2)-C(6)	1.837(7)	P(2)-C(17)	1.861(7)
C(1)-C(2)	1.417(9)	C(1)-C(5)	1.421(9)
C(2)-C(3)	1.413(9)	C(3)-C(4)	1.442(10)
C(4)-C(5)	1.424(10)	C(6)-C(10)	1.437(9)
C(6)-C(7)	1.437(10)	C(7)-C(8)	1.411(10)
C(8)-C(9)	1.401(10)	C(9)-C(10)	1.418(10)
C(11)-C(13)	1.548(8)	C(11)-C(12)	1.560(9)
C(14)-C(16)	1.515(9)	C(14)-C(15)	1.545(9)
C(17)-C(18)	1.519(9)	C(17)-C(19)	1.562(10)
C(20)-C(22)	1.538(10)	C(20)-C(21)	1.542(9)

Cl(2)-Ni(1)-Cl(1)	125.37(8)	Cl(2)-Ni(1)-P(2)	107.81(8)
Cl(1)-Ni(1)-P(2)	105.81(8)	Cl(2)-Ni(1)-P(1)	115.41(8)
Cl(1)-Ni(1)-P(1)	97.00(7)	P(2)-Ni(1)-P(1)	102.98(7)
C(11)-P(1)-C(1)	104.6(3)	C(11)-P(1)-C(14)	103.9(3)
C(1)-P(1)-C(14)	107.8(3)	C(11)-P(1)-Ni(1)	115.8(2)
C(1)-P(1)-Ni(1)	113.0(2)	C(14)-P(1)-Ni(1)	111.1(2)
C(20)-P(2)-C(6)	102.5(3)	C(20)-P(2)-C(17)	106.2(3)
C(6)-P(2)-C(17)	103.6(3)	C(20)-P(2)-Ni(1)	117.8(2)
C(6)-P(2)-Ni(1)	112.7(2)	C(17)-P(2)-Ni(1)	112.7(3)
C(2)-C(1)-C(5)	110.5(6)	C(2)-C(1)-P(1)	126.4(5)
C(5)-C(1)-P(1)	123.1(5)	P(1)-C(1)-Fe(1)	127.2(3)
C(3)-C(2)-C(1)	107.4(6)	C(2)-C(3)-C(4)	107.2(6)
C(5)-C(4)-C(3)	109.3(6)	C(5)-C(4)-Fe(1)	69.7(4)
C(1)-C(5)-C(4)	105.4(6)	C(10)-C(6)-C(7)	108.1(6)
C(10)-C(6)-P(2)	124.9(5)	C(7)-C(6)-P(2)	126.9(5)
P(2)-C(6)-Fe(1)	124.5(3)	C(8)-C(7)-C(6)	107.8(6)
C(9)-C(8)-C(7)	107.7(6)	C(8)-C(9)-C(10)	110.4(6)
C(9)-C(10)-C(6)	105.9(7)	C(13)-C(11)-C(12)	109.9(6)
C(13)-C(11)-P(1)	110.8(5)	C(12)-C(11)-P(1)	114.6(4)
C(16)-C(14)-C(15)	110.6(6)	C(16)-C(14)-P(1)	116.6(5)
C(15)-C(14)-P(1)	109.4(5)	C(18)-C(17)-C(19)	109.9(6)
C(18)-C(17)-P(2)	109.2(5)	C(19)-C(17)-P(2)	111.5(5)
C(22)-C(20)-C(21)	110.1(5)	C(22)-C(20)-P(2)	115.5(5)
C(21)-C(20)-P(2)	114.8(5)		

Table 4.

Bond lengths [A] and angles [deg] for 98SRC119.

Ni(1)-Cl(2)	2.221(2)	Ni(1)-Cl(1)	2.243(2)
Ni(1)-P(2)	2.300(2)	Ni(1)-P(1)	2.303(2)
Fe(1)-C(9)	2.008(8)	Fe(1)-C(4)	2.024(6)
Fe(1)-C(7)	2.031(7)	Fe(1)-C(5)	2.032(7)
Fe(1)-C(3)	2.036(7)	Fe(1)-C(10)	2.036(7)
Fe(1)-C(8)	2.037(8)	Fe(1)-C(2)	2.037(7)
Fe(1)-C(1)	2.050(7)	Fe(1)-C(6)	2.056(6)
P(1)-C(11)	1.837(7)	P(1)-C(1)	1.850(6)
P(1)-C(14)	1.878(7)	P(2)-C(20)	1.814(7)
P(2)-C(6)	1.837(7)	P(2)-C(17)	1.861(7)
C(1)-C(2)	1.417(9)	C(1)-C(5)	1.421(9)
C(2)-C(3)	1.413(9)	C(3)-C(4)	1.442(10)
C(4)-C(5)	1.424(10)	C(6)-C(10)	1.437(9)
C(6)-C(7)	1.437(10)	C(7)-C(8)	1.411(10)
C(8)-C(9)	1.401(10)	C(9)-C(10)	1.418(10)
C(11)-C(13)	1.548(8)	C(11)-C(12)	1.560(9)
C(14)-C(16)	1.515(9)	C(14)-C(15)	1.545(9)
C(17)-C(18)	1.519(9)	C(17)-C(19)	1.562(10)
C(20)-C(22)	1.538(10)	C(20)-C(21)	1.542(9)

Cl(2)-Ni(1)-Cl(1)	125.37(8)	Cl(2)-Ni(1)-P(2)	107.81(8)
Cl(1)-Ni(1)-P(2)	105.81(8)	Cl(2)-Ni(1)-P(1)	115.41(8)
Cl(1)-Ni(1)-P(1)	97.00(7)	P(2)-Ni(1)-P(1)	102.98(7)
C(9)-Fe(1)-C(4)	103.7(3)	C(9)-Fe(1)-C(7)	68.4(3)
C(4)-Fe(1)-C(7)	152.4(3)	C(9)-Fe(1)-C(5)	118.2(3)
C(4)-Fe(1)-C(5)	41.1(3)	C(7)-Fe(1)-C(5)	166.0(3)
C(9)-Fe(1)-C(3)	121.1(3)	C(4)-Fe(1)-C(3)	41.6(3)
C(7)-Fe(1)-C(3)	118.3(3)	C(5)-Fe(1)-C(3)	70.2(3)
C(9)-Fe(1)-C(10)	41.0(3)	C(4)-Fe(1)-C(10)	122.5(3)
C(7)-Fe(1)-C(10)	69.8(3)	C(5)-Fe(1)-C(10)	106.5(3)
C(3)-Fe(1)-C(10)	159.0(3)	C(9)-Fe(1)-C(8)	40.5(3)
C(4)-Fe(1)-C(8)	116.4(3)	C(7)-Fe(1)-C(8)	40.6(3)
C(5)-Fe(1)-C(8)	152.0(3)	C(3)-Fe(1)-C(8)	103.5(3)
C(10)-Fe(1)-C(8)	69.3(3)	C(9)-Fe(1)-C(2)	159.0(3)
C(4)-Fe(1)-C(2)	68.9(3)	C(7)-Fe(1)-C(2)	108.5(3)
C(5)-Fe(1)-C(2)	69.9(3)	C(3)-Fe(1)-C(2)	40.6(3)
C(10)-Fe(1)-C(2)	159.3(3)	C(8)-Fe(1)-C(2)	123.7(3)
C(9)-Fe(1)-C(1)	156.3(3)	C(4)-Fe(1)-C(1)	67.5(3)
C(7)-Fe(1)-C(1)	129.4(3)	C(5)-Fe(1)-C(1)	40.7(3)
C(3)-Fe(1)-C(1)	67.9(3)	C(10)-Fe(1)-C(1)	123.8(3)
C(8)-Fe(1)-C(1)	163.2(3)	C(2)-Fe(1)-C(1)	40.6(3)
C(9)-Fe(1)-C(6)	68.2(2)	C(4)-Fe(1)-C(6)	162.2(3)
C(7)-Fe(1)-C(6)	41.1(3)	C(5)-Fe(1)-C(6)	127.5(3)
C(3)-Fe(1)-C(6)	156.1(3)	C(10)-Fe(1)-C(6)	41.1(3)
C(8)-Fe(1)-C(6)	68.4(3)	C(2)-Fe(1)-C(6)	124.1(2)
C(1)-Fe(1)-C(6)	113.3(2)	C(11)-P(1)-C(1)	104.6(3)
C(11)-P(1)-C(14)	103.9(3)	C(1)-P(1)-C(14)	107.8(3)
C(11)-P(1)-Ni(1)	115.8(2)	C(1)-P(1)-Ni(1)	113.0(2)
C(14)-P(1)-Ni(1)	111.1(2)	C(20)-P(2)-C(6)	102.5(3)
C(20)-P(2)-C(17)	106.2(3)	C(6)-P(2)-C(17)	103.6(3)
C(20)-P(2)-Ni(1)	117.8(2)	C(6)-P(2)-Ni(1)	112.7(2)
C(17)-P(2)-Ni(1)	112.7(3)	C(2)-C(1)-C(5)	110.5(6)
C(2)-C(1)-P(1)	126.4(5)	C(5)-C(1)-P(1)	123.1(5)
C(2)-C(1)-Fe(1)	69.2(4)	C(5)-C(1)-Fe(1)	68.9(4)
P(1)-C(1)-Fe(1)	127.2(3)	C(3)-C(2)-C(1)	107.4(6)
C(3)-C(2)-Fe(1)	69.7(4)	C(1)-C(2)-Fe(1)	70.2(4)
C(2)-C(3)-C(4)	107.2(6)	C(2)-C(3)-Fe(1)	69.7(4)
C(4)-C(3)-Fe(1)	68.7(4)	C(5)-C(4)-C(3)	109.3(6)

C(5)-C(4)-Fe(1)	69.7(4)	C(3)-C(4)-Fe(1)	69.6(4
C(1)-C(5)-C(4)	105.4(6)	C(1)-C(5)-Fe(1)	70.3(4
C(4)-C(5)-Fe(1)	69.1(4)	C(10)-C(6)-C(7)	108.1(6
C(10)-C(6)-P(2)	124.9(5)	C(7)-C(6)-P(2)	126.9(5
C(10)-C(6)-Fe(1)	68.7(4)	C(7)-C(6)-Fe(1)	68.5(4
P(2)-C(6)-Fe(1)	124.5(3)	C(8)-C(7)-C(6)	107.8(6
C(8)-C(7)-Fe(1)	69.9(4)	C(6)-C(7)-Fe(1)	70.4(4
C(9)-C(8)-C(7)	107.7(6)	C(9)-C(8)-Fe(1)	68.6(5
C(7)-C(8)-Fe(1)	69.5(4)	C(8)-C(9)-C(10)	110.4(6
C(8)-C(9)-Fe(1)	70.8(5)	C(10)-C(9)-Fe(1)	70.5(4
C(9)-C(10)-C(6)	105.9(7)	C(9)-C(10)-Fe(1)	68.4(4
C(6)-C(10)-Fe(1)	70.2(4)	C(13)-C(11)-C(12)	109.9(6
C(13)-C(11)-P(1)	110.8(5)	C(12)-C(11)-P(1)	114.6(4
C(16)-C(14)-C(15)	110.6(6)	C(16)-C(14)-P(1)	116.6(5
C(15)-C(14)-P(1)	109.4(5)	C(18)-C(17)-C(19)	109.9(6
C(18)-C(17)-P(2)	109.2(5)	C(19)-C(17)-P(2)	111.5(5
C(22)-C(20)-C(21)	110.1(5)	C(22)-C(20)-P(2)	115.5(5
C(21)-C(20)-P(2)	114.8(5)		

Table 5.

Anisotropic displacement parameters (A^2 x 10^3) for 98SRC119.

The anisotropic displacement factor exponent takes the form:
-2 pi^2 [h^2 a*^2 U11 + ... + 2 h k a* b* U12]

	U11	U22	U33	U23	U13	U1
Ni(1)	19(1)	23(1)	12(1)	0(1)	-2(1)	1(
Fe(1)	24(1)	17(1)	8(1)	1(1)	-1(1)	0(
Cl(1)	19(1)	35(1)	25(1)	3(1)	1(1)	1(
Cl(2)	35(1)	42(1)	14(1)	8(1)	-3(1)	5(
P(1)	20(1)	17(1)	8(1)	2(1)	0(1)	2(
P(2)	20(1)	21(1)	7(1)	0(1)	-2(1)	-2(
C(1)	15(3)	16(3)	4(3)	-2(3)	1(3)	4(
C(2)	25(5)	19(4)	14(4)	0(3)	2(3)	-4(
C(3)	39(5)	13(5)	16(4)	3(3)	-13(3)	0(
C(4)	47(6)	15(5)	15(4)	-10(3)	3(4)	-4(
C(5)	23(5)	21(5)	16(4)	0(3)	-6(3)	-3(
C(6)	16(4)	10(4)	12(3)	-5(3)	-6(3)	-5(
C(7)	22(5)	26(5)	25(4)	-9(3)	7(3)	3(
C(8)	47(6)	15(4)	20(4)	3(3)	-7(4)	10(
C(9)	46(6)	25(5)	7(4)	3(3)	-4(3)	-12(
C(10)	23(5)	16(5)	24(4)	-2(3)	1(3)	-9(
C(11)	27(5)	15(4)	13(4)	2(3)	2(3)	-1(
C(12)	24(5)	31(5)	20(4)	0(3)	-5(3)	-4(
C(13)	29(5)	29(5)	27(4)	19(4)	11(4)	2(
C(14)	19(5)	27(5)	22(4)	2(3)	6(3)	6(
C(15)	40(6)	31(5)	30(4)	5(4)	4(4)	11(
C(16)	44(6)	35(6)	28(4)	-1(4)	10(4)	17(
C(17)	34(5)	11(5)	24(4)	-6(3)	-3(3)	-1(
C(18)	55(7)	38(6)	9(4)	-8(4)	0(4)	1(
C(19)	29(5)	44(6)	17(4)	-5(4)	-3(3)	-7(
C(20)	19(4)	18(5)	18(4)	-4(3)	-2(3)	-2(
C(21)	34(5)	36(5)	14(4)	3(3)	5(3)	-3(
C(22)	30(5)	27(5)	24(4)	-8(3)	9(4)	7(

Table 6.

Hydrogen coordinates (x 10^4) and isotropic displacement parameters (A^2 x 10^3) for 98SRC119.

	x	y	z	U(iso)
H(2)	1638(5)	2090(7)	121(3)	23
H(3)	1831(5)	3417(8)	-1151(4)	28
H(4)	3521(6)	3523(8)	-1448(4)	31
H(5)	4372(5)	2316(7)	-346(4)	24
H(7)	1712(5)	5131(8)	955(4)	29
H(8)	2093(6)	6293(8)	-332(4)	33
H(9)	3771(5)	6218(8)	-503(4)	31
H(10)	4486(5)	5078(7)	679(4)	25
H(11)	1845(5)	865(7)	1446(3)	22
H(12A)	1668(26)	-118(16)	161(10)	37
H(12B)	1129(12)	-973(39)	812(9)	37
H(12C)	2072(15)	-1531(24)	482(18)	37
H(13A)	2715(25)	-373(18)	2411(11)	42
H(13B)	2660(26)	-1697(19)	1860(6)	42
H(13C)	1759(5)	-1068(37)	2232(15)	42
H(14)	3549(5)	-1471(8)	557(4)	27
H(15A)	4844(24)	-2121(19)	1200(13)	51
H(15B)	4291(10)	-1202(44)	1811(6)	51
H(15C)	5138(16)	-569(27)	1356(17)	51
H(16A)	4124(11)	-153(48)	-515(9)	53
H(16B)	4728(29)	-1454(10)	-292(16)	53
H(16C)	5037(20)	46(42)	-26(8)	53
H(17)	3468(5)	6146(8)	2677(4)	28
H(18A)	3181(7)	4773(48)	3746(10)	51
H(18B)	4182(27)	5350(31)	3875(7)	51
H(18C)	4035(32)	3819(20)	3566(5)	51
H(19A)	5068(11)	6285(30)	2775(17)	45
H(19B)	4819(6)	5847(42)	1895(8)	45
H(19C)	5171(8)	4723(14)	2507(23)	45
H(20)	1760(5)	3524(7)	1931(3)	22
H(21A)	2233(26)	1858(14)	2851(12)	42
H(21B)	1307(5)	2579(32)	3101(19)	42
H(21C)	2231(26)	3003(22)	3523(8)	42
H(22A)	1656(25)	5822(16)	2216(8)	41
H(22B)	2003(15)	5578(22)	3095(16)	41
H(22C)	1042(9)	4995(10)	2827(21)	41

Table 2. Atomic coordinates (x 10^4) and equivalent isotropic displacement parameters (A^2 x 10^3) for 98SRC120. U(eq) is defined as one third of the trace of the orthogonalized Uij tensor.

	x	y	z	U(eq)
Pd(1)	6822(1)	2500	2500	18(1)
Fe(1)	4118(1)	2500	2500	18(1)
Cl(1)	7884(1)	1580(1)	1944(1)	30(1)
P(1)	5934(1)	1460(1)	2062(1)	18(1)
C(1)	4843(2)	1533(2)	2579(5)	17(1)
C(2)	4552(3)	1731(3)	4063(5)	18(1)
C(3)	3678(3)	1710(3)	4074(6)	28(1)
C(4)	3401(3)	1492(3)	2610(6)	30(1)
C(5)	4116(3)	1385(3)	1682(5)	27(1)
C(6)	6255(3)	574(3)	3149(5)	22(1)
C(7)	5612(3)	-85(3)	3022(5)	28(1)
C(8)	6458(3)	771(3)	4796(5)	30(1)
C(9)	5891(3)	1125(3)	76(5)	30(1)
C(10)	6574(3)	545(3)	-385(6)	35(1)
C(11)	5837(5)	1792(4)	-1033(6)	77(3)

able 4. Bond lengths [A] and angles [deg] for 98SRC120.

d(1)-P(1)	2.2982(13)	Pd(1)-Cl(1)	2.3595(12
e(1)-C(1)	2.010(4)	Fe(1)-C(5)	2.025(5)
e(1)-C(2)	2.028(4)	Fe(1)-C(4)	2.060(4)
e(1)-C(3)	2.061(5)	P(1)-C(1)	1.812(4)
(1)-C(9)	1.855(5)	P(1)-C(6)	1.858(4)
(1)-C(5)	1.434(6)	C(1)-C(2)	1.439(6)
(2)-C(3)	1.401(6)	C(3)-C(4)	1.423(7)
(4)-C(5)	1.423(6)	C(6)-C(7)	1.524(6)
(6)-C(8)	1.536(6)	C(9)-C(11)	1.501(7)
(9)-C(10)	1.527(6)		

(1)-Pd(1)-P(1)#1	103.43(6)	P(1)-Pd(1)-Cl(1)#1	171.28(4)
(1)#1-Pd(1)-Cl(1)#1	84.55(4)	P(1)-Pd(1)-Cl(1)	84.55(4)
(1)#1-Pd(1)-Cl(1)	171.28(4)	Cl(1)#1-Pd(1)-Cl(1)	87.72(6)
(1)#1-Fe(1)-C(1)	109.4(2)	C(1)-Fe(1)-C(5)	41.6(2)
(1)-Fe(1)-C(2)	41.7(2)	C(5)-Fe(1)-C(2)	69.3(2)
(1)-Fe(1)-C(4)	69.2(2)	C(5)-Fe(1)-C(4)	40.8(2)
(2)-Fe(1)-C(4)	68.1(2)	C(1)-Fe(1)-C(3)	69.1(2)
(5)-Fe(1)-C(3)	68.7(2)	C(2)-Fe(1)-C(3)	40.1(2)
(4)-Fe(1)-C(3)	40.4(2)	C(1)-P(1)-C(9)	103.1(2)
(1)-P(1)-C(6)	101.0(2)	C(9)-P(1)-C(6)	104.9(2)
(1)-P(1)-Pd(1)	120.21(14)	C(9)-P(1)-Pd(1)	114.8(2)
(6)-P(1)-Pd(1)	111.1(2)	C(5)-C(1)-C(2)	106.7(4)
(5)-C(1)-P(1)	129.2(4)	C(2)-C(1)-P(1)	124.1(3)
(5)-C(1)-Fe(1)	69.7(2)	C(2)-C(1)-Fe(1)	69.8(2)
(1)-C(1)-Fe(1)	127.1(2)	C(3)-C(2)-C(1)	108.9(4)
(3)-C(2)-Fe(1)	71.2(3)	C(1)-C(2)-Fe(1)	68.5(2)
(2)-C(3)-C(4)	108.2(4)	C(2)-C(3)-Fe(1)	68.7(2)
(4)-C(3)-Fe(1)	69.8(3)	C(3)-C(4)-C(5)	108.1(4)
(3)-C(4)-Fe(1)	69.8(3)	C(5)-C(4)-Fe(1)	68.3(3)
(4)-C(5)-C(1)	108.0(4)	C(4)-C(5)-Fe(1)	71.0(3)
(1)-C(5)-Fe(1)	68.7(2)	C(7)-C(6)-C(8)	111.9(4)
(7)-C(6)-P(1)	111.5(3)	C(8)-C(6)-P(1)	112.2(3)
(11)-C(9)-C(10)	110.5(4)	C(11)-C(9)-P(1)	113.3(4)
(10)-C(9)-P(1)	115.2(3)		

Symmetry transformations used to generate equivalent atoms:
#1 x,-y+1/2,-z+1/2

Table 5.

Anisotropic displacement parameters (A^2 x 10^3) for 98SRC120.
The anisotropic displacement factor exponent takes the form:
-2 pi^2 [h^2 a*^2 U11 + ... + 2 h k a* b* U12]

	U11	U22	U33	U23	U13	U12
Pd(1)	19(1)	15(1)	19(1)	3(1)	0	0
Fe(1)	17(1)	17(1)	21(1)	2(1)	0	0
Cl(1)	27(1)	26(1)	39(1)	-1(1)	8(1)	7(1)
P(1)	24(1)	14(1)	16(1)	1(1)	2(1)	0(1)
C(1)	23(2)	11(2)	17(2)	2(2)	-3(2)	-1(2)
C(2)	18(3)	15(3)	21(3)	5(2)	3(2)	-2(2)
C(3)	26(3)	24(3)	34(3)	6(2)	7(2)	-3(3)
C(4)	23(3)	21(3)	46(3)	4(3)	-8(3)	-7(2)
C(5)	34(3)	17(3)	30(3)	-2(2)	-7(2)	-1(3)
C(6)	26(3)	16(3)	25(3)	3(2)	1(2)	2(2)
C(7)	37(3)	15(3)	31(3)	8(2)	6(2)	-2(3)
C(8)	27(3)	34(3)	30(3)	11(2)	-4(2)	-3(3)
C(9)	39(3)	30(3)	21(3)	-10(2)	3(3)	6(3)
C(10)	55(4)	20(3)	30(3)	-5(2)	14(3)	-2(3)
C(11)	164(7)	51(5)	18(3)	11(3)	18(4)	52(5)

Table 6.

Hydrogen coordinates (x 10^4) and isotropic displacement parameters (A^2 x 10^3) for 98SRC120.

	x	y	z	U(iso)
H(2)	4896(3)	1856(3)	4900(5)	22
H(3)	3330(3)	1821(3)	4913(6)	34
H(4)	2836(3)	1430(3)	2305(6)	36
H(5)	4112(3)	1240(3)	649(5)	32
H(6)	6781(3)	374(3)	2680(5)	27
H(7A)	5516(13)	-209(11)	1959(5)	42
H(7B)	5087(6)	86(7)	3484(28)	42
H(7C)	5818(8)	-556(6)	3543(27)	42
H(8A)	6901(12)	1170(12)	4831(5)	46
H(8B)	6646(16)	293(4)	5314(9)	46
H(8C)	5957(5)	977(16)	5293(10)	46
H(9)	5354(3)	828(3)	-24(5)	36
H(10A)	6569(13)	91(9)	298(21)	53
H(10B)	7118(4)	808(6)	-331(33)	53
H(10C)	6473(11)	365(14)	-1417(13)	53
H(11A)	6307(15)	2152(14)	-878(31)	116
H(11B)	5311(13)	2077(16)	-885(33)	116
H(11C)	5857(27)	1580(4)	-2059(6)	116

Table 2. Atomic coordinates (x 10^4) and equivalent isotropic displacement parameters (A^2 x 10^3) for C26H45NFEPDCL2P2.CH2CL2. U(eq) is defined as one third of the trace of the orthogonalized Uij tensor.

	x	y	z	U(eq)
Pd(1)	5680(1)	524(1)	7918(1)	18(1)
Fe(1)	7479(1)	2432(1)	6525(1)	17(1)
P(1)	5257(1)	1336(1)	6763(1)	18(1)
Cl(2)	5871(1)	-422(1)	9097(1)	30(1)
P(2)	7289(1)	947(1)	8160(1)	18(1)
Cl(1)	4052(1)	-24(1)	7831(1)	36(1)
C(11)	9573(4)	1463(4)	6976(4)	23(1)
C(9)	8730(4)	3029(4)	6994(4)	23(1)
C(4)	7536(5)	2099(4)	5271(4)	24(1)
C(1)	6194(4)	1896(4)	6144(4)	17(1)
N(1)	10124(4)	1280(3)	7755(3)	25(1)
C(7)	7329(4)	2764(4)	7739(4)	22(1)
C(2)	6236(4)	2820(4)	5906(4)	21(1)
C(3)	7063(5)	2931(4)	5377(4)	24(1)
C(6)	7825(4)	1921(4)	7650(3)	18(1)
C(12)	10202(5)	1801(5)	6248(4)	32(2)
C(5)	7009(4)	1461(4)	5747(4)	20(1)
C(8)	7890(4)	3431(4)	7341(4)	23(1)
C(10)	8719(4)	2092(4)	7171(4)	18(1)
C(21)	4348(4)	2237(4)	6984(5)	29(1)
C(15)	8166(4)	22(3)	7943(4)	22(1)
C(16)	7927(5)	-438(4)	7111(4)	31(1)
C(25)	4503(4)	1115(5)	5143(4)	27(1)
C(24)	4662(4)	624(4)	5964(3)	22(1)
C(13)	10816(5)	534(5)	7672(4)	37(2)
C(18)	7461(5)	1242(4)	9281(4)	27(1)
C(26)	5214(5)	-254(4)	5829(4)	32(2)
C(20)	6641(5)	1823(5)	9618(4)	36(2)
C(19)	8474(5)	1654(5)	9441(4)	34(2)
C(17)	8267(5)	-679(4)	8633(4)	34(2)
C(22)	3260(5)	1941(5)	6981(5)	39(2)
C(23)	4576(5)	2719(6)	7779(7)	67(3)
C(14)	10631(2)	2027(3)	8073(3)	40(2)
Cl(3)	4423(2)	865(2)	10831(1)	95(1)
C(27)	3817(2)	633(2)	9917(2)	87(4)
Cl(4)	2494(2)	572(2)	10030(2)	186(3)

Table 3. Bond lengths [A] and angles [deg] for C26H45NFEPDCL2P2.CH2CL2.

Pd(1)-P(1)	2.2861(16)	Pd(1)-P(2)	2.3024(15)
Pd(1)-Cl(1)	2.3557(15)	Pd(1)-Cl(2)	2.3749(15)
Fe(1)-C(1)	2.011(6)	Fe(1)-C(6)	2.011(6)
Fe(1)-C(7)	2.016(6)	Fe(1)-C(5)	2.018(6)
Fe(1)-C(10)	2.037(6)	Fe(1)-C(2)	2.038(6)
Fe(1)-C(9)	2.059(6)	Fe(1)-C(3)	2.062(6)
Fe(1)-C(8)	2.063(6)	Fe(1)-C(4)	2.071(6)
P(1)-C(1)	1.815(6)	P(1)-C(24)	1.851(6)
P(1)-C(21)	1.862(6)	P(2)-C(6)	1.824(6)
P(2)-C(15)	1.860(6)	P(2)-C(18)	1.862(6)
C(11)-N(1)	1.479(8)	C(11)-C(10)	1.524(8)
C(11)-C(12)	1.531(8)	C(9)-C(8)	1.401(8)
C(9)-C(10)	1.434(7)	C(4)-C(3)	1.412(9)
C(4)-C(5)	1.416(8)	C(1)-C(5)	1.431(8)
C(1)-C(2)	1.438(8)	N(1)-C(14)	1.409(5)
N(1)-C(13)	1.465(8)	C(7)-C(8)	1.408(8)
C(7)-C(6)	1.438(8)	C(2)-C(3)	1.414(9)
C(6)-C(10)	1.455(8)	C(21)-C(23)	1.495(10)
C(21)-C(22)	1.539(9)	C(15)-C(17)	1.530(8)
C(15)-C(16)	1.535(9)	C(25)-C(24)	1.523(8)
C(24)-C(26)	1.529(9)	C(18)-C(20)	1.511(9)
C(18)-C(19)	1.527(9)	Cl(3)-C(27)	1.7137
C(27)-Cl(4)	1.8023		

P(1)-Pd(1)-P(2)	103.07(5)	P(1)-Pd(1)-Cl(1)	84.48(6)
P(2)-Pd(1)-Cl(1)	172.44(6)	P(1)-Pd(1)-Cl(2)	171.07(6)
P(2)-Pd(1)-Cl(2)	85.84(5)	Cl(1)-Pd(1)-Cl(2)	86.62(6)
C(1)-Fe(1)-C(6)	108.7(2)	C(1)-Fe(1)-C(7)	107.7(2)
C(6)-Fe(1)-C(7)	41.8(2)	C(1)-Fe(1)-C(5)	41.6(2)
C(6)-Fe(1)-C(5)	110.6(2)	C(7)-Fe(1)-C(5)	137.9(2)
C(1)-Fe(1)-C(10)	140.1(2)	C(6)-Fe(1)-C(10)	42.1(2)
C(7)-Fe(1)-C(10)	69.8(2)	C(5)-Fe(1)-C(10)	113.1(2)
C(1)-Fe(1)-C(2)	41.6(2)	C(6)-Fe(1)-C(2)	137.4(2)
C(7)-Fe(1)-C(2)	108.4(2)	C(5)-Fe(1)-C(2)	69.2(2)
C(10)-Fe(1)-C(2)	177.6(2)	C(1)-Fe(1)-C(9)	175.3(2)
C(6)-Fe(1)-C(9)	69.4(2)	C(7)-Fe(1)-C(9)	67.9(2)
C(5)-Fe(1)-C(9)	143.0(2)	C(10)-Fe(1)-C(9)	41.0(2)
C(2)-Fe(1)-C(9)	137.1(2)	C(1)-Fe(1)-C(3)	68.8(2)
C(6)-Fe(1)-C(3)	177.5(2)	C(7)-Fe(1)-C(3)	137.9(2)
C(5)-Fe(1)-C(3)	68.0(2)	C(10)-Fe(1)-C(3)	140.2(2)
C(2)-Fe(1)-C(3)	40.3(2)	C(9)-Fe(1)-C(3)	113.0(2)
C(1)-Fe(1)-C(8)	135.7(2)	C(6)-Fe(1)-C(8)	69.3(2)
C(7)-Fe(1)-C(8)	40.4(2)	C(5)-Fe(1)-C(8)	177.3(2)
C(10)-Fe(1)-C(8)	68.7(2)	C(2)-Fe(1)-C(8)	108.9(2)
C(9)-Fe(1)-C(8)	39.7(2)	C(3)-Fe(1)-C(8)	112.0(2)
C(1)-Fe(1)-C(4)	69.0(2)	C(6)-Fe(1)-C(4)	140.1(2)
C(7)-Fe(1)-C(4)	176.4(3)	C(5)-Fe(1)-C(4)	40.5(2)
C(10)-Fe(1)-C(4)	113.6(3)	C(2)-Fe(1)-C(4)	68.2(3)
C(9)-Fe(1)-C(4)	115.3(3)	C(3)-Fe(1)-C(4)	40.0(2)
C(8)-Fe(1)-C(4)	141.1(2)	C(1)-P(1)-C(24)	101.2(3)
C(1)-P(1)-C(21)	103.3(3)	C(24)-P(1)-C(21)	105.2(3)
C(1)-P(1)-Pd(1)	120.86(19)	C(24)-P(1)-Pd(1)	111.1(2)
C(21)-P(1)-Pd(1)	113.5(2)	C(6)-P(2)-C(15)	105.0(3)
C(6)-P(2)-C(18)	101.1(3)	C(15)-P(2)-C(18)	106.1(3)
C(6)-P(2)-Pd(1)	121.44(19)	C(15)-P(2)-Pd(1)	111.60(19)
C(18)-P(2)-Pd(1)	110.3(2)	N(1)-C(11)-C(10)	109.0(5)
N(1)-C(11)-C(12)	115.0(5)	C(10)-C(11)-C(12)	111.9(5)
C(8)-C(9)-C(10)	109.5(5)	C(8)-C(9)-Fe(1)	70.3(3)
C(10)-C(9)-Fe(1)	68.7(3)	C(3)-C(4)-C(5)	107.6(5)
C(3)-C(4)-Fe(1)	69.7(3)	C(5)-C(4)-Fe(1)	67.8(3)
C(5)-C(1)-C(2)	106.8(5)	C(5)-C(1)-P(1)	124.9(4)
C(2)-C(1)-P(1)	128.2(5)	C(5)-C(1)-Fe(1)	69.5(3)
C(2)-C(1)-Fe(1)	70.2(3)	P(1)-C(1)-Fe(1)	128.6(3)
C(14)-N(1)-C(13)	109.2(5)	C(14)-N(1)-C(11)	113.8(5)
C(13)-N(1)-C(11)	112.9(5)	C(8)-C(7)-C(6)	109.1(5)
C(8)-C(7)-Fe(1)	71.6(3)	C(6)-C(7)-Fe(1)	68.9(3)

C(3)-C(2)-C(1)	107.7(5)	C(3)-C(2)-Fe(1)	70.8(3)
C(1)-C(2)-Fe(1)	68.2(3)	C(4)-C(3)-C(2)	109.1(5)
C(4)-C(3)-Fe(1)	70.3(3)	C(2)-C(3)-Fe(1)	68.9(3)
C(7)-C(6)-C(10)	106.6(5)	C(7)-C(6)-P(2)	118.2(4)
C(10)-C(6)-P(2)	135.0(4)	C(7)-C(6)-Fe(1)	69.3(3)
C(10)-C(6)-Fe(1)	69.9(3)	P(2)-C(6)-Fe(1)	127.8(3)
C(4)-C(5)-C(1)	108.7(5)	C(4)-C(5)-Fe(1)	71.8(3)
C(1)-C(5)-Fe(1)	68.9(3)	C(9)-C(8)-C(7)	108.2(5)
C(9)-C(8)-Fe(1)	70.0(3)	C(7)-C(8)-Fe(1)	68.0(3)
C(9)-C(10)-C(6)	106.6(5)	C(9)-C(10)-C(11)	123.9(5)
C(6)-C(10)-C(11)	129.1(5)	C(9)-C(10)-Fe(1)	70.3(3)
C(6)-C(10)-Fe(1)	68.0(3)	C(11)-C(10)-Fe(1)	132.6(4)
C(23)-C(21)-C(22)	109.9(6)	C(23)-C(21)-P(1)	112.1(5)
C(22)-C(21)-P(1)	115.0(4)	C(17)-C(15)-C(16)	109.7(5)
C(17)-C(15)-P(2)	115.7(5)	C(16)-C(15)-P(2)	111.2(4)
C(25)-C(24)-C(26)	111.3(5)	C(25)-C(24)-P(1)	112.3(4)
C(26)-C(24)-P(1)	112.4(4)	C(20)-C(18)-C(19)	111.6(6)
C(20)-C(18)-P(2)	112.9(5)	C(19)-C(18)-P(2)	111.7(4)
Cl(3)-C(27)-Cl(4)	113.7		

Symmetry transformations used to generate equivalent atoms:

Table 4. Anisotropic displacement parameters (A^2 x 10^3) for C26H45NFEPDCL2P2.CH2CL2. The anisotropic displacement factor exponent takes the form: -2 pi^2 [h^2 a*^2 U11 + ... + 2 h k a* b* U12]

	U11	U22	U33	U23	U13	U12
Pd(1)	17(1)	17(1)	21(1)	2(1)	2(1)	-2(1)
Fe(1)	14(1)	16(1)	21(1)	1(1)	1(1)	-1(1)
P(1)	14(1)	18(1)	23(1)	2(1)	2(1)	-2(1)
Cl(2)	30(1)	29(1)	31(1)	13(1)	0(1)	-4(1)
P(2)	17(1)	18(1)	19(1)	2(1)	1(1)	-1(1)
Cl(1)	25(1)	45(1)	38(1)	14(1)	-2(1)	-17(1)
C(11)	20(3)	17(3)	32(3)	-1(2)	3(2)	-2(2)
C(9)	19(3)	18(3)	31(3)	5(3)	1(3)	-3(2)
C(4)	18(3)	30(3)	23(3)	0(2)	1(3)	-2(3)
C(1)	14(3)	18(3)	19(3)	4(2)	-2(2)	2(2)
N(1)	18(3)	25(3)	31(3)	-2(2)	-6(2)	4(2)
C(7)	21(3)	21(3)	24(3)	-5(2)	-1(2)	1(2)
C(2)	14(3)	21(3)	27(3)	6(2)	-8(2)	-4(2)
C(3)	26(4)	24(3)	21(3)	7(2)	-7(3)	-1(3)
C(6)	16(3)	20(3)	19(3)	0(2)	-1(2)	-3(2)
C(12)	20(4)	36(4)	39(4)	4(3)	13(3)	5(3)
C(5)	18(3)	20(3)	23(3)	0(2)	1(2)	1(2)
C(8)	23(3)	16(3)	32(3)	-3(2)	-6(3)	-1(2)
C(10)	14(3)	19(3)	23(3)	2(2)	-5(2)	-3(2)
C(21)	16(3)	20(3)	52(4)	7(3)	7(3)	-2(2)
C(15)	24(3)	15(3)	26(3)	3(3)	-1(3)	1(2)
C(16)	32(3)	21(3)	39(3)	-6(3)	3(3)	6(3)
C(25)	17(3)	39(4)	26(3)	6(3)	-5(2)	-4(3)
C(24)	21(3)	25(3)	22(3)	5(2)	-2(2)	-8(2)
C(13)	21(3)	37(3)	55(4)	-1(4)	-5(3)	6(3)
C(18)	39(4)	24(3)	18(3)	2(2)	-1(3)	0(3)
C(26)	34(4)	23(3)	39(4)	-5(3)	1(3)	-3(3)
C(20)	40(5)	44(4)	24(3)	-4(3)	4(3)	3(3)
C(19)	38(4)	40(4)	24(3)	6(3)	-6(3)	-8(3)
C(17)	35(4)	24(4)	42(4)	14(3)	3(3)	8(3)
C(22)	19(3)	43(4)	55(5)	-10(4)	4(3)	5(3)
C(23)	27(4)	63(6)	112(8)	-60(6)	-17(5)	18(4)
C(14)	27(4)	37(4)	56(5)	-5(3)	-9(4)	4(3)
Cl(3)	144(3)	88(2)	51(1)	-12(1)	4(2)	17(2)
C(27)	56(6)	136(11)	69(7)	-38(7)	19(5)	-16(7)
Cl(4)	58(2)	115(3)	384(8)	-130(4)	75(3)	-30(2)

Table 5. Hydrogen coordinates (x 10^4) and isotropic displacement parameters (A^2 x 10^3) for C26H45NFEPDCL2P2.CH2CL2.

	x	y	z	U(iso)
H(11)	9281	897	6798	27
H(9)	9220	3326	6696	27
H(4)	8093	1990	4947	29
H(7)	6734	2855	8016	26
H(2)	5798	3264	6070	25
H(3)	7264	3466	5138	28
H(12A)	10507	2356	6399	48
H(12B)	9790	1889	5767	48
H(12C)	10704	1370	6120	48
H(5)	7166	860	5793	24
H(8)	7731	4033	7312	28
H(21)	4417	2675	6533	35
H(15)	8819	296	7877	26
H(16A)	7974	-13	6665	46
H(16B)	7269	-675	7131	46
H(16C)	8388	-914	7016	46
H(25A)	4183	1675	5249	41
H(25B)	4095	760	4782	41
H(25C)	5129	1219	4879	41
H(24)	4006	469	6179	27
H(13A)	11331	692	7288	56
H(13B)	10470	19	7467	56
H(13C)	11099	401	8208	56
H(18)	7439	681	9596	32
H(26A)	5861	-131	5613	48
H(26B)	4857	-617	5438	48
H(26C)	5271	-565	6351	48
H(20A)	6751	1933	10201	54
H(20B)	6019	1525	9546	54
H(20C)	6632	2379	9321	54
H(19A)	8517	2219	9161	51
H(19B)	8978	1263	9232	51
H(19C)	8564	1739	10030	51
H(17A)	8445	-392	9147	51
H(17B)	8770	-1101	8481	51
H(17C)	7650	-984	8702	51
H(22A)	3128	1592	7472	59
H(22B)	3133	1589	6492	59
H(22C)	2841	2458	6979	59
H(23A)	5215	2994	7736	101
H(23B)	4575	2304	8235	101
H(23C)	4085	3170	7875	101
H(14A)	10163	2454	8279	60
H(14B)	11018	2293	7637	60
H(14C)	11057	1842	8520	60
H(27A)	4056	69	9700	104
H(27B)	3975	1092	9511	104